

University of Alberta

**Characterization of Clay Minerals in the Athabasca Oil Sands in Water
Extraction and Nonaqueous Solvent Extraction Processes**

by

Mohammad Ali Hooshlar Fard

A thesis submitted to the Faculty of Graduate Studies and Research
in partial fulfillment of the requirements for the degree of

Doctor of Philosophy

in

Materials Engineering

Department of Chemical and Materials Engineering

©Mohammad Ali Hooshlar Fard

Fall 2011

Edmonton, Alberta

Permission is hereby granted to the University of Alberta Libraries to reproduce single copies of this thesis and to lend or sell such copies for private, scholarly or scientific research purposes only. Where the thesis is converted to, or otherwise made available in digital form, the University of Alberta will advise potential users of the thesis of these terms.

The author reserves all other publication and other rights in association with the copyright in the thesis and, except as herein before provided, neither the thesis nor any substantial portion thereof may be printed or otherwise reproduced in any material form whatsoever without the author's prior written permission.

Dedicated to my beloved parents,
Jamileh Nategh & Aliasghar Hooshiar

Abstract

Production of oil from the second largest oil deposit in the world, i.e., the Alberta oil sands containing approximately 13% of total proven oil reserves in the world (169.9 billion barrels), has been shown to be significantly influenced by clay minerals. Clay minerals in particular play a key role in the settling behaviour of massive amounts of aqueous tailings resulting from water-based bitumen extraction. A nonaqueous extraction process is of special interest to extract bitumen from oil sands due to its potential advantages, such as high bitumen recovery even from low grade oil sands ores and the elimination of slow settling, sludge tailings ponds with stable suspensions. While clay minerals have been characterized in water-based bitumen extraction from the oil sands to some extent, the gap of knowledge in the characterization of clay minerals in a nonaqueous bitumen extraction process has led to the current research.

A nonaqueous bitumen extraction process was established where only toluene and heptane, with no water additions, were used to extract bitumen from oil sands ore samples. Bitumen recovery and product quality were studied under different process conditions, such as the ratio of toluene to heptane and settling time. Bitumen recovery was found to be insensitive to the characteristics of the oil

sands ores, such as processability and fines content, although the high fines ore sample was more sensitive to the extraction conditions. A product with high purity, containing more than 99.5 wt% bitumen on a solvent-free basis, was produced at room temperature under the optimum extraction conditions tested.

Quantitative x-ray diffraction (XRD) analysis revealed an enrichment of kaolinite in the extraction products (froth stream in water-based extraction and supernatant in nonaqueous extraction) when compared with the ore. High resolution transmission electron microscopy (HRTEM) investigations showed the presence of monolayer discrete smectitic clay minerals (not detectable by XRD). Illite-smectite expandability results calculated from HRTEM data have made it possible to explain the extraordinarily high surface activity in the primary froth stream. Scanning electron microscopy (SEM) observations showed some important features (clay-organic aggregates) which affect the settling behaviour of the solids after nonaqueous extraction.

Acknowledgements

Hereby, I would like to thank everybody who helped me during my PhD:

Dr. Peter Uhlik with whom I performed almost every experiment. I can never thank him enough for his great help.

Dr. Heather Kaminsky for her guidance, especially in the beginning of my PhD. She has collaborated in writing a great deal of Chapter Three of the current thesis.

My undergraduate student, Alyssa Shinbine, for helping with high-resolution transmission electron microscopy (HRTEM) measurements.

Dr. Olusola B Adeyinka for his guidance in establishing the nonaqueous bitumen extraction process.

Dr. Oladipo Omotoso for his guidance, especially with x-ray diffraction (XRD) and transmission electron microscopy (TEM).

The following amazing technicians who trained me to use several instruments: Greg Popowich for TEM, Randy Mandryk for Microtome, Shiraz Merali & Diane Caird for XRD, Daniel Salomon, Rakesh Bhatnagar and Tina Barker for SEM, Andree Koenig for the centrifuge and Tuyet Le for Karl-Fischer titrator and elemental analyzer.

Dr. Arash Karimi for his help in using the micro-thermogravimetric analyzer (micro-TGA).

Dr. Kavithaa Logan for her guidance with micro-TGA, the elemental analyzer and the Karl-Fischer titrator.

My friend, Arash Ilbagi, for his great help in using TGA.

Dr. Yadollah Maham for his suggestions in performing TGA experiments.

Dr. Murray Gray, Dr. Al Meldrum and Dr. Dr. Hani Henein for letting me using their laboratory equipment.

Dr. Arek Derkowski for his great help in writing the Future Work Chapter.

My great friends, Dr. Navid Paydavosi and Mehdi Alipour, for their help in editing the current thesis.

My great office mates, Dr. Heather Kaminsky, Patrick Kerr and Stephen Gibson for providing a great working atmosphere during my PhD.

Dr. Payman Esmaili and Ron D. Myers of Imperial Oil Ltd. for their suggestions during several meetings.

The Centre for Oil Sands Innovation (COSI) for funding my PhD project.

Finally, my fantastic supervisors, Dr. Thomas H. Etsell, Dr. Qi Liu, and Dr. Douglas G. Ivey, for their guidance and supervision. I have had the opportunity to have access to their insights and knowledge at any time during the last four years. Their great suggestions have helped me in performing laboratory experiments, analyzing scientific data and writing scientific papers.

Table of Contents

1)	Introduction.....	1
1.1.	Important role of clay minerals in bitumen extraction.....	6
1.2.	The influence of clay minerals on the settling behaviour of the tailings	7
1.3.	The role of clay minerals in bitumen recovery	9
1.4.	Clay-organic interactions during bitumen extraction.....	11
1.5.	Importance of clay mineralogy in relation to the bitumen extraction process	20
1.6.	Objectives of the research	21
1.7.	References.....	23
2)	Background.....	28
2.1.	Clay minerals: Microstructures and properties	28
2.1.1.	Joining of the sheets.....	30
2.1.2.	1:1 Layer clay minerals.....	31
2.1.3.	2:1 Layer clay minerals.....	32
2.1.4.	Polytypes and layer stacking.....	35
2.1.5.	Turbostratic disorder	36
2.1.6.	Mixed-layer clay minerals	36
2.1.7.	Swelling	37
2.1.8.	Surface area.....	38
2.1.9.	Charge distribution and cation exchange capacity (CEC)	38
2.2.	Basics of characterization techniques	39
2.2.1.	Electron diffraction	39
2.2.2.	TEM analysis	40
2.2.3.	X-ray diffraction (XRD)	41

2.3.	References.....	45
3)	High resolution transmission electron microscopy study of clay mineral particles from streams of simulated water based bitumen extraction of Athabasca oil sands.....	47
3.1.	Introduction.....	47
3.2.	Materials and methods	49
3.2.1.	Sample preparation and batch extraction.....	49
3.2.2.	TEM sample preparation.....	50
3.2.3.	Determination of cation exchange capacity (CEC)	53
3.3.	Results and discussion	54
3.3.1.	Morphology of clay mineral particles.....	54
3.3.2.	Particle thickness measurement by HRTEM	59
3.3.3.	Determination of iron content from amorphous and crystalline Fe Oxides	67
3.3.4.	CEC Measurements	68
3.3.5.	Special case of the 0.2-2 μm size fraction of the primary froth.....	70
3.4.	Conclusions.....	71
	Acknowledgements.....	72
3.5.	References.....	73
4)	Clay minerals in nonaqueous extraction of bitumen from Alberta oil sands. Part 1: nonaqueous extraction procedure.....	77
4.1.	Introduction.....	77
4.2.	Materials and experimental procedures	80
4.2.1.	Samples.....	80
4.2.2.	Solvent extraction tests	80
4.2.3.	Analytical methods	82
4.3.	Results and discussion	84

4.3.1.	Bitumen recovery	84
4.3.2.	Product quality	88
4.3.3.	Settling time	93
4.4.	Conclusions	96
	Acknowledgements	97
4.5.	References	98
5)	Clay minerals in nonaqueous extraction of bitumen from Alberta oil sands. Part 2: characterization of clay minerals	100
5.1.	Introduction	100
5.2.	Materials and experimental procedures	102
5.2.1.	Oil sands ore samples	102
5.2.2.	Solvent extraction	102
5.2.3.	Clay particle separation	103
5.2.4.	X-ray diffraction (XRD) analyses	103
5.2.5.	Transmission electron microscopy (TEM) investigations	104
5.2.6.	Scanning electron microscopy (SEM) investigations	106
5.3.	Results and discussion	106
5.3.1.	Characterization of clay minerals in the oil sands ores	106
5.3.1.1.	Low-pressure SEM investigations	106
5.3.1.2.	TEM analyses	108
5.3.2.	Comparison between clay minerals in the oil sands ore and extraction product	109
5.3.2.1.	XRD analyses	109
5.3.2.2.	HRTEM investigations	116
5.3.2.3.	Low-pressure SEM investigations	121
5.3.3.	Characterization of the tailings	123

5.4.	Conclusions.....	127
	Acknowledgements.....	128
5.5.	References.....	129
6)	Summary.....	132
6.1.	Study of the nature of clay minerals in both good and poor processing raw oil sands ores and the clay lenses.....	132
6.2.	Study of the behaviour and characteristics of clay minerals during nonaqueous extraction	133
6.2.1.	Bitumen recovery.....	134
6.2.2.	Product quality	135
6.2.3.	Settling time	136
6.2.4.	Settling behaviour of the tailings	136
6.3.	Comparison study of the behaviour of clay minerals during water extraction	138
7)	Conclusions and future work	141
7.1.	Conclusions.....	141
7.2.	Future work.....	143
7.2.1.	Establishment of a systematic sampling method	143
7.2.2.	Detailed characterization of the clay minerals and Fe nanominerals in the representative oil sands end members (estuarine sand, estuarine clay, marine sand, and marine clay) and artificial oil sands samples.....	144
7.2.3.	Study of the influence of clay minerals on solvent extraction in a completely water-free environment	146
7.2.4.	Study of the influence of different smectites on water-based and nonaqueous bitumen extraction	147
7.2.5.	The role of clay minerals on solvent recovery.....	148
7.3.	References.....	150

List of Tables

Table 1-1. Typical composition of MFT (Thomas et al., 2010) and its clay mineral contents (Adeyinka et al., 2009).	6
Table 1-2. Adsorption capacities of asphaltenes on different minerals (Pernyeszi et al., 1998).	18
Table 2-1. Free-swelling data for clay minerals (Grim, 1962).	38
Table 2-2. Cation exchange capacity of some clay minerals (Grim, 1962).	39
Table 3-1. Length and width measurements for dispersed particles in primary froth and middlings samples. Mean area was calculated by multiplying the average length by the average width.	57
Table 3-2. Statistical parameters for particles observed by HRTEM. (*aspect ratio is calculated by using the area values from Table 3-1 and thicknesses only for illitic particles.)	60
Table 3-3. Illite-smectite expandability calculated from HRTEM measurements (%S Max) and comparison with expandability measured by XRD (%S XRD). T – total measured thickness of particles; N – total number of interlayers in measured particles; No - number of measured particles.	66
Table 3-4. CEC values before and after Jackson treatment.	69
Table 4-1. Composition of oil sands ore samples.	80
Table 4-2. Supernatant assays based on solvent-free mass balance calculations*.	89
Table 4-3. Calculated values for heptane to bitumen ratio at different toluene/heptane ratios for the two oil sands samples.	92
Table 5-1. Length and width measurements for dispersed particles in oil sands ores A and B. Mean area was calculated by multiplying the average length by average width.	109
Table 5-2. Statistical parameters for particles observed by HRTEM - %Smax and d-spacing are calculated maximum illite-smectite expandability and basal spacing, respectively.	121

List of Figures

Fig. 1.1. Worlds oil reserves in 2009 (billion barrels) (Alberta Energy, 2011).....	1
Fig. 1.2. Typical arrangement of oil sands particles (Camp, 1976).....	3
Fig. 1.3. Relationships between fines, clays, and ultrafines contents in oil sands ores (Tu et al., 2005). Arrows indicate the ores that do not follow the correlation.	3
Fig. 1.4. General scheme for hot water bitumen extraction process.....	4
Fig. 1.5. Relationship between bitumen recovery and a) the illite/kaolinite ratio and b) the amount of ultra-thin illite in the raw oil sands ore (Mercier et al., 2008).	10
Fig. 1.6. Role of biwetttable clay minerals in stabilizing water droplets in bitumen (water-oil emulsion) (Sparks et al., 2003).	13
Fig. 1.7. Confocal laser scanning micrograph of the bitumen froth showing aggregates of clay-water- bitumen (spheres) trapped between bitumen sheets (plates). The area of normal bitumen is indicated by the arrow. (Muñoz et al., 2003).	13
Fig. 1.8. Secondary electron field emission SEM image of kaolinite particles coated with oil deposits (Lebedeva and Fogden, 2011). Scale bar = 500 nm.....	16
Fig. 1.9. Adsorption of organic matter on the surface of clay minerals (Sparks et al., 2003).	17
Fig. 2.1. A tetrahedral sheet made by corner linked SiO_4 (Bennett & Hulbert, 1986).	28
Fig. 2.2. An octahedral sheet made by edge to edge linked octahedra (Grim, 1962).	29
Fig. 2.3. Coordination in a close-packed plane of atoms; each atom possessing two sets of sites, I and II, around it where one set will be octahedral and the other tetrahedral (Moore & Reynolds, 1997). A: Octahedral sheet. B: Octahedral sites (I and II). C: It is not possible that both type I and II octahedral sites are occupied by anions (oxygen atoms or hydroxyl groups) because the shaded volume would have to be occupied by both of them. D: Octahedral sites surrounded by six anions.	30
Fig. 2.4. Joining octahedral and tetrahedral sheets together to form a 1:1 layer silicate (Moore & Reynolds, 1997).....	30

Fig. 2.5. Structure of kaolinite as an example of a 1:1 layer clay mineral (Grim, 1962).	31
Fig. 2.6. Formation of a 2:1 layer silicate by joining two tetrahedral sheets to one octahedral sheet ○ = oxygen, ● = hydroxyl, • = cations in tetrahedral sites, ⊙ = cations in octahedral sites (Moore & Reynolds, 1997).	33
Fig. 2.7. An undistorted 0.7 nm layer of space group Cm showing all three octahedral sites and relative displacement of octahedral and tetrahedral sheets (Bailey, 1963).	34
Fig. 2.8. a) Cis-vacant and b) trans-vacant configurations in octahedral sheets in dioctahedral clay minerals (Sainz-Diaz et al., 2001).	35
Fig. 2.9. Crystal structure of smectitic I/S. Large dark circles are fixed K, open circles are water molecules and small dark circles are exchangeable cations (Altaner & Ylagan, 1997).	37
Fig. 2.10. Bragg diffraction (Cullity, 1978).	40
Fig. 2.11. TEM images showing lattice fringes for a) smectite, b) illite, and c) illite-smectite (Ahn & Peacor, 1986).	41
Fig. 2.12. Pure illite and glauconite XRD patterns (Moore & Reynolds, 1997). .	43
Fig. 2.13. Pure kaolinite and chlorite XRD patterns (Moore & Reynolds, 1997). 43	
Fig. 2.14. Pure smectite XRD pattern (Moore & Reynolds, 1997).	43
Fig. 2.15. Illite-smectite (50-50) XRD pattern (Moore & Reynolds, 1997).	43
Fig. 3.1. HRTEM image of illite RM30 used as a standard for particle thickness measurements and basal spacing calculations. The enlarged part is on the right ($D_1 = t$ (thickness of the individual particle, measured from the middle of the first layer to middle of the last layer)/ n (number of interlayers per individual particle)).	52
Fig. 3.2. TEM images of dispersed samples showing pseudo-hexagonal idiomorphic (A), subhedral (B), anhedral (C) and oval (D) particles. L – length and W – width.	55
Fig. 3.3. Distributions of length and width of particles from extraction products measured from TEM images.	58
Fig. 3.4. HRTEM images of the 0.2-2 μm middlings sample showing a) thin and b) thick particles.	59

Fig. 3.5. HRTEM image of the 0.2-2 μm primary froth sample is showing thick (15 layers) and thin (2 layers) particles.....	61
Fig. 3.6. Distribution of number of layers per particle measured from data obtained from HRTEM images.....	62
Fig. 3.7. HRTEM images of <0.2 μm primary froth sample. Iron-rich regions are circled.....	63
Fig. 3.8. HRTEM image of 0.2-2 μm middlings sample showing inconsistent basal spacings (circles) and lateral layer termination (squares).....	64
Fig. 3.9. Maximum percent smectite obtained from TEM plotted against expandability measured by XRD. Published data are from Środoń et al. (1992) and Uhlík et al. (2000).	67
Fig. 3.10. Soluble Fe content (wt%) after sodium dithionite extraction and ammonium oxalate extraction is compared with the total amount of Fe determined by XRF (Kaminsky, 2008).....	68
Fig. 4.1. A comparison between water content measured by the Karl Fischer titration method (KF) and Dean Stark analysis (DS) in the extraction products. .	83
Fig. 4.2. Bitumen distribution in all three products. Error bars show differences in the values of two or three extraction tests.....	85
Fig. 4.3. Bitumen recovery and corresponding solvent to bitumen (S:B) ratio.	86
Fig. 4.4. Total bitumen recovery based on the mass of the remaining bitumen in the tailings after a 2nd wash.....	88
Fig. 4.5. Supernatant assays from mass balance calculations – average values are from Table 4-2, using water content values from the KF titration method. Standard deviation is $\pm 1\%$ for bitumen and solids (measured by Dean Stark) and $\pm 0.05\%$ for water (measured by Karl Fischer titration).....	91
Fig. 4.6. Water content in extraction products by Karl Fischer titration. Standard deviation is $\pm 0.05\%$	93
Fig. 4.7. Water and solids contents of the supernatant with a toluene to heptane ratio of 30/70 at different settling times analyzed by the KF titration and TGA, respectively. Standard deviation is $\pm 0.05\%$ for water contents.	94
Fig. 4.8. Water and solids contents of the supernatant with a toluene to heptane ratio of 0/100 at different settling times analyzed by the KF titration and TGA, respectively. Standard deviation is $\pm 0.05\%$ for water contents.	95

Fig. 5.1. Environmental SEM images of the raw oil sands ore showing the very fine (clay) particles attached to the large sands grains. Bitumen is most probably present in dark channels among sand grains. Arrows show some small clay particles as an example.	107
Fig. 5.2. Cryo-SEM secondary electron images of raw oil sands ores, A and B, showing agglomerates of clay particles in ore B.	107
Fig. 5.3. TEM images of dispersed samples from the 0.2-2 μm fraction of oil sands ore A showing pseudo-hexagonal (P) and lath-like (L) particles.	108
Fig. 5.4. XRD profiles of oriented samples of the 0.2-2 μm fraction of the oil sands ores as well as their nonaqueous extraction products (supernatants at a toluene to heptane ratio of 30/70 and a settling time of 7.5 min). Ch-chlorite, I/S – mixed-layered illite-smectite, I-illite, K-kaolinite, Q-quartz, EG-sample saturated with ethylene glycol, RH-relative humidity, SUP-supernatant.	111
Fig. 5.5. K/I ratio (black bars) and relative enrichment of kaolinite to the supernatant (gray bars) for the entire clay fraction (< 2 μm) from the ore and supernatant after 1 and 7.5 min of settling, based on quantitative XRD analysis. T/H - toluene to heptane ratio.	114
Fig. 5.6. K/I ratio for the entire clay fraction (<2 μm) from the ore and products after water-based batch extraction of samples A and B, based on quantitative XRD analysis. PF - primary froth, MID - middlings, TAIL -tailings.	115
Fig. 5.7. HRTEM lattice fringe image from KGa-1B. Measured d (basal spacing) = 0.7 nm.	117
Fig. 5.8. HRTEM lattice fringe images from the clay fractions of sample B: a), b) the oil sands ore and c), d), e), f) the extraction product (supernatant) showing particles varying in thickness. bi: bilayer, m: monolayer.	118
Fig. 5.9. Distribution of number of layers per particle measured from data obtained from HRTEM images. Samples are clay fractions (< 2 μm) separated from ore B (dashed line) and supernatant produced from sample B at a toluene to heptane ratio of 30/70 after 7.5 min of settling.	119
Fig. 5.10. BSE SEM image of the A supernatant after 1 min of settling.	123
Fig. 5.11. BSE SEM image of the B supernatant after 1 min of settling.	123
Fig. 5.12. BSE SEM image the of A supernatant after 7.5 min of settling.	123
Fig. 5.13. BSE SEM image of the B supernatant after 7.5 min of settling.	123

Fig. 5.14. Comparison of clay fraction (<2 μm) composition of the ore and products after nonaqueous extraction (supernatant and tailings), showing the kaolinite enrichment in the supernatant. 0/100 = toluene to heptane ratio. 124

Fig. 5.15. BSE low pressure SEM images of tailings from nonaqueous extraction with a toluene to heptane weight ratio of 30/70. Sample A (left), sample B (right), scale bars are 100 μm. Large grains: quartz/feldspar, small particles: clays. Arrows show some small clay particles. The circle shows an area of clay agglomerates. 125

Fig. 5.16. Sum of the consolidated and partly consolidated tailings solids volume vs. gravity settling time. (Solids% = (Volume of consolidated tailings + Volume of partly consolidated tailings)/Total volume)..... 127

Chapter 1

Introduction

Alberta's oil sands deposit is one of the largest sources of oil on the planet. In 2009, the proven oil reserve in Alberta, at 171.3 billion barrels, held approximately 13% of total proven oil reserves in the world, of which 99% (169.9 billion barrels) were associated with oil sands. The oil sands deposit makes Alberta the second largest oil reserve in the world after Saudi Arabia (Fig. 1.1). Alberta's oil sands reserve also accounts for more than 95% of Canada's oil reserves. The production of crude oil from Alberta's oil sands (1.31 million barrels/day in 2008) is anticipated to increase to three million barrels per day by 2018, according to the Alberta Energy and Utilities Board (AEUB). In 2009, Alberta supplied 7% of the United States oil demand, or 15% of U.S. crude oil imports by exporting approximately 1.4 million barrels per day (bbl/d) of crude oil to the U.S. (Alberta Energy, 2011).

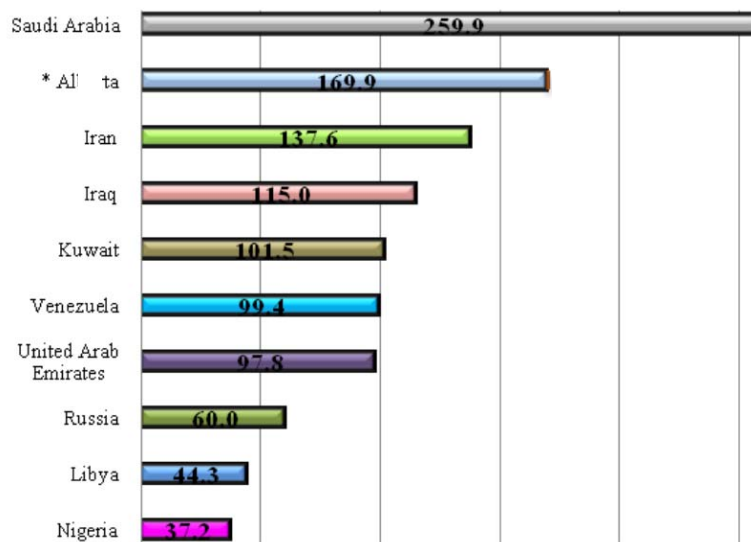


Fig. 1.1. Worlds oil reserves in 2009 (billion barrels) (Alberta Energy, 2011).

Oil sands, consisting of layers of sand deposits mixed with highly viscous petroleum (bitumen), are commonly referred to as tar sands or bituminous sands. Alberta's oil sands consist of approximately 55-80 wt% sands (mainly quartz), 4-18 wt% bitumen, 5-34 wt% fine solids (particles smaller than 45 μm), and 2-15 wt% water (Bichard, 1987; Kasperski, 2001). It is generally believed that the arrangement of the oil sands components is as depicted in Fig. 1.2 (Camp, 1976). The quantity of fines present within the oil sands plays a major role in the water-based bitumen extraction process. An ore possessing more than 10 wt% bitumen and less than 10 wt% fines of the total mineral content would be considered a good candidate for the water-based bitumen extraction process. Conversely, an oil sand ore would be a poor processing ore if it contains less than 8 wt% bitumen and more than 35 wt% fines.

In the oil sands industry, the fines (fraction smaller than 45 μm) content of an oil sands ore has been used as an important parameter in determining the processability of the ore, although it has been known for a long time that it is, in fact, the clay (fraction smaller than 2 μm) and ultrafine clay (fraction smaller than 0.2 μm) contents that matter most in this regard. Supporters of the use of fines content in determining the processability of an oil sands ore argue that the fines, clay, and ultrafine clay contents of an ore correlate closely. This argument has been examined by Tu et al. (2005). They showed that although there is an approximately linear correlation between the ultrafine clay (fraction smaller than 0.3 μm in their study), clay (fraction smaller than 3 μm in their study), and fines contents, the ultrafine clays content in some ores was unproportionally high relative to the fines content (Fig. 1.3).

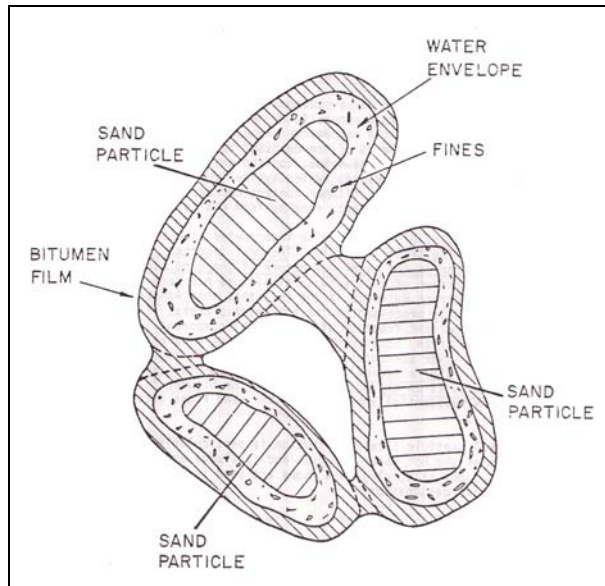


Fig. 1.2. Typical arrangement of oil sands particles (Camp, 1976).

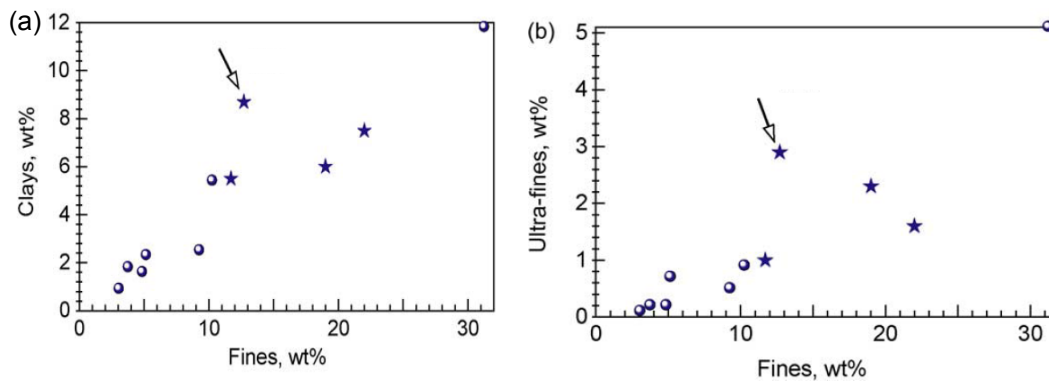


Fig. 1.3. Relationships between fines, clays, and ultrafines contents in oil sands ores (Tu et al., 2005). Arrows indicate the ores that do not follow the correlation.

Two methods are currently used to produce crude bitumen from the oil sands: surface mining and in-situ methods. Approximately 80% of the proven reserves (169.9 billion barrels) are recoverable by in-situ methods and 20% by surface mining. Surface mining can be used for oil sands deposits within 75 meters of the surface while in-situ methods must be used for oil sands below this threshold. In 2009, surface mining accounted for 55% of Alberta's production of crude bitumen

(1.5 million barrels per day) as opposed to 45% for in-situ methods (Alberta Energy, 2011).

Clark Hot Water Extraction (CHWE), a water-based process, is used to extract bitumen from the oil sands in surface mining methods (Camp, 1976). Fig 1.4 illustrates the basic steps of hot water bitumen extraction. Detailed information about hot water bitumen extraction is available in the review paper by Masliyah et al. (2004). The large volume of tailings generated from this process poses a major environmental challenge to the oil sands industry. Currently, 170 square kilometres of land area in Northern Alberta is covered by oil sands tailings ponds with a total volume of 840 million cubic metres (Alberta Energy Resources Conservation Board, 2010). The increasing rate of bitumen production also means a larger volume of the tailings. Currently, two hundred million litres (0.2 million m³) of oil sands tailings are produced daily, and the volume of tailings is estimated to increase 30% by 2020 (Grant et. al, 2008).

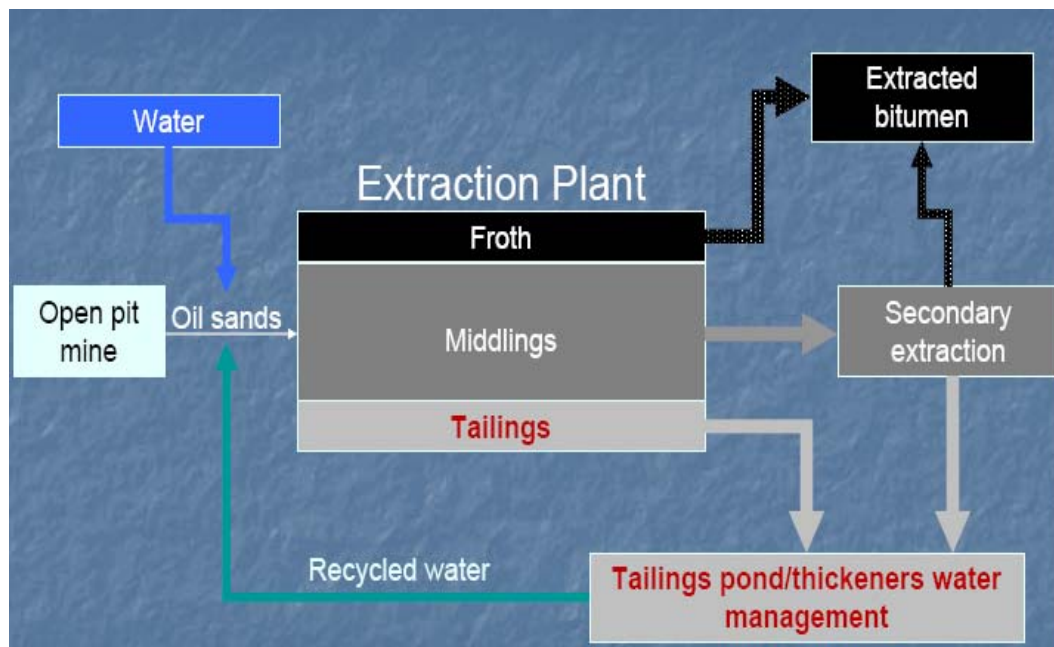


Fig. 1.4. General scheme for hot water bitumen extraction process.

In addition to generating a massive volume of tailings, the water-based bitumen extraction process consumes large amount of water. Almost 90% of the 359 million cubic metres of water annually allotted for use in the oil sands industry is not recycled or returned to its original source (Sustainable Development Business Case Report, 2006).

Mature fine tailings (MFT), a mixture of fines, residual organics (bitumen and solvents), and water, are the most problematic component of the tailings. It was estimated by Kasperski (1992) that 1.3 m³ of MFT is produced from mining of one cubic meter of oil sands ore by the technology used in 1992. From an oil production standpoint, approximately 0.25 m³ (1.57 barrels) MFT is generated for each barrel of produced bitumen. Based on 2.6 billion barrels of bitumen produced since 1968, the accumulated volume of MFT is larger than 650 million m³. This number is expected to pass one billion cubic metres by 2020 with the current production rate (Chalaturnyk et al., 2002; PTAC, 2007). The settling of fines to about 30 wt% solids takes approximately ten years (MacKinnon, 1989). The high surface area of the MFT is one of the prime reasons for its long settling time. Although the reasons for this high surface area are to date not completely understood, ultrafine kaolinite and mixed-layer clay minerals with expandable smectitic layers are two commonly suggested possibilities (Omotoso and Mikula, 2004).

The composition of MFT is variable. A typical composition of MFT (Table 1-1) was reported by Thomas et al. (2010). The mineral content at the top of MFT is about 10 wt% and reaches to about 50 wt% at the bottom giving an average mineral content of about 30 wt%. Fines, the fraction smaller than 45 µm, are the dominant size fraction in the solids (>97 wt% based on Thomas et al., 2010). The clay fraction of the tailings (fraction smaller than 2 µm) is reported to be composed of 22-76 wt% kaolinite, 7-10 wt% illite, 1-8 wt% montmorillonite and traces of chlorite, quartz, calcite, dolomite, siderite, feldspar, ankerite, zircon, ilmenite, leucosene, and rutile (Kasperski, 1992). Not only is the settling

behaviour of the tailings highly influenced by the rheology of MFT, but so is bitumen extraction. Adeyinka et al. (2009) showed that the rheological behaviour of MFT is predominantly controlled by the clay fraction of the fines. Table 1-1 shows the mineral composition of MFT studied by Adeyinka et al (2009). They reported a total surface area of 186 m²/g based on XRD calculations. Table 1-1 also shows the calculated specific surface area for each clay mineral in the MFT. For instance, it can be seen that the presence of only 10% smectitic layers in kaolinite (kaolinite-smectite 90:10) increased the surface area from 61 to 273 m²/g (Adeyinka et al., 2009).

Table 1-1. Typical composition of MFT (Thomas et al., 2010) and its clay mineral contents (Adeyinka et al., 2009).

<u>Water</u> (wt%)	<u>Hydrocarbon</u> (wt%)	<u>Solids (wt%)</u>			
62	3	35			
Mineral composition of the clay fraction (<2 µm) of solids (wt%)	Illite-smectite (77:23)	Illite	Kaolinite-smectite (90:10)	Kaolinite	
	44	20	10	26	
Specific surface area (m ² /g)	293	68	273	61	

1.1. Important role of clay minerals in bitumen extraction

The structure and properties of clay minerals present in the oil sands will be discussed in detail in the background section. It seems necessary to briefly explain the composition of bitumen and its components before focusing on clay-bitumen interactions.

Although the structure of bitumen is not yet completely defined, it is known that bitumen consists of three main components: maltenes, resins and asphaltenes with asphaltenes being heavier (with respect to molecular weight), more polar and also more aromatic than other components. Maltenes are the part of the bitumen that is soluble in normal alkane (paraffin) solvents such as pentane and heptane. There is

a general agreement that resins are soluble in higher molecular weight normal alkanes, but are insoluble in lower molecular weight alkanes. Asphaltenes can be differentiated from the other components of bitumen by their insolubility in normal paraffins such as n-pentane and n-heptane. There are large polycyclic and polyaromatic rings in the asphaltenes molecules containing oxygen, nitrogen, sulphur, and metals (Clementz, 1976).

Because of their very high surface area and charge density, clay minerals are the most reactive solids that bitumen molecules are exposed to during the bitumen extraction process. The irreversible adsorption of organic matter, e.g., bitumen (or bitumen components such as asphaltenes), on clay mineral surfaces dramatically changes the physical and chemical properties of the clay minerals as well as the chromatography of crude oil composition. Both influence the extraction process (Clementz, 1976; Dongbao et al., 2010). Clementz believes that any measurement of the charge of the clay mineral, its expandability, or the nature of its surface will be affected by the adsorption of organic matter on the clay mineral surfaces. For instance, an underestimate in the amount of expandable clay minerals (smectites or mixed-layer smectitic layers within illite or kaolinite) may occur due to the broadening of {001} reflections caused by the adsorption of organic matter on the clay mineral surfaces. Similar underestimation is common in cation exchange capacity (CEC) measurements. Asphaltene molecules contain positively charged nitrogen groups in their structures and, hence, are attracted to the negatively charged surfaces of clay minerals.

1.2. The influence of clay minerals on the settling behaviour of the tailings

Adeyinka et al. (2009) demonstrated the importance of clay-organic interactions on the settling behaviour of the tailings. They showed that adsorption of organic matter on the clay mineral surfaces increases the MFT viscosity due to the

stronger particle interactions. Consequently, higher viscosity of MFT will result in longer settling times for the tailings.

The amount of nanosized (20-300 nm) clay mineral particles was found to almost entirely control the final volume of MFT. The aggregation of such clay mineral particles in the presence of flocculating cations (present in common salts) was indicated to be the main cause for the formation of a thixotropic gel and, therefore, produced a huge volume of MFT (Kotylar et al., 1996; Kotylar et al., 1998a). Kotylar et al. (1992) claimed that this phenomenon is responsible for nearly all of the water-holding capacity of MFT as the gel-like structure contains as much as 90% of the process water (Ripmeester et al., 1993). The nano sized clay solids can also help the coarser fraction of the tailings in forming auxiliary structures by providing a viscous supporting medium for them. Characterization of the nanosized clay minerals is, therefore, a crucial necessity in understanding the mechanism of the gelation process.

Tu et al. (2005) showed that the settling behaviour of the oil sands slurries is very sensitive to the ultrafine clay minerals content of the ore. Their results demonstrated that the existence of more than 1.5 wt% ultrafine clay minerals in the oil sands ore makes the slurries non-segregating. Kaminsky (2008) also showed that hydrophilic ultrafine clay minerals free of organic matter intensely concentrate in the middlings during water-based batch extraction of bitumen. Not only has the amount of the clay or ultrafine clay minerals, but the type and their properties, directly influence the characteristics of the tailings and MFT. The expandable clay minerals (either discrete or mixed-layer) have been found to be the most influential in this regard. For instance, the surface area of the MFT and its volume will be doubled if 10 wt% smectite is added to MFT solids (Omotoso & Mikula, 2004).

1.3. The role of clay minerals in bitumen recovery

Another environmental problem associated with bitumen extraction is the residual organic matter (bitumen and solvents) in the tailings ponds. Since any loss in bitumen recovery corresponds to the existence of residual bitumen in the tailings ponds, higher bitumen recovery is not only important from an economical point of view but is also advantageous from an environmental perspective. In addition to affecting the settling behaviour of the tailings, clay minerals play an important role in bitumen recovery due to clay-organic interactions. The “armouring” effect of clay particles adsorbed on bitumen droplet surfaces lowers the probability for the bitumen droplets to attach to air bubbles.

Dang-Vu et al. (2009) showed that both bitumen recovery and froth quality are directly related to the wettability of the fine solids. In addition, Adegoroye et al. (2010) found that bitumen recovery from the oil sands is inversely related to the amount of the organic-coated solids in the raw oil sands ore. Dang-Vu et al. (2009) argued that the simultaneous presence of both fines and asphaltenes influences bitumen recovery significantly.

Kasongo et al. (2000) also observed that the simultaneous presence of montmorillonite and calcium ions during water-based bitumen extraction decreased bitumen recovery significantly, while the presence of illite and kaolinite did not have such an effect on bitumen recovery. For example, bitumen recovery decreased from 93% to less than 70% in the presence of 40 ppm calcium ions and 1 wt% montmorillonite. They showed that the adsorption of calcium ions on montmorillonite surfaces increased the adhesive forces between them and bitumen droplets making bitumen aeration more difficult and, therefore, lowering bitumen recovery. Conversely, kaolinite and illite surfaces did not show such an affinity to calcium ions (Kasongo et al., 2000; Liu et al. 2004).

Mercier et al. (2008) studied the relationship between several characteristics of clay minerals in the oil sands ores and bitumen recovery. Their XRD-based investigations on ten oil sands ore samples indicated that there is a correlation between bitumen recovery and the ratio of illite to kaolinite in the raw oil sands ore (Fig. 1.5). Their results also showed that the percentage of the ultrathin illite particles (particles with crystallite thicknesses less than four composite layers) in the oil sands ore decreases bitumen recovery dramatically (Fig. 1.5b). Mercier et al. were not able to determine whether ultrathin kaolinite particles have the same influence on bitumen recovery, as the amount of such particles detected in their study was virtually zero.

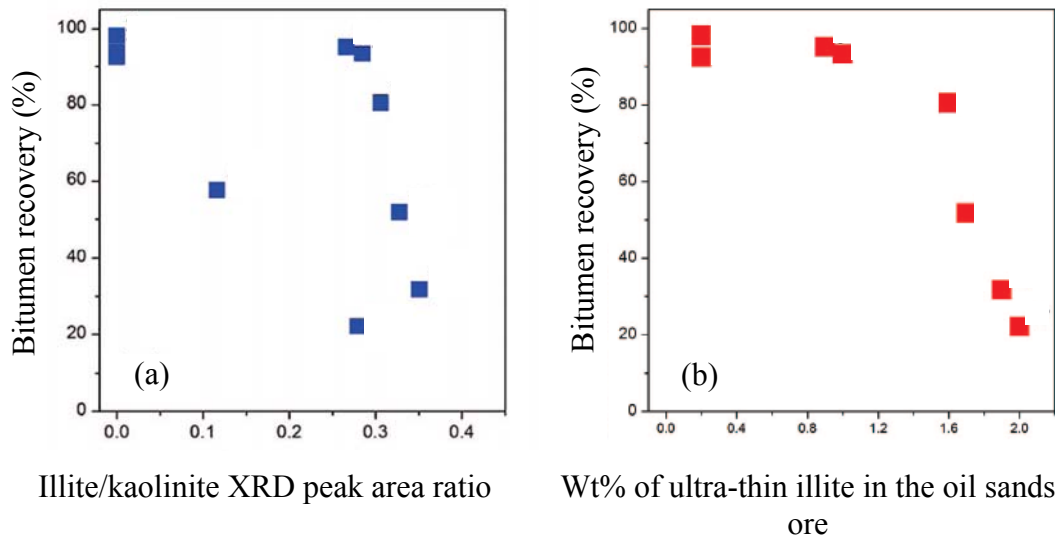


Fig. 1.5. Relationship between bitumen recovery and a) the illite/kaolinite ratio and b) the amount of ultra-thin illite in the raw oil sands ore (Mercier et al., 2008).

It should be noted that due to the large scale of oil sands production, a slight difference in bitumen recovery has a significant economic impact. Current water extraction process recovers about 91% of the bitumen from the oil sands and the current production rate is about 1.3 million barrels/day. A one percentage point drop in bitumen recovery would lead to a loss of revenue of \$1.42 million per day at the current oil price of about \$100 per barrel.

1.4. Clay-organic interactions during bitumen extraction

Although the majority of solids in the oil sands are hydrophilic and, hence, settle to the tailings, some of them with high organic matter content show biwettable (and/or hydrophobic) characteristics (Kotlyar et al., 1988, 1998b; Darkovich et al., 1989; Bensebaa et al., 2000). These solids (clay minerals), together with organic matter, usually form aggregates. Other materials such as quartz, heavy minerals, calcium carbonate, siderite, and iron oxides have also been found in aggregate structures. These aggregates can be either biwettable or completely hydrophobic depending on the organic matter content (Sparks et al., 2003).

Before discussing more about the nature of the organic rich clay surfaces, it is necessary to explain the common understanding of the hydrophobic (oleophilic), biwettable, and hydrophilic particles in the bitumen extraction process. In the oil sands literature, particles that respond well to bitumen aeration and hence can be found mostly in the froth are considered hydrophobic (or oleophilic). These particles attach themselves to the air bubbles during conventional mineral floatation. The term biwettable is usually used for particles that have a tendency to concentrate at the interfaces (usually water-oil interface). The hydrophilic particles are those that are dispersed in water and can be found mainly in the middlings (Sparks et al., 2003).

Darkovich et al. (1989) believe that the biwettablity of the solid surfaces is due to a humic matter coating, as this coating is moderately hydrophobic in character. They showed that the insoluble organic carbon content determines the degree of hydrophobicity. These solids were identified as “ultrafine clays” coated strongly with toluene insoluble organic matter with asphaltene-like characteristics (Kotlyar et al., 1998b). Adegroye et al. (2009) showed that removing the organic matter from the surfaces of the clay minerals reduces their carbon, hydrogen, and nitrogen contents and makes the clay mineral particles hydrophilic. They also showed that the method used for the organic matter removal (hydrogen peroxide

or low temperature ashing in their case) influences the surface properties; e.g., cation exchange capacity of the clay mineral. In addition, they determined that hydrogen peroxide is more effective in removing organic matter than low temperature ashing. The carbon content of the tailings was reduced from 13.11 wt% to 2.09 wt% after low temperature ashing and to 0.39 wt% after hydrogen peroxide. The same trend was observed in the froth as hydrogen peroxide and low temperature ashing reduced the carbon content from 17.01 to 0.52 and 5.01, respectively.

These hydrophobic (and biwettable) solids are the most problematic from the bitumen recovery standpoint as they provide adsorption sites for bitumen during extraction. The finest size fractions of these solids (clay mineral particles) also intensely stabilize the bitumen droplets suspended in water (oil-water emulsions) (Levine & Sanford, 1985; Levine et al., 1989). Kotlyar et al. (1993) showed that these colloidal inorganic solids (clay mineral particles) stabilize a gel-like structure containing up to 90 wt% of the process water. Sparks et al. (2003) presented a model explaining the role of biwettable clay minerals in the stabilization of water droplets in a continuous bitumen phase (Fig. 1.6) (water-in-oil emulsions). They also mentioned that the opposite type of emulsion (oil-in-water emulsions) may happen under the correct conditions. Such aggregates, composed of clay minerals, water, and bitumen, were observed by confocal laser scanning microscopy (CLSM) in the bitumen froth (Fig. 1.7) (Muñoz et al., 2003). Muñoz et al. indicated that clay mineral (inorganic) particles were enriched in the degraded bitumen in all cases.

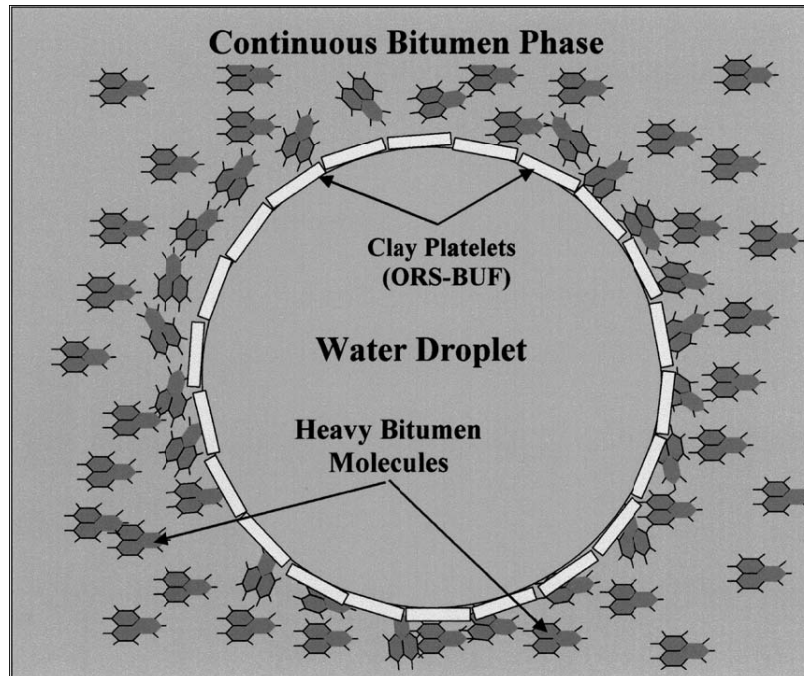


Fig. 1.6. Role of biwetttable clay minerals in stabilizing water droplets in bitumen (water-oil emulsion) (Sparks et al., 2003).

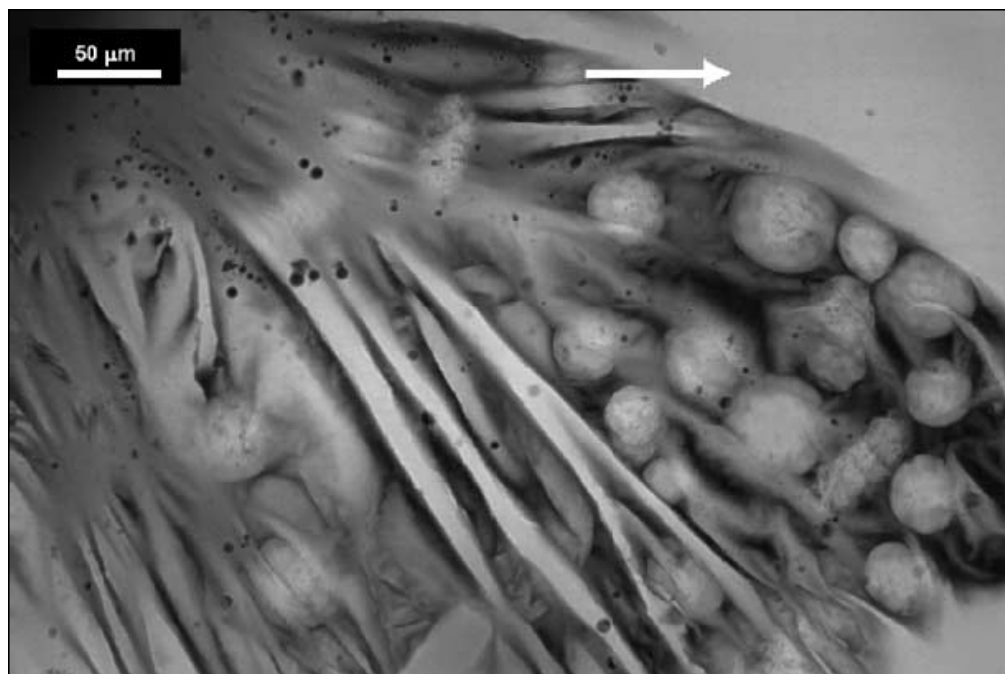


Fig. 1.7. Confocal laser scanning micrograph of the bitumen froth showing aggregates of clay-water-bitumen (spheres) trapped between bitumen sheets (plates). The area of normal bitumen is indicated by the arrow. (Muñoz et al., 2003).

In this model, asphaltene molecules and humic matter (components of bitumen) are preferentially adsorbed on the surface of clay-water clusters and the entire complex is dispersed in the maltene continuous phase of bitumen (Fig. 1.6) in the same way that asphaltene micelles are dispersed in the maltenes. Additional stabilization of this system by the resin component of bitumen forms a colloidal system. Such a colloidal system is extremely difficult to break down.

Kotlyar et al. (1998a) believe that the ultrafine clay minerals are most probably the main contributor to the existence of intractable water (usually accompanied by salt) in the bitumen froth. The remaining salts and clay mineral solids are extremely harmful for the bitumen upgrading process, as the residual salts cause corrosion problems in many downstream locations due to their high chloride content. In addition, organic-rich clay minerals may cause the formation of coke in undesired areas of the upgrading plant (Kotlyar et al., 1998a). Tu et al. (2005) showed that the formation of these organic-rich solids is strongly related to the adsorption of heavy components from bitumen on the clay minerals surfaces. They also showed that these adsorbed components of bitumen (pentane-insoluble in this case) are very strongly bound to the clay minerals surfaces (Tu et al., 2006).

Kaolinite, illite, smectite, and chlorite, the most abundant clay minerals in the oil sands, do not always behave similarly during bitumen extraction (Clementz, 1976). Differences in the behaviour of different clay minerals during bitumen extraction have been reported by researchers, although there is a shortage of such studies. For instance, the presence or absence of expandable smectites, such as montmorillonite, plays an important role in the formation of clay-organic complexes. Czarnecka & Gillott (1980) showed that bitumen and its fractions (maltenes and asphaltenes) were adsorbed on the surfaces of the four common clay minerals in Athabasca oil sands (illite, kaolinite, montmorillonite, and chlorite). The adsorption of these organic molecules on the clay mineral surfaces makes them less hydrophilic. They also showed that the adsorption of the organic

matter on montmorillonite was higher for nitrobenzene than for chloroform, while the situation was reversed for kaolinite, illite, and chlorite. The main reason for this difference is the expandable structure of smectitic clay minerals; e.g., montmorillonite. Exchangeable cations and interlayer water in montmorillonite can be replaced by polar organics. Within the smectite family, the adsorption of the organic matter is extremely dependent on the nature of the exchangeable cation (Czarnecka and Gillott, 1980).

The type of the clay minerals' exchangeable cations (calcium, magnesium, sodium, etc.) and the type of the solvent affect the amount of adsorbed bitumen. Clementz (1976) showed that calcium and magnesium montmorillonite have more interlayer surface available for adsorption of organic matter (e.g., asphaltenes) in a given solvent than sodium and potassium montmorillonite.

Another difference between expandable clay minerals, e.g., montmorillonite and non-swelling clay minerals such as kaolinite and illite, is their sensitivity to the dielectric constant of the organic solvent. The swelling capacity of montmorillonite is affected by the dielectric constant of the organic solvent. This may change the mechanism of bitumen adsorption in solvents with high dielectric constants (e.g., nitrobenzene) than in solvents like chloroform with lower dielectric constant, as bitumen molecules become more ionized in nitrobenzene. Therefore, adsorption happens through an ion-exchange mechanism (Clementz, 1976).

Clementz believes that among the above parameters the type of solvent is the main factor controlling the adsorption of bitumen components on the surface of clay minerals (Clementz, 1976). The influence of the solvent type is more pronounced for montmorillonite than for illite and kaolinite.

Kaolinite surfaces were found to be more inclined to adsorb asphaltene molecules when compared to non-clay minerals such as CaCO_3 , TiO_2 , Fe_3O_4 , FeS_2 , and

SiO₂. Dudášová et al. (2008) showed that not only is the amount of adsorbed asphaltenes higher on kaolinite surfaces, but the affinity for adsorption is also higher on kaolinite surfaces. Their results indicated that the adsorption of asphaltenes on mineral surfaces depends more on the type of mineral than on the nature/origin of asphaltenes.

Lebedeva and Fogden (2011) showed that under certain conditions the wettability of the kaolinite aggregates changes from hydrophilic to oleophilic. They also showed that the asphaltene-like deposits on kaolinite surfaces are primarily nanoparticles. These nanoparticles were about 10 nm in size and capable of forming larger aggregates (Fig. 1.8).

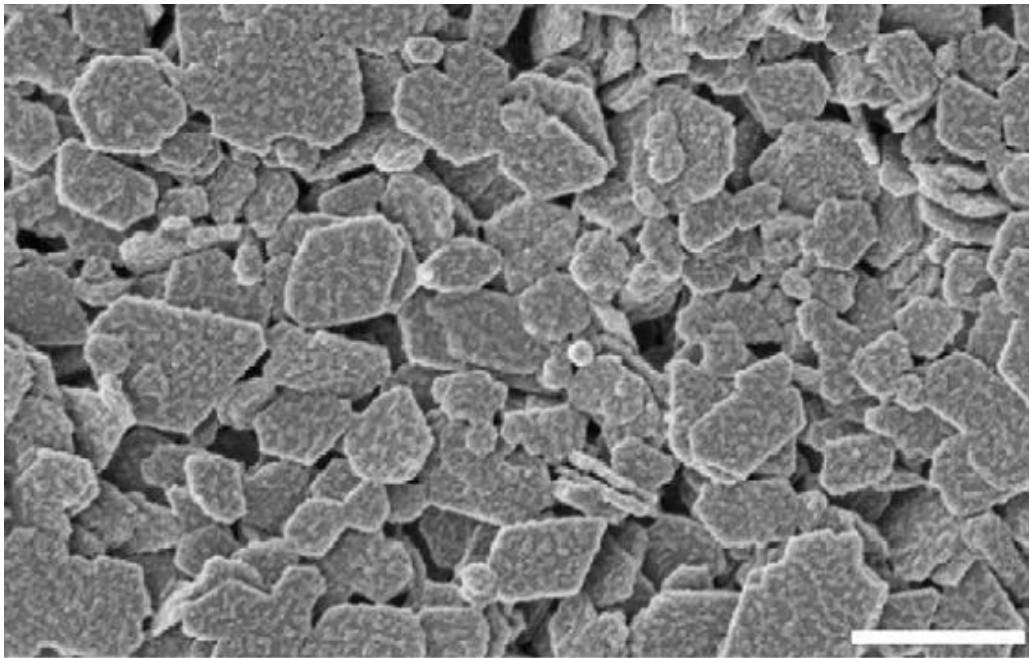


Fig. 1.8. Secondary electron field emission SEM image of kaolinite particles coated with oil deposits (Lebedeva and Fogden, 2011). Scale bar = 500 nm.

Their finding is in agreement with the model previously presented by Sparks et al. (2003) for the adsorption of organic matter on surfaces of clay minerals (not only kaolinite) in oil sands. In their model, the adsorption of organic matter on the

surface of clay minerals is patchy (Fig. 1.9). Sparks et al. indicated that the nature of the adsorbed organic matter is both asphaltic and humic.

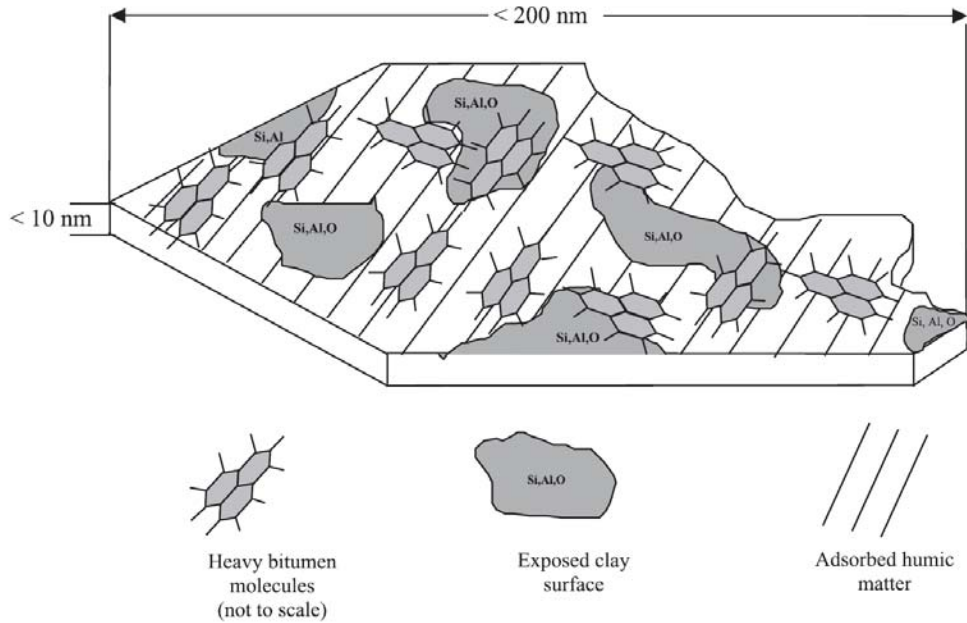


Fig. 1.9. Adsorption of organic matter on the surface of clay minerals (Sparks et al., 2003).

The charge distribution of clay mineral surfaces and the surface charge, as well as the size of the organic molecules, are the key parameters controlling the adsorption of organic molecules on clay mineral surfaces. For an organic molecule to be adsorbed on the surface of a clay mineral, both the attraction between the surface charges and the charge distribution on the clay mineral surface are important. The clay mineral surface must provide enough space for the organic molecule to be adsorbed. The distribution of surface charges on clay mineral surfaces is determined by structural factors such as ionic substitutions (Boyd et al., 2008). Structural factors of clay minerals including ionic substitutions will be discussed comprehensively in Chapter 2. Despite the numerous efforts by a great number of researchers, organic-clays interactions are not yet fully understood. Using advanced characterization techniques, such as

scanning transmission x-ray microscopy (STXM) and near edge x-ray absorption fine structure (NEXAFS) spectroscopy, promises a break through in understanding of organic-clay interactions in the near future (Omotoso et al., 2006; Covelli et al., 2009).

Pernyeszi et al. (1998) showed the hydrophobization of kaolinite and illite surfaces by microcalorimetry. They suggested a complete hydrophobization of kaolinite particles under certain conditions. They also compared the adsorption of asphaltenes on the surface of clay minerals in mixtures of n-heptane and toluene. Their results indicated the great affinity of kaolinite surfaces for asphaltenes. Tu et al. (2006) showed that kaolinite surfaces have a higher propensity for adsorbing similar asphaltene-like organic matter (pentane-insoluble) than illite surfaces.

In n-heptane/toluene mixtures, Pernyeszi et al. (1998) suggested a two-stage adsorption mechanism. They believe that the mono-molecule adsorption of asphaltenes happens in the first step, followed by micellar or aggregated adsorption. It has to be pointed out that the monolayer capacities of adsorbed asphaltenes (n in Table 1-2) reported for bentonite by Pernyeszi et al. seems to be too low to the author of this thesis. They described this extremely low adsorption capacity of bentonite (a form of smectite) in toluene and n-heptane/toluene mixtures by the interlayer spacing of bentonite ($d = 1.5-1.6$ nm). They believe that large asphaltene aggregates are not able to penetrate the interlayer spacing of bentonite. Their explanation is contradictory to many studies on the similar smectite (montmorillonite) discussed previously.

Table 1-2. Adsorption capacities of asphaltenes on different minerals (Pernyeszi et al., 1998).

<u>Adsorbent mineral</u>	<u>Solvent</u>	<u>n (mg/g)</u>
Quartz	Toluene	6.4
Kaolinite	Toluene	33.9
Illite	Toluene	17.1
Bentonite	Toluene	9.4
Kaolinite	10% n-heptane/toluene	66.3
Bentonite	10% n-heptane/toluene	8.7

Kaolinite	30% n-heptane/toluene	16.6
Bentonite	30% n-heptane/toluene	8.6
Bentonite	35% n-heptane/toluene	8.9

n = monolayer capacity of adsorbed asphaltene.

It is not only the type of clay mineral which can affect bitumen extraction by influencing the organic-clay interactions. The degree of crystallinity of kaolinite, for example, is also found to influence its reactions with the organic matter. For instance, Ignasiak et al. (1983) observed that while well-crystallized, ordered kaolinite remained with bitumen during extraction, poorly ordered kaolinite was associated with precipitated asphaltenes. Another example of how minor structural differences in clay minerals influence bitumen extraction is presented by Kaminsky et al. (2009). They showed that not only was kaolinite enriched in the froth and illite-smectite in the middlings and tailings, but also the type of illite-smectite (with respect to the degree of smectite mixed-layering in the illite-smectite structure) detected in the froth was different from that of the other streams.

In summary, the following parameters affect the adsorption of bitumen components on clay mineral surfaces:

- Type of clay minerals (e.g., kaolinite vs. illite vs. expandable clay minerals)
- Structure of clay minerals (e.g., the degree of crystallinity (for kaolinite) and ionic substitution)
- Degree of expandability and exchangeable cations (for expandable clay minerals; e.g., montmorillonite)
- Surface area, CEC, and density and distribution of surface charges of the clay minerals
- The media (aqueous vs. organic solvents)
- Dielectric constant of the media (for organic solvents)

1.5. Importance of clay mineralogy in relation to the bitumen extraction process

As mentioned before, the interactions between clay minerals and bitumen result in clay-organic complexes. It is especially important to determine the types and properties of existing clay minerals in the oil sands to establish any nonaqueous extraction process, because clay-organic complexes are stable enough to resist strong solvents (Clementz, 1976). The settling behaviour of tailings is directly controlled by flocculation/dispersion characteristics of existing clay minerals. Even a small amount of smectite, either discrete or as a mixed-layer, has a great influence on the settling and consolidation of tailings. Mutual interactions between clay mineral characteristics and water chemistry have major influences on the extraction process. None of these interactions can be studied successfully without having sufficient knowledge about the types, microstructures, and properties of existing clays in the oil sands.

Several studies have been done to determine the types of existing clays in oil sands. Kaminsky (2008) has performed an extensive review of previous studies of clay mineralogy in oil sands. Based on such studies, the most abundant clay minerals in the Alberta oil sands are kaolinite and illite. Smectite, chlorite, vermiculite, and mixed-layer clay minerals are also present in the oil sands in smaller quantities. Surprisingly, however, the surface area and cation exchange capacity of oil sands extraction tailings are considerably higher than the expected values for kaolinite and illite. Omotoso & Mikula (2004) showed that this is due to smectite mixed layering in kaolinite and illite. However, such arguments remain highly debatable in the oil sands industry. The structure of interstratified clay minerals is not fully understood and more studies are required to characterize the structure and properties of existing mixed-layer clay minerals in the oil sands. A better understanding of interstratified clay minerals may finally lead to technological processes with improved settling behaviour of tailings as well as greater conservation of water in the bitumen extraction process. Detailed studies

of clay mineralogy will result in a better understanding of the types, structures, and properties of existing clay minerals in oil sands, ultimately leading to improved bitumen extraction processes with no or reduced water consumption or perhaps an alternative process such as mild heating.

1.6. Objectives of the research

As mentioned, it has been demonstrated by many researchers that the adsorption of organic matter (e.g., bitumen components, such as asphaltenes) on the clay mineral surfaces has a huge influence on the bitumen extraction process and also dramatically changes the physical and chemical properties of the clay minerals. Therefore, one has to be very careful when using the general knowledge about the characteristics of the clay minerals present in the oil sands (kaolinite, illite, smectite, and chlorite). In addition, for this reason, characterizing the clay minerals in a natural system (during actual bitumen extraction) is of great importance. The interactions between the organic matter and clay minerals also make characterization of clay minerals in the oil sands very challenging (Covelli et al., 2009). To the author's knowledge, there is only one study that characterized the clay minerals from the very beginning to the end of water-based bitumen extraction (Kaminsky, 2008) and none for nonaqueous bitumen extraction. The motivation for the present research was to characterize the clay minerals during an actual nonaqueous bitumen extraction process.

In the commercial water-based bitumen extraction, problems such as low bitumen liberation and flotation caused by clay-organic interactions have been overcome by the addition of caustic and by increasing the extraction temperature (Mikula et al., 2003). The addition of caustic elevates the pH which releases natural surfactants (Schramm et al., 1985; Smith & Schramm, 1992) thereby reducing the oil-water surface tension and clay mineral hydrophobicity. As a result, clay minerals are dispersed into a slow-settling tailings stream. The containment of

such tailings is expensive and also problematic from an environmental perspective. Preventing the dispersion of clay minerals in the tailings stream is one of the motivations for alternative bitumen extraction processes, such as the nonaqueous extraction process presented in the current research.

In the present study, a systematic characterization procedure using XRD, SEM, and TEM as the main methods was first established to study the clay minerals during a simulated water-based batch extraction of bitumen from the oil sands. Afterwards, the same methodology was applied to characterize the clay minerals during nonaqueous bitumen extraction. In order to do so, a lab-scale nonaqueous bitumen extraction procedure was established. Some critical parameters, such as bitumen recovery, product quality and extraction time, were studied/modified in order to validate the established nonaqueous extraction process. It has to be pointed out that the main goal for the nonaqueous extraction method was not to establish a commercial nonaqueous bitumen extraction process, but to separate the clay minerals from the oil sands in a way similar to the way they will be separated in future commercial nonaqueous bitumen extraction. Characterization of the clay minerals during both water-based and nonaqueous bitumen extraction processes revealed some similarities and also differences in the way they behave in the presence or absence of added water during bitumen extraction.

1.7. References

Adegoroye, A., Uhlik, P., Omotoso, O., Xu, Z., & Masliyah, J. (2009). A comprehensive analysis of organic matter removal from clay-sized minerals extracted from oil sands using low temperature ashing and hydrogen peroxide. *Energy and Fuels*, 23, 7, 3716-20.

Adegoroye, A., Wang, L., Omotoso, O., Xu, Z., & Masliyah, J. (2010). Characterization of organic-coated solids isolated from different oil sands. *Canadian Journal of Chemical Engineering*, 88, 3, 462-70.

Adeyinka, O. B., Samiei, S., Xu, Z., & Masliyah, J. H. (2009). Effect of particle size on the rheology of Athabasca clay suspensions. *The Canadian Journal of Chemical Engineering*, 87, 3, 422-34.

Alberta Energy Resources Conservation Board. (2010). News Release – ERCB Approves Fort Hills and Syncrude tailings pond plans with conditions. www.ercb.ca/portal/server.pt/gateway/PTARGS_6_0_308_0_0_43/http%3B/ercbContent/publishedcontent/publish/ercb_home/news/news_releases/2010/nr2010_05.aspx (accessed April 21, 2011).

Alberta Energy (2011). Oil sands. Alberta Government, www.energy.gov.ab.ca/OurBusiness/oilsands.asp (accessed April 21, 2011).

Bensebaa, F., Kotlyar, L., Pleizier, G., Sparks, B., Deslandes, Y., & Chung, K. (2000). Surface chemistry of end cuts from Athabasca bitumen. *Surface and Interface Analysis*, 30, 1, 207-11.

Bichard, J.A. (1987). Oil sands composition and behaviour research: The research papers of John A. Bichard 1957-65. *Alberta Oil Sands Technology and Research Authority (AOSTRA)*, Edmonton, Canada.

Boyd, S.A., Johnston, C.T., Laird, D.A., Teppen, B.J., & Li, H. (2008). A comprehensive analysis of organic contaminant adsorption by clays. 1st CONRAD Clay Workshop, May 2008, Calgary, Alberta, Canada.

Camp, F. W. (1976). The tar sands of Alberta, 3rd ed., Cameron Engineers Inc., Colorado, USA.

Chalaturnyk, R. J., Scott, J. D., & Ozum, B. (2002). Management of oil sands tailings. *Petroleum Science and Technology*, 20, 1025–46.

Clementz, D. M. (1976). Interaction of petroleum heavy ends with montmorillonite. *Clays and Clay Minerals*, 24, 6, 312-19.

Covelli, D., Hernández-Cruz, D., Haines, B. M., Munoz, V., Omotoso, O., Mikula, R., et al. (2009). NEXAFS microscopy studies of the association of hydrocarbon thin films with fine clay particles. *Journal of Electron Spectroscopy and Related Phenomena*, 173, 1, 1-6.

Czarnecka, E., & Gillott, J. E. (1980). Formation and characterization of clay complexes with bitumen from Athabasca oil sand. *Clays and Clay Minerals*, 28, 3, 197-203.

Dang-Vu, T., Jha, R., Wu, S., Tannant, D. D., Masliyah, J., & Xu, Z. (2009). Effect of solid wettability on processability of oil sands ores. *Energy & Fuels*, 23, 5, 2628-36.

Darcovich, K., Kotlyar, L. S., Tse, W. C., Ripmeester, J. A., Capes, C. E., & Sparks, B. D. (1989). Wettability study of organic-rich solids separated from Athabasca oil sands. *Energy & Fuels*, 3, 3, 386-91.

Dongbao, F., Woods, J. R., Kung, J., Kingston, D. M., Kotlyar, L. S., Sparks, B. D., et al. (2010). Residual organic matter associated with toluene-extracted oil sands solids and its potential role in bitumen recovery via adsorption onto clay minerals. *Energy & Fuels*, 24, 4, 2249-56.

Dudášová, D., Simon, S., Hemmingsen, P. V., & Sjöblom, J. (2008). Study of asphaltenes adsorption onto different minerals and clays: Part 1. experimental adsorption with UV depletion detection. *Colloids and Surfaces A: Physicochemical and Engineering Aspects*, 317, 1-3, 1-9.

Grant, J., Dyer, S. & Woynillowicz, D. (2008). Fact or fiction: Oil sands reclamation. The Pembina Institute.
http://pubs.pembina.org/reports/Fact_or_Fiction-report.pdf (accessed August 11, 2011).

Ignasiak, T. M., Kotlyar, L., Longstaffe, F. J., Strausz, O. P., & Montgomery, D. S. (1983). Separation and characterization of clay from Athabasca asphaltene. *Fuel*, 62, 3, 353-62.

Kaminsky, H.A.W., (2008). Characterization of an Athabasca oil sands ore and process streams. Ph.D.Thesis, Department of Chemical and Materials Engineering, University of Alberta, Canada.

Kaminsky, H. A. W., Etsell, T. H., Ivey, D. G., & Omotoso, O. (2009). Distribution of clay minerals in the process streams produced by the extraction of bitumen from Athabasca oil sands. *The Canadian Journal of Chemical Engineering*, 87, 1, 85-93.

- Kasongo, T., Zhou, Z., Xu, Z. & Masliyah J.H. (2000). Effect of clays and calcium ions on bitumen extraction from Athabasca oil sands using flotation. *The Canadian Journal of Chemical Engineering*, 78, 674-81.
- Kasperski, K. L. (1992). A review of properties and treatment of oil sands tailings. *AOSTRA Journal of Research*, 8, 1, 11-53.
- Kasperski, K. L. (2001). Review of research on aqueous extraction of bitumen from mined oil sands. [Division No. CWRC 01-17 (CF)]. Natural Resources Canada, CANMET-WRC.
- Kotlyar, L. S., Ripmeester, J. A., Sparks, B. D., & Montgomery, D. S. (1988). Characterization of organic-rich solids fractions isolated from Athabasca oil sand using a cold water agitation test. *Fuel*, 67, 2, 221-26.
- Kotlyar, L. S., Capes, C. E., Sparks, B. D., Sparks, B. D., Sparks, B. D., Sparks, B. D., et al. (1992). Gel-forming attributes of colloidal solids from fine tails formed during extraction of bitumen from Athabasca oil sands by the hot water process. *AOSTRA Journal of Research*, 8, 55-61.
- Kotlyar, L. S., Deslandes, Y., Sparks, B. D., Kodama, H., & Schutte, R. (1993). Characterization of colloidal solids from Athabasca fine tails. *Clays and Clay Minerals*, 41, 3, 341-45.
- Kotlyar, L. S., Sparks, B. D., & Schutte, R. (1996). Effects of salt on the flocculation behaviour of nano particles in oil sands fine tailings. *Clays and Clay Minerals*, 44, 1, 121-131.
- Kotlyar, L. S., Sparks, B. D., LePage, Y., & Woods, J. R. (1998a). Effect of particle size on the flocculation behaviour of ultra-fine clays in salt solutions. *Clay Minerals*, 33, 1, 103-107.
- Kotlyar, L. S., Sparks, B. D., Woods, J. R., Raymond, S., Le Page, Y., & Shelfantook, W. (1998b). Distribution and types of solids associated with bitumen. *Petroleum Science and Technology*, 16, 1-2, 1-19.
- Lebedeva, E. V., & Fogden, A. (2011). Wettability alteration of kaolinite exposed to crude oil in salt solutions. *Colloids and Surfaces A: Physicochemical and Engineering Aspects*, 377, 1-3, 115-22.
- Levine, S., & Sanford, E. (1985). Stabilisation of emulsion droplets by fine powders. *Canadian Journal of Chemical Engineering*, 63, 2, 258-68.
- Levine, S., Bowen, B. D., & Partridge, S. J. (1989). Stabilization of emulsions by fine particles I. partitioning of particles between continuous phase and oil/water interface. *Colloids and Surfaces*, 38, 2, 325-43.

Liu, J., Xu, Z., & Masliyah, J. (2004). Role of fine clays in bitumen extraction from oil sands. *American Institute of Chemical Engineers (AIChE) Journal*, 50, 8, 1917-27.

Masliyah, J., Zhou, Z., Xu, Z., Czarnecki, J., & Hamza, H. (2004). Understanding water-based bitumen extraction from athabasca oil sands. *Canadian Journal of Chemical Engineering*, 82, 4, 628-54.

MacKinnon, M.D. (1989). Development of the tailings pond at Syncrude's oil sands plant: 1978–1987. *AOSTRA Journal of Research*, 5, 2, 109–33.

Mercier, P. H. J., Patarachao, B., Kung, J., Kingston, D. M., Woods, J. R., Sparks, B. D., et al. (2008). X-ray diffraction (XRD)-derived processability markers for oil sands based on clay mineralogy and crystallite thickness distributions. *Energy & Fuels*, 22, 5, 3174-93.

Mikula, R. J., Munoz, V. A., Wang, N., Bjornson, B., Cox, D., Moisan, B., et al. (2003). Characterization of bitumen properties using microscopy and near infrared spectroscopy: Processability of oxidized or degraded ores. *Journal of Canadian Petroleum Technology*, 42, 8, 50-54.

Muñoz, V. A., Kasperski, K. L., Omotoso, O. E., & Mikula, R. J. (2003). The use of microscopic bitumen froth morphology for the identification of problem oil sand ores. *Petroleum Science & Technology*, 21, 9, 1509-29.

Omotoso, O. E., & Mikula, R. J. (2004). High surface areas caused by smectitic interstratification of kaolinite and illite in Athabasca oil sands. *Applied Clay Science*, 25, 1-2, 37-47.

Omotoso, O. E., Mikula, R. J., Urquhart, S., Sulimma, H., & Stephens, P. W. (2006). Characterization of clays from poorly processing oil sands using synchrotron techniques. *Clay Science*, 12, 2, 88-93.

Pernyeszi, T., Patzkó, Á., Berkesi, O., & Dékány, I. (1998). Asphaltene adsorption on clays and crude oil reservoir rocks. *Colloids and Surfaces A: Physicochemical and Engineering Aspects*, 137, 1-3, 373-84.

Ripmeester, J. A., Kotlyar, L. S., & Sparks, B. D. (1993). ²H NMR and the sol—gel transition in suspensions of colloidal clays. *Colloids and Surfaces A: Physicochemical and Engineering Aspects*, 78, 57-63.

Schramm, L. L., & Smith, R. G. (1985). The influence of natural surfactants on interfacial charges in the hot-water process for recovering bitumen from the Athabasca oil sands. *Colloids and Surfaces*, 14, 1, 67-85.

Smith, R. G., & Schramm, L. L. (1992). The influence of mineral components on the generation of natural surfactants from Athabasca oil sands in the alkaline hot water process. *Fuel Processing Technology*, 30, 1, 1-14.

Sparks, B. D., Kotlyar, L. S., O'Carroll, J. B., & Chung, K. H. (2003). Athabasca oil sands: Effect of organic coated solids on bitumen recovery and quality. *Journal of Petroleum Science and Engineering*, 39, 3-4, 417-30.

Sustainable Development Business Case Report (2006). "Clean Conventional Fuel - Oil and Gas", version 1, November.

<http://www.sdtc.ca/uploads/documents/en/CleanConventionalFuel-OilandGas.pdf> (accessed August 9, 2011).

Thomas, T., Afacan, A., Masliyah, J., Xu., Z., Wang, Y. & Liu, J. (2010). Recovery of Hydrocarbons from Mature. Fine Tailings of Oil Sands Extraction. Proceedings of the 2nd International Oil Sands Tailings Conference, December 2010, Edmonton, Alberta, Canada, 141-8.

Tu, Y., O'Carroll, J. B., Kotlyar, L. S., Sparks, B. D., Ng, S., Chung, K. H., et al. (2005). Recovery of bitumen from oil sands: Gelation of ultra-fine clay in the primary separation vessel. *Fuel*, 84, 6, 653-60.

Tu, Y., Kingston, D., Kung, J., Kotlyar, L. S., Sparks, B. D., & Chung, K. H. (2006). Adsorption of pentane insoluble organic matter from oilsands bitumen onto clay surfaces. *Petroleum Science & Technology*, 24, 3, 327-38.

Water Use in Alberta Oil Sands. (2007). PTAC – May 29, Water Innovation in the Oil Patch Forum.

<http://www.ptac.org/env/dl/envf0702p05.pdf> (accessed August 11, 2011).

Chapter 2

Background

2.1. Clay minerals: Microstructures and properties

While clays are referred to as particles smaller than 2 μm equivalent spherical diameter (the diameter of a spherical particle with the same settling behavior), clay minerals are classified as layered silicates (phyllosilicates). Layer silicates are constructed from at least two sheets - tetrahedral and octahedral. A tetrahedral sheet is composed of corner-linked SiO_4 tetrahedra (Fig. 2.1) (Bennett & Hulbert, 1986). The O-O and Si-O bonds have bond distances of about 0.264 nm and 0.162 nm in each tetrahedron, respectively. Although Si^{4+} is the dominant cation, it can be substituted with other cations such as Al^{3+} and Fe^{3+} . An octahedral sheet is composed of octahedra connected by their external boundaries. It consists of two planes of closely packed oxygen and hydroxyl ions, encompassing cations occupying octahedral spaces between the two planes. These octahedral spaces are typically occupied by Al^{3+} , Mg^{2+} , Fe^{2+} and Fe^{3+} , although other transition elements have also reportedly filled these sites (Fig. 2.2) (Grim, 1962).

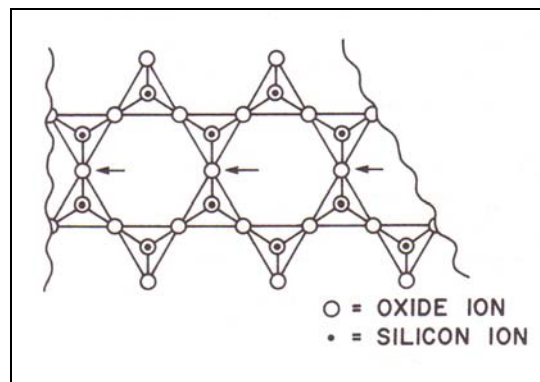


Fig. 2.1. A tetrahedral sheet made by corner linked SiO_4 (Bennett & Hulbert, 1986).

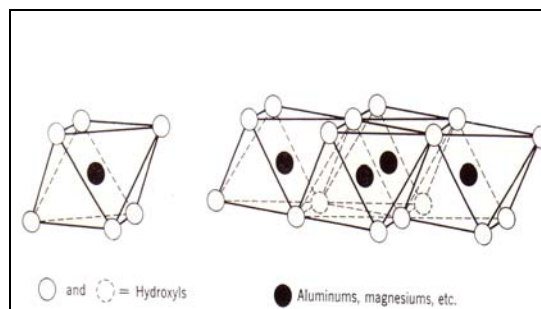


Fig. 2.2. An octahedral sheet made by edge to edge linked octahedra (Grim, 1962).

Depending on the cation to anion ratio, an octahedral sheet may be classified as either trioctahedral or dioctahedral. However, in reference to brucite, $\text{Mg}(\text{OH})_2$, and gibbsite, $\text{Al}(\text{OH})_3$, which possess the simplest examples of the microstructures of the two families of clay minerals, trioctahedral or dioctahedral sheets are commonly referred to as brucite-like or gibbsite-like, respectively. Brucite-like sheets possess a cation-to-anion ratio of 1:2. Considering a close-packed oxygen or hydroxyl ion plane, each anion has three crystallographic equivalent octahedral sites surrounding it (Fig. 2.3). All three surrounding sites are occupied with divalent cations; hence, the term trioctahedral. Alternatively, gibbsite-like sheets possess a cation-to-anion ratio of 1:3. Therefore, only two of three octahedral sites can be occupied by trivalent cations to establish electrical neutrality (Moore & Reynolds, 1997).

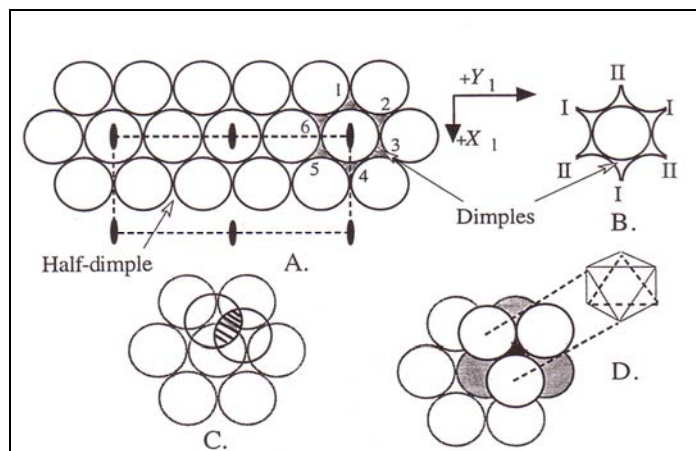


Fig. 2.3. Coordination in a close-packed plane of atoms; each atom possessing two sets of sites, I and II, around it where one set will be octahedral and the other tetrahedral (Moore & Reynolds, 1997). A: Octahedral sheet. B: Octahedral sites (I and II). C: It is not possible that both type I and II octahedral sites are occupied by anions (oxygen atoms or hydroxyl groups) because the shaded volume would have to be occupied by both of them. D: Octahedral sites surrounded by six anions.

2.1.1. Joining of the sheets

Octahedral and tetrahedral sheets can be combined easily due to their special structures. Because the oxygen-to-oxygen and OH^- -to- OH^- ionic dimensions are very similar, $2/3$ of the hydroxyl ions in the octahedral sheet can be replaced by the apical oxygens in the tetrahedral sheet, forming a 1:1 layer silicate. The remaining hydroxyl ions occupy the empty spaces among the apical oxygens of the tetrahedral sheet (the centers of the hexagonal rings, as in Figs. 2.4 & 2.5).

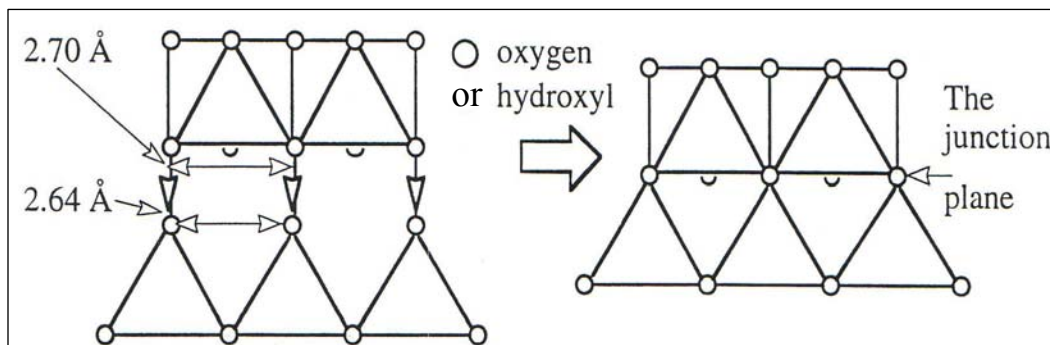


Fig. 2.4. Joining octahedral and tetrahedral sheets together to form a 1:1 layer silicate (Moore & Reynolds, 1997).

2.1.2. 1:1 Layer clay minerals

Most 1:1 layer clay minerals possess either a minute layer charge, or no layer charge at all. This minute layer charge is because the cation sites in tetrahedral sheets are usually all filled by Si^{4+} . As well, the octahedral sites are occupied by either Al^{3+} or Mg^{2+} . Additional charges in one sheet are neutralized by substitutions in the other sheet. Kaolinite ($\text{Al}_2\text{Si}_2\text{O}_5(\text{OH})_4$) has no layer charge ($Z=0$). Accordingly, completely crystallized kaolinite is the most effective representative of a 1:1 layer clay family. The kaolinite 1:1 layer structure, in which one octahedral sheet is joined to a tetrahedral one, is illustrated in Fig. 2.5. These two sheets possess very similar dimensions in their a and b axes (crystallographic axes), allowing octahedral-tetrahedral formation to occur with ease. The resulting 1:1 layer has an approximate thickness of 0.7 nm. All kaolin minerals include a 1:1 layer in their structures. However, the way in which these layers are stacked is different for varying members of the kaolin family. Differences also arise in the position of Al ions in octahedral sites.

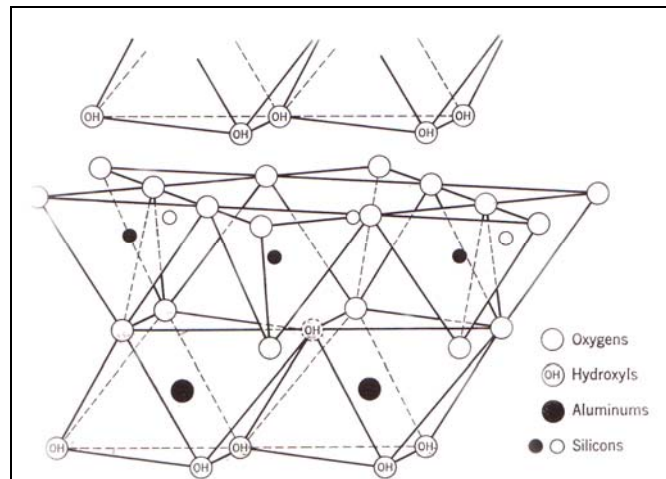


Fig. 2.5. Structure of kaolinite as an example of a 1:1 layer clay mineral (Grim, 1962).

In a 1:1 structure, hydrogen bonds hold the unit layers together tightly, but the plane between the unit layers is a cleavage plane. Because of its strong hydrogen bonding, kaolinite displays less pronounced cleavage than most clay minerals. As well, these hydrogen bonds do not permit the dispersion of small kaolinite particles in water (Grim, 1962). In reality, the joining of the sheets is not as depicted in Fig. 2.4 and 2.5. The two sheets possess different lateral dimensions, resulting in distortions or adjustments in one or both sheets. An ideal tetrahedral sheet with no substitution is about 6% larger than a dioctahedral sheet, but about 3% smaller than a trioctahedral sheet (Moore & Reynolds, 1997).

2.1.3. 2:1 Layer clay minerals

Fig. 2.6 shows the process of joining two tetrahedral sheets to one octahedral sheet. All the hydroxyl ions have been replaced by apical oxygens, except for the two indicated by the large black balls. Displacement of the sheets can be seen more clearly by focusing on the two remaining hydroxyl ions. As depicted in Fig. 2.6, these hydroxyl ions are not exactly on the top of each other. The displacement alters the symmetry from trigonal to monoclinic. For 2:1 layer clay minerals and micas, the ideal displacement is $a/3$. The two most important factors affecting the structure symmetry are the type of octahedral site occupation in the dioctahedral sheet, and the displacement of the layers. To comprehend the first factor, it is necessary to understand the three octahedral sites in the octahedral sheet. The three octahedral sites do not have equivalent symmetry as layer displacement occurs.

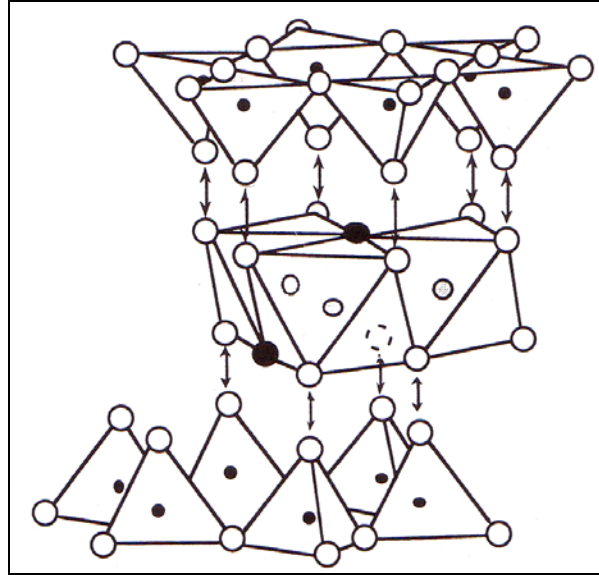


Fig. 2.6. Formation of a 2:1 layer silicate by joining two tetrahedral sheets to one octahedral sheet
 ○ = oxygen, ● = hydroxyl, • = cations in tetrahedral sites, ⊙ = cations in octahedral sites
 (Moore & Reynolds, 1997).

Fig. 2.7 depicts octahedral sites, the A sites, located on the mirror plane. The equivalent octahedral sites, B and C, are located on opposite sites of the plane. A, B and C sites differ only because of interlayer shift.

Some texts refer to these octahedral sites as M(1) and M(2). In dioctahedral clay minerals, the symmetry is different depending on which octahedral site is empty. For example, if sites B and C are occupied by Al^{3+} ions (as depicted in Fig. 2.7), the symmetry will be maintained. However, if the above condition is not met, the mirror plane will no longer exist. If the vacant site is located on the mirror plane, the A site, the configuration is described as trans-vacant, meaning the mirror transverses the vacant site. Dioctahedral clay minerals possessing an occupied site on the mirror plane are classified as cis-vacant (Bailey, 1963).

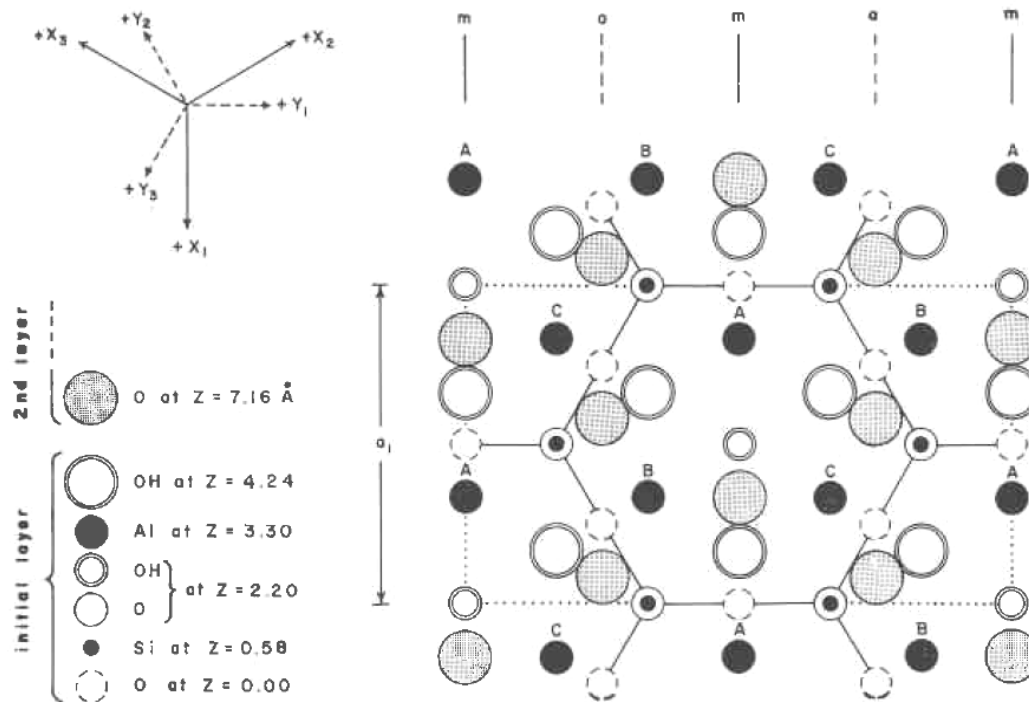


Fig. 2.7. An undistorted 0.7 nm layer of space group Cm showing all three octahedral sites and relative displacement of octahedral and tetrahedral sheets (Bailey, 1963).

Another way to understand these configurations is to visualize the disposition of hydroxyl ions in the octahedral sheet with respect to the vacant site. As depicted in Fig. 2.8, the configuration is cis-vacant if hydroxyl groups are located in the same site with respect to the vacant site. The configuration is trans-vacant if the two hydroxyl groups are located at opposite sides of the vacant site. Fig. 2.8 reiterates that trans-vacant configuration has a centre of symmetry but cis-vacant does not (Sainz-Diaz et al., 2001).

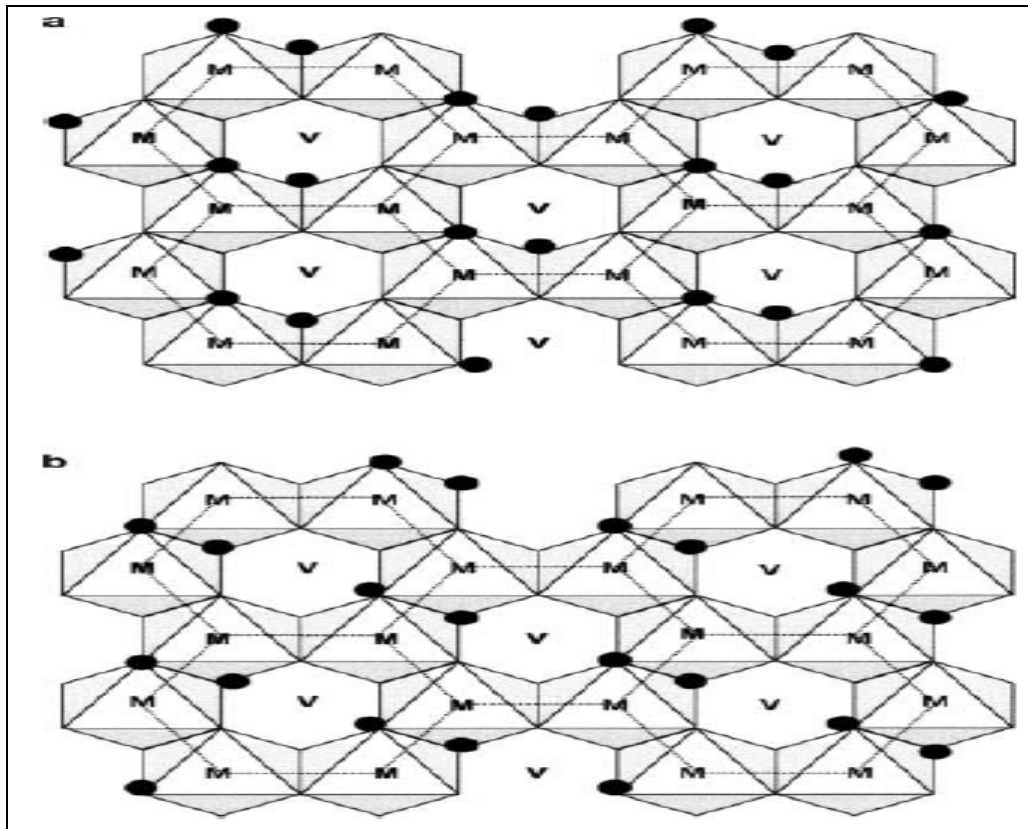


Fig. 2.8. a) Cis-vacant and b) trans-vacant configurations in octahedral sheets in dioctahedral clay minerals (Sainz-Diaz et al., 2001).

2.1.4. Polytypes and layer stacking

Many different clay minerals can be formed from 1:1 or 2:1 layers depending on the layer configuration along the z-axis or (001) direction. The terms “translation” and “rotation” are generally used to describe this configuration. The term “translation” describes the interlayer shift in kaolinite, while rotation of layers happens in dickite. Rotations and/or translations that occur unsystematically can cause disorder. Furthermore, systematic displacements result in polytypes. The term “systematic” refers to the distributions that occur according to a pattern with respect to the symmetry of the layers.

2.1.5. Turbostratic disorder

Turbostratic disorder is the most extreme type of stacking disorder. Occurring when layers are displaced and/or rotated by any amount with respect to each other, turbostratic disorder may take place if there is no keying effect between layers. The layer positions and orientations also must be arbitrary with respect to each other. For instance, turbostratic disorder occurrence in kaolinite is not possible because of the strong hydrogen bonding between oxygen in tetrahedral layers and hydroxyl ions in the upper octahedral layers. However, turbostratic disorder is found in smectites because the interlayer spaces are large and mutual attraction forces between layers are weak. It can be inferred that minerals with turbostratic disorder are constructed by two-dimensional crystallites because they do not possess any regular pattern along the *z*-axis. This type of structure produces a two-dimensional diffraction pattern.

2.1.6. Mixed-layer clay minerals

A mixed-layer clay mineral is not a simple physical mixture of two or more clay minerals. It is produced by the stacking order of silicate layers along the *z*-axis, known as layer interstratifications. Stacking order may be either regular or irregular. Regular stacking produces a clay mineral with characteristics unlike those of the original layers. For instance, rectorite can be considered to be made of illite and smectite layers in a regular stacking order. Irregular, or random, stacking order produces interstratified clay minerals with random mixed layering, which do not possess unique properties.

Therefore, unique naming is not used and irregularly stacked clay minerals have compound names such as illite-smectite, kaolinite-smectite or chlorite-vermiculite (Grim, 1962). Regardless of stacking order, the typical thickness for a single layer of interstratified clay mineral is three or four silicate layers. At present, most studies on mixed-layer clay minerals have focused on illite-smectite

interstratification, as it is the most common variety. To explain the nature of interlaying, several models have been developed, including the classic (non-polar) and polar models. The classic interpretation assumes the mixed layers to be identical to the end member species. Therefore, each layer is either smectite or illite in this model. In the polar model, on the other hand, some layers are neither smectite nor illite as illustrated in Fig. 2.9. The polar model assumes that layers are formed by two different tetrahedral sheets. Fig. 2.9 shows the crystal structure of illite-smectite based on the mentioned models (Dudek et al., 2006; Altaner & Ylagan, 1997).

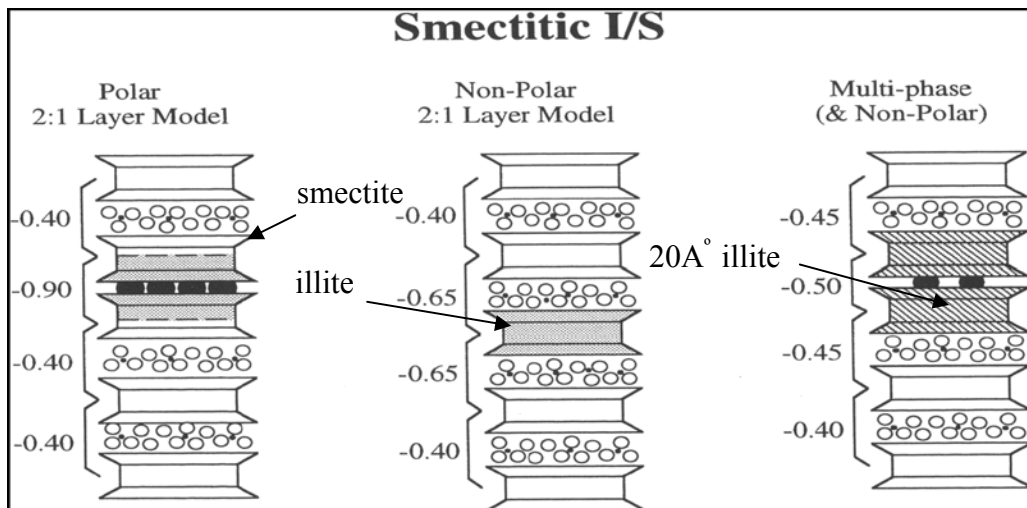


Fig. 2.9. Crystal structure of smectitic I/S. Large dark circles are fixed K, open circles are water molecules and small dark circles are exchangeable cations (Altaner & Ylagan, 1997).

2.1.7. Swelling

While virtually all clay minerals swell in water, the degree of swelling varies with the structure of the clay minerals. Weaker bonds in interlayer spaces result in more swelling (e.g., smectite should swell more than illite or kaolinite). Table 2-1 shows the percentage of relative swelling in typical clay minerals. Swelling is low in well-ordered clay minerals (illite and kaolinite) but greater in poorly ordered

clays (montmorillonite). Exchangeable cations, particle size distribution, and water chemistry also influence clay-swelling characteristics.

Table 2-1. Free-swelling data for clay minerals (Grim, 1962).

<u>Clay mineral</u>	<u>Na-</u> <u>montmorillonite</u>	<u>Ca-montmorillonite</u>	<u>illite</u>	<u>kaolinite</u>
Swelling %	1400-2000	45-145	15-120	5-60

2.1.8. Surface area

It is important to consider surface area because it influences surface phenomena. Swelling clay minerals have a much higher specific surface area (SSA) making them more surface active. Nitrogen gas adsorption at 77 K is the most common technique to determine the SSA of non-swelling clay minerals (Bergaya et al., 2006). For hydratable (swelling) clay minerals, however, the ethylene glycol monoethyl ether (EGME) method is the accepted method for measuring the SSA (Quirk & Murray, 1999).

2.1.9. Charge distribution and cation exchange capacity (CEC)

As described above, clay minerals usually have charges on their surfaces because of several ion substitutions in their silicate layers. This layer charge controls how the basal planes of a clay mineral interact with the surrounding environment. Clay minerals maintain electrical neutrality by absorbing ions on their surfaces. Ion distribution on interlayer surfaces depends on the layer charge distribution, which is determined by structural factors. Some factors include isomorphous substitutions in both tetrahedral and octahedral sheets, rotations of layers relative to each other, and layer stacking disorders.

Ions typically are absorbed in the interlayer spaces and can be exchanged with other ions, which may dramatically influence clay properties. The most common exchangeable cations in clay minerals are Ca^{2+} , Mg^{2+} , H^+ , K^+ , NH_4^+ and Na^+ . In addition to the isomorphous substitutions, cations also can be absorbed via broken bonds along edges and hydrogen replacement in exposed hydroxyls by other cations. Broken bonds are the main cause of cation exchange capacity in kaolinite and provide a significant portion of the cation exchange capacity in illite and chlorite. In contrast, isomorphous substitutions play the major role in smectites. Table 2-2 shows the range of cation exchange capacity for some important clay minerals. It can be seen that montmorillonite and vermiculite have considerably higher capacities than illite or kaolinite (Grim, 1962; Moore & Reynolds, 1997).

Table 2-2. Cation exchange capacity of some clay minerals (Grim, 1962).

Clay mineral	kaolinite	Illite	montmorillonite	vermiculite	chlorite
CEC(meq/100gr)	3-15	10-40	80-150	100-150	10-40

2.2. Basics of characterization techniques

2.2.1. Electron diffraction

An incident beam will be scattered by atoms in all directions. Diffracted beams can be detected only in specific directions in which they reinforce one another. Based on Bragg's law, the rays scattered by atoms in all planes are in phase if the path difference between them is a whole number multiple of the wavelength, $n\lambda$. Fig. 2.10 shows the Bragg condition that leads to the Bragg equation:

$$n\lambda = 2d\sin\theta \quad (2-1)$$

where d is the basal spacing for reflecting planes, λ is the electron wavelength, and θ is the Bragg angle (Cullity, 1978).

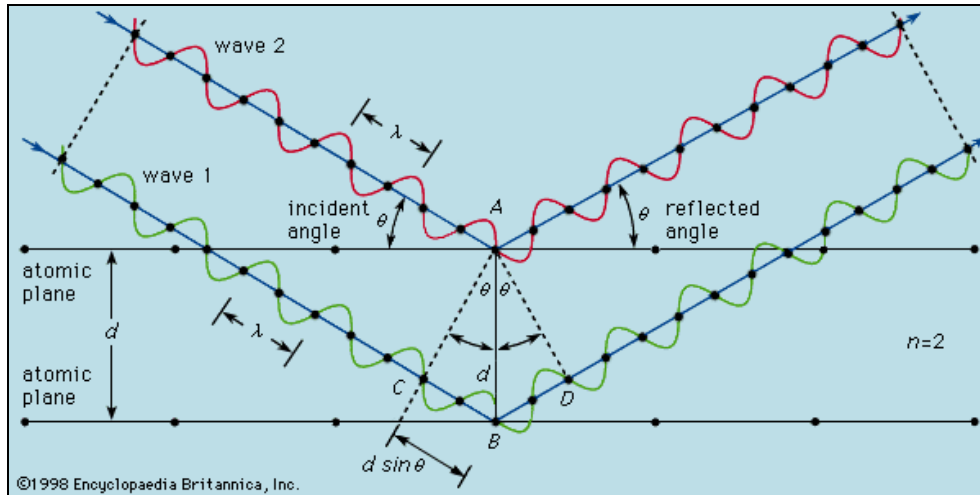


Fig. 2.10. Bragg diffraction (Cullity, 1978).

2.2.2. TEM analysis

In this study, two types of samples are prepared for TEM investigations. The first type is made by placing a droplet of a dilute suspension of clay minerals in distilled water, on a carbon-coated copper grid. Because of their plate-like shape, clay mineral particles are positioned on the grid with their basal planes nearly parallel to the grid surface.

The other type of TEM sample is prepared by cutting ultrathin sections of embedded clay minerals in a resin. Two key points should be considered in this procedure. First, the ultrathin section plate should be normal to the bedding, usually an extra pure resin, to have the basal planes parallel to the beam. Second, to preserve the original relations within individual grains, the sample should be

cut perpendicular to the basal plane; otherwise cutting introduces artefacts to the lattice fringes.

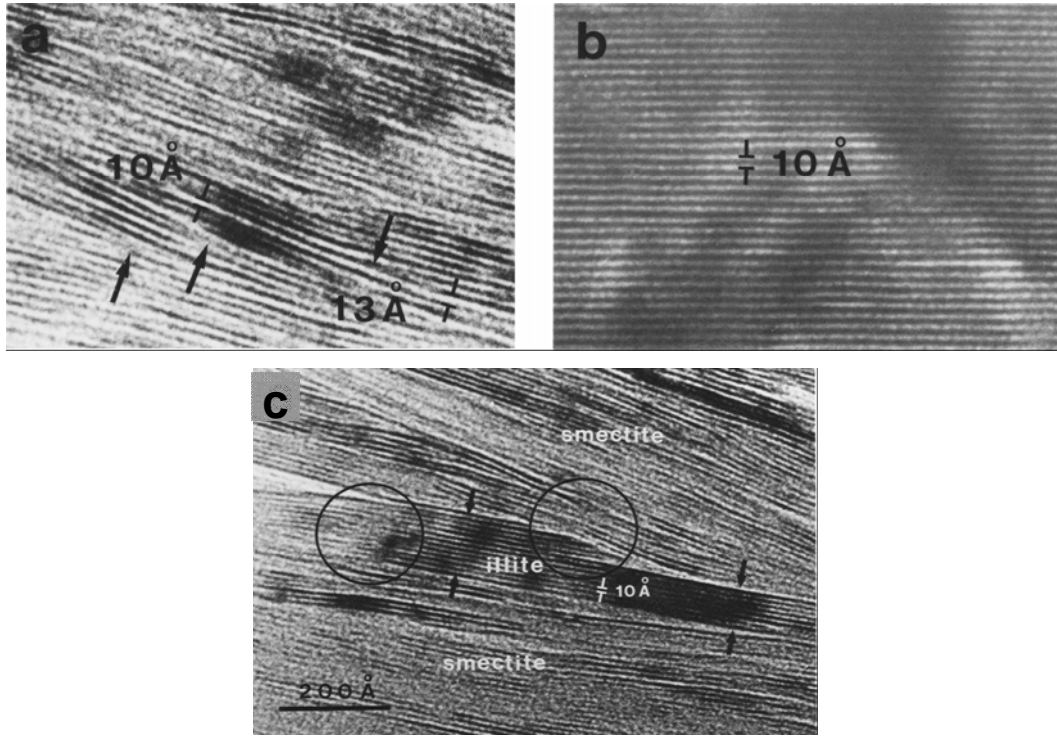


Fig. 2.11. TEM images showing lattice fringes for a) smectite, b) illite, and c) illite-smectite (Ahn & Peacor, 1986).

Sample preparation by the second technique can be time consuming, but provides the opportunity to look at the clay minerals in directions parallel to their basal planes, which allows the particle thickness and interlayer spacing to be measured. By measuring the thicknesses of multiple particles, useful information can be obtained about clay mineralogy; e.g., smectite has fewer layers per crystal compared with illite and kaolinite. Fig. 2.11 shows typical lattice fringe images taken from thin section samples. Smectite, illite, and mixed-layer illite-smectite can be distinguished from one another by this method (Ahn & Peacor, 1986).

2.2.3. X-ray diffraction (XRD)

The principles of x-ray diffraction are similar to electron diffraction, which is explained above. In general, it is necessary to identify peak positions, intensities, widths, and symmetries to provide information for analyzing an XRD pattern. Various phases in the sample are generally identified by comparing peak positions with standard XRD patterns; this is usually not the case for clays. To identify clay minerals by XRD, special structural characteristics of clay minerals need to be taken into account. Clay minerals have a similar crystal structure in the x-y plane, as described above. Because of this special crystal structure, hkl reflections cannot be used widely for identification of clay minerals by XRD. The main usage of hkl reflections is to determine the polytypes. Randomly ordered powder XRD, giving hkl reflections, is also useful for identifying clay and non-clay portions of the sample in quantitative analyses.

To identify clay minerals by XRD, oriented samples must be used to improve the intensity of the (001) reflections. The glass slide method or Millipore® filter transfer method can be used to prepare oriented samples from a dispersed suspension of clay minerals. Flocculation of clay mineral particles in the suspension should be avoided, as it can cause random orientations. Several pretreatments, such as ethylene glycol solvation, glycerol solvation, saturation with various cations and heat treatments, should be applied to XRD samples for correct identification of the clay minerals. These pretreatments are established by considering the particular structures and properties of each family of clay minerals. For instance, smectite can easily be identified from illite and kaolinite by comparing diffraction patterns taken from air-dried and ethylene glycol solvated samples, because XRD patterns from illite and kaolinite are not affected by ethylene glycol solvation. For easily expandable smectite, on the other hand, ethylene glycol treatment shifts the (001) reflection from 1.5 nm for the air-dried condition to 1.69 nm.

Figs. 2.12-2.15 show XRD patterns for pure illite, chlorite, smectite and illite-smectite. The peaks are sharp, equidistant and symmetrical for pure clay minerals,

but not for mixed-layer ones. An entire diffraction pattern is necessary for identifying mixed-layer clay minerals. Peak broadening and asymmetric peaks, typical features in a mixed-layer clay mineral XRD pattern, are widely used for analyzing these patterns. The degree of mixed-layering can be determined based on Mering's principles, which state that (00l) peaks for mixed-layer clays occur between the reflections for the end member individual clay minerals. Positions of these reflections are determined by the degree of the interstratification (Moore & Reynolds, 1997).

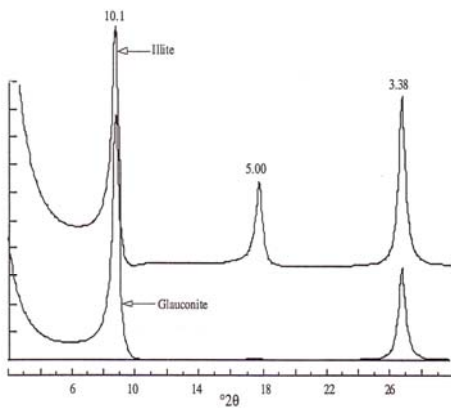


Fig. 2.12. Pure illite and glauconite XRD patterns (Moore & Reynolds, 1997).

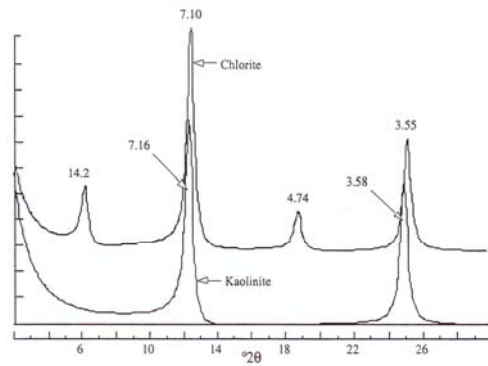


Fig. 2.13. Pure kaolinite and chlorite XRD patterns (Moore & Reynolds, 1997).

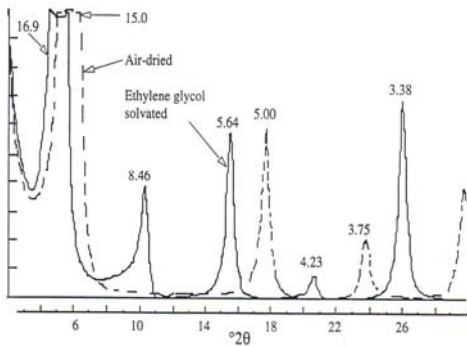


Fig. 2.14. Pure smectite XRD pattern (Moore & Reynolds, 1997).

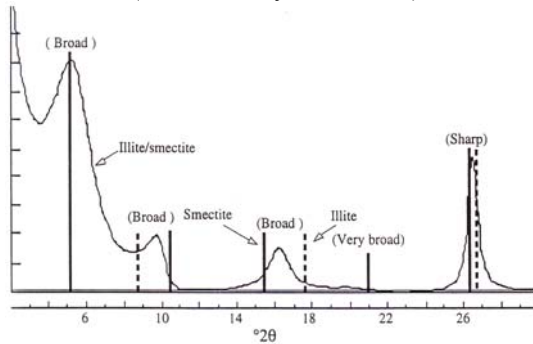


Fig. 2.15. Illite-smectite (50-50) XRD pattern (Moore & Reynolds, 1997).

It is theoretically possible to analyze any sample quantitatively, based on the intensities of the peaks present in the XRD pattern. In practice, however,

quantitative XRD for clay minerals requires extensive experience. Computer programs such as NEWMOD[®] modeling are available for quantitative XRD of clay minerals. Providing calibration standards is the most challenging step for using programs like NEWMOD[®]. Peak positions and their integrated areas, obtained from source clay mineral XRD profiles, are used as standard parameters for these programs. Reynolds (1989) and Brindley (1980) have given detailed principles for quantitative XRD.

2.3. References

- Ahn, J. H., & Peacor, D. R. (1986). Transmission and analytical electron microscopy of the smectite-to-illite transition. *Clays and Clay Minerals*, 34, 2, 165-179.
- Altaner, S. P., & Ylagan, R. F. (1997). Comparison of structural models of mixed-layer illite/smectite and reaction mechanisms of smectite illitization. *Clays and Clay Minerals*, 45, 4, 517-33.
- Bailey, S. W. (1963). Polymorphism of kaolin minerals. *American Mineralogist*, 48, 11-2, 1196-1209.
- Bennett R. H., & Hulbert M. H. (1986). Clay Microstructure. International Human Resources Development Corporation, Press Prentice Hall, Boston, MA.
- Bergaya, F., Theng, B. K. G. & Lagaly, G. (editors), (2006). Handbook of Clay Science. Developments in Clay Science, Volume 1, Elsevier Science, Amsterdam.
- Brindley, G. W., (1980). in Brindley, G. W. and Brown, G. (editors), Crystal structures of clay minerals and their x-ray identification: Monograph 5, Mineralogical Society, London, 411-38.
- Cullity, B.D. (1978). Elements of X-Ray diffraction, 2nd Edition, Addison-Wesley Publishing Company, Inc. Menlo Park, CA., USA.
- Dudek, T., Cuadros, J., & Fiore, S. (2006). Interstratified kaolinite-smectite: Nature of the layers and mechanism of smectite kaolinization. *American Mineralogist*, 91, 1, 159-170.
- Grim, R. E. (1962). Applied clay mineralogy, McGraw-Hill Book Company, Inc., USA.
- Moore, D. M. and Reynolds, Jr. R. C. (1997) 2nd Edition, X-Ray Diffraction and the Identification and Analysis of Clay Minerals, Oxford University Press, USA.
- Quirk, J. P., & Murray, R. S. (1999). Appraisal of the ethylene glycol monoethyl ether method for measuring hydratable surface area of clays and soils. *Soil Science Society of America Journal*, 63, 4, 839-49.
- Reynolds, R. C., Jr. (1985). NEWMOD[®] a computer program for calculation of one dimensional diffraction patterns of mixed-layer clays: Reynolds, R. C., 8 Brook Rd., Hanover, NH.

Reynolds, R. C. Jr. (1989). in Calvert, C. S., Pevear, D. R., & Mumpton, F. A., (editors), *Quantitative Mineral Analysis of Clays: Workshop Lectures*, Vol. 1, Clay Minerals Society, Boulder, CO, 4-36.

Sainz-Diaz, C. I., Hernández-Laguna, A., & Dove, M. T. (2001). Theoretical modeling of cis-vacant and trans-vacant configurations in the octahedral sheet of illites and smectites. *Physics and Chemistry of Minerals*, 28, 5, 322-31.

Chapter 3

High resolution transmission electron microscopy study of clay mineral particles from streams of simulated water based bitumen extraction of Athabasca oil sands¹

3.1. Introduction

Alberta's oil sands deposits represent the second largest reserve of oil in the world, with approximately 1.7 trillion barrels of bitumen in-place and 169.9 billion barrels proven oil reserves that can be recovered by current technology (Alberta Energy, 2011). These reserves are in the form of oil sands, comprised of 55–80% inorganic materials (primarily quartz), 4–18% bitumen and 2–15% water (Bichard, 1987). This composition makes the recovery of oil from oil sands a considerably more challenging prospect than the recovery of oil from conventional crude reserves. One of the major challenges is the role clay minerals play in the efficiency of the extraction process and the tractability of the tailings produced. Over the years, a general trend has been observed: as the fines content of an ore increases, the bitumen recovery from that ore decreases (Sanford, 1983). Mikula et al. (2008) showed that clay minerals, not the entire fines fraction, and the fluid phase determine the settling behaviour of tailings. Kasongo et al. (2000) reported that, through batch flotation experiments, the addition of montmorillonite (1 wt%) and calcium ions (40 mg/L) had a synergistic effect in decreasing bitumen recovery, whereas the addition of other clay minerals (kaolinite and illite, also at 1 wt%) did not have such an impact on recovery. On the other hand, Moran et al. (2000) used a micropipette manipulator to study the adhesion

¹ The contents of this chapter originally appeared in the journal *Applied Clay Science*. Copyright © 2011 Elsevier B.V. All rights reserved. Hooshiar, A., Uhlík, P., Kaminsky, H. W., Shinbine, A., Omotoso, O., Liu, Q., et al. (2010). High resolution transmission electron microscopy study of clay mineral particles from streams of simulated water based bitumen extraction of Athabasca oil sands. *Applied Clay Science*, 48(3), 466-474.

between a bitumen droplet and an air bubble and found that the bitumen droplet did not attach to an air bubble even when only 0.5 wt% of kaolinite was added to the solution. This implied that bitumen recovery would be affected in the presence of 0.5 wt% of kaolinite. Further work by Wallace et al. (2004) identified a relationship between increased soluble potassium and decreased bitumen recovery, pointing to a negative impact of degraded illite or illite-smectite on recovery. Finally, work by Tu et al. (2005) showed that the ultrafine ($< 0.3 \mu\text{m}$) clays may be responsible for the gelation and sludging behaviour of some ores, which negatively affects bitumen recovery and tailings management. These studies underscore the importance of characterizing the clay minerals in the oil sands, as they all indicate that the clay activity of the ore is the largest predictor of poor recovery.

Kaminsky et al. (2009) characterized low-grade oil sands in detail, predominantly by x-ray diffraction (XRD). Kaolinite, illite, illite-smectite, kaolinite-smectite and chlorite were found to be the dominant clay minerals in their samples based on the XRD results. Their work has shown that kaolinite and chlorite are preferentially partitioned to the froth stream during processing, while illite-smectite is preferentially partitioned to the middlings. Their work also showed that the illite-smectite XRD reflection in the primary bitumen froth product exhibited a higher degree of low angle asymmetry after ethylene glycol solvation than the illite-smectite in the middlings. In this paper, results of transmission electron microscopy (TEM) and high resolution transmission electron microscopy (HRTEM) investigations on the nature of the clay minerals, especially the mixed-layer clay minerals, are reported. In addition, the amount of iron content in the streams from simulated water based bitumen extraction is determined.

3.2. Materials and methods

3.2.1. Sample preparation and batch extraction

A low-grade oil sands ore (1.5 kg), containing 8.5% bitumen from a Suncor lease, was processed in a Syncrude-styled batch extraction unit using the CANMET procedure that has been reported to represent hydro transport conditioning at 50°C (Wang and Mikula, 2002). The warm tap water and oil sands were mixed. After 20 minutes of conditioning, air was injected through the mixing rotor. During this process, bitumen that was liberated from the sand and clay floated to the top of separation vessel. After 10 minutes of flotation, the mixing and air flow were stopped and the surface froth was scooped off the surface as the primary froth fraction. The residual slurry was stirred for 30 s and was then allowed to settle for two minutes. The portion still in suspension was decanted as middlings. The fraction which settled is the tailings. The solids from the streams were cleaned and separated from the residual water and organics by the Dean Stark procedure (Syncrude, 1979). While the technique for middlings/tailings separation was arbitrary, the middlings fraction generally represented the fine tailings stream that ended up as mature fine tailings (MFT) for a given extraction water chemistry. The cleaned solids were then homogenized and the >45 µm particles were removed by sieving in a Ro-tap™ sieve shaker, using deionized water. The sub-sieve fraction was separated into fines (2-45 µm), clays (0.2–2 µm) and ultrafine clays (<0.2 µm) by centrifuging.

The modified Jackson treatment by Šucha et al. (1991) was applied to a portion of each separated clay fraction from several samples. In this procedure, sodium acetate was used to remove carbonates (<2 wt% of siderite and/or ankerite was present in the samples, Kaminsky et al., 2009), hydrogen peroxide to remove organic materials and sodium dithionite (Na₂S₂O₄) and citrate to remove iron

oxides. After extraction of iron oxides, the samples were centrifuged in order to remove the solids from the extract. Solids were washed with deionized water and centrifuged again. Samples labelled with Na are those saturated with sodium ions, after residual organic matter and iron oxide removal. Some slurries of the samples were also selected to determine the amount of amorphous or nanocrystalline iron oxides by the ammonium oxalate procedure (Smith, 1984). Both procedures, Jackson and ammonium oxalate, were used to separate soluble Fe from selected samples. The extracts were analyzed by atomic absorption spectroscopy (AAS) in order to determine the Fe content.

3.2.2. TEM sample preparation

Two types of samples were used in TEM analysis – dispersed samples and ultrathin sections. The preparation of the dispersed samples involved diluting clay solids with deionized water to an approximate concentration of 1 mg/40 mL. The resulting slurry was sonicated to fully disperse the clays in the slurry. One drop of the solution was then placed on a lacey, carbon-coated, copper grid.

The dispersed samples were examined in both JEOL 2022 FS and JEOL 2010 transmission electron microscopes (TEMs). The length and width of the clay mineral particles in the images obtained were then measured and compiled.

Ultrathin sections were prepared using fragments of the dried solids that were separated from the extraction streams or from raw oil sands ores. The solids were coated with agar and immersed in water, and then embedded in resin using the method of Tessier (1984) and Elsass et al. (1998). In this method, the agar-coated solids sample was sequentially immersed in water, methanol, propylene oxide and finally in Spurr resin to ensure all pores and free spaces had been impregnated. After polymerization of the resin, ultrathin sections (~70 nm thick) were cut using

a Reichert Ultracut E microtome and a diamond knife. The microtome slices were captured on a lacey, carbon-coated, copper grid.

One-dimensional, bright field high-resolution TEM (HRTEM) images were taken with a JEOL 2010 microscope operated at 200 kV and equipped with a CCD camera and an energy-dispersive x-ray (EDX) spectrometer. The camera settings were adjusted to enable real-time low-light imaging. The electron beam was defocused to minimize specimen damage, so that the image was barely visible on the phosphorescent screen, and the magnification was increased to between 400 kX and 1.5 MX. Lattice fringe images were obtained by adjusting the sample height to the point of minimum contrast and then adjusting the focus until fringes were obtained. Proper orientation for imaging was found by obtaining the maximum contrast for the lattice fringes of the aluminosilicate layers normal to the stacking direction of the layers in each case. These phase contrast images result from (00l) diffracted beams. Selected area diffraction (SAD) patterns were recorded in some cases.

The origin of the sequential dark and bright lines in these types of images is a phenomenon called phase contrast. These lines are representative of aluminosilicate layers. Each dark line is representative of a layer with high electrostatic potential versus a bright line for a low electrostatic potential interlayer (Środoń et al., 1990) at the slightly under focused imaging conditions. Therefore, the distance between the two sequential similar lines (dark-dark or bright-bright) corresponds to the basal spacing of the clay mineral, which is a unique characteristic of the mineral. Theoretically, it is possible to identify the existing minerals in the sample by measuring their basal spacing on the lattice fringes images. A HRTEM image of an illite RM30 ultrathin section used as a standard for calibrating particle thickness measurements and basal spacing calculations is illustrated in Fig. 3.1. The basal spacing of this sample is 1 nm. Further information about the characteristics and properties for the standard clay mineral sample, illite RM 30, is available in the extensive study by Eberl et al.

(1987). The number of interlayers per particle and particle thickness were used for calculation of the expandability of illite-smectite according to the equation by Środoń et al. (1990):

$$\%S_{\text{Max}} = \frac{(T + N_0 D_s) - (D_l (N + N_0))}{(N + N_0)(D_s - D_l)} \times 100\% \quad (3-1)$$

N_0 is the number of crystals measured for a given sample, T is the “total” measured thickness and N is the “total” number of measured interlayers, D_s and D_l are basal spacings for smectite (1.35 nm) and illite (1 nm), respectively. Expandability means the percentage of smectitic interlayers per illite-smectite crystal. The calculated expandability is called the maximum expandability, %S Max, since the edge layers are considered to be smectitic in nature (Środoń et al., 1990).

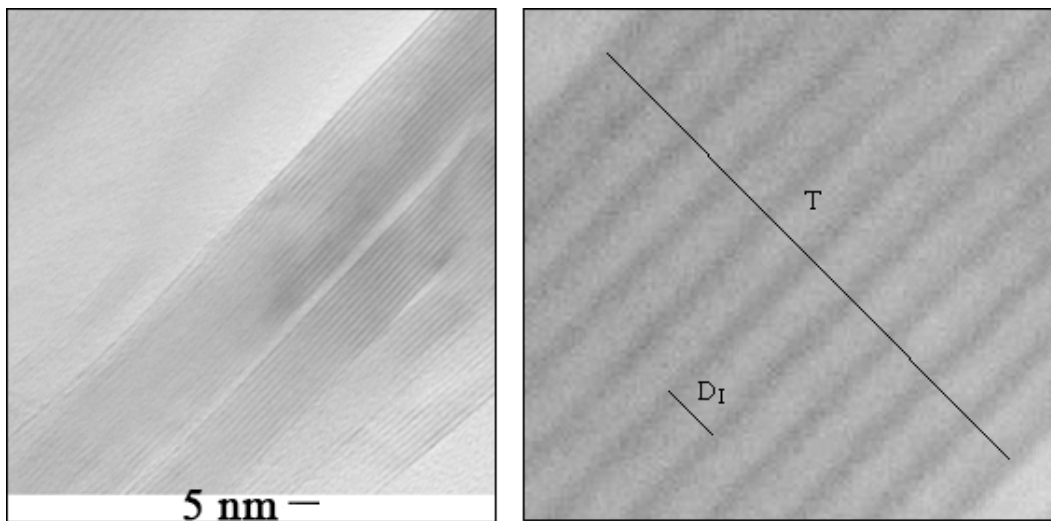


Fig. 3.1. HRTEM image of illite RM30 used as a standard for particle thickness measurements and basal spacing calculations. The enlarged part is on the right ($D_l = t$ (thickness of the individual particle, measured from the middle of the first layer to middle of the last layer)/ n (number of interlayers per individual particle)).

3.2.3. Determination of cation exchange capacity (CEC)

Two methods, methylene blue (MB) titration and copper (II) triethylenetetramine (Cu-trien) adsorption were used to determine the CEC of the clay samples. In the MB method, 0.2 g of the dried solids were dispersed in 50 mL of 0.015 M NaHCO₃ along with 2 mL of 10% w/w NaOH. The resultant mixture was stirred using a magnetic stir bar and sonicated until the sample was completely dispersed. Once the samples were dispersed, 2 ml of 10% v/v H₂SO₄ were added and the pH measured to ensure it was below 3. The sample was then titrated in 1 mL or 0.5 mL intervals with a fresh solution of 0.006 N MB. After each addition of MB, a transfer pipette was used to place one drop of the titrated mixture onto a piece of Whatman #4 qualitative filter paper. The droplet was examined for the presence of a blue halo, which would indicate the end point of the titration. When a light blue halo appeared around the drop, the sample was left to stir for two more minutes and then another drop was placed on the filter paper to make sure the drops had been taken from a homogenized, fully dispersed solution. The end point was reached when the halo was still present after the second drop. At the end point of the titration, the volume of MB added to the slurry was recorded and used to calculate the methylene blue index (MBI) and MB surface area (SA) according to the methods of Hang and Brindley (1970):

$$\text{MBI (meq/100 g)} = [(\text{volume of MB} \times \text{normality of MB}) / (\text{mass solids})] \times 100 \quad (3-2)$$

$$\text{SA (m}^2\text{/g)} = \text{MBI} \times 130 \times 0.0602 \quad (3-3)$$

For the Cu-trien CEC method, a 0.01 M solution of copper (II) triethylenetetramine (Cu-trien) was used. 1.463 g of triethylenetetramine was dissolved in 100 mL of deionized water and mixed with an identical molar equivalent of copper (II) sulphate. The solution was then appropriately diluted (Meier and Kahr, 1999). At least two specimens with different masses (120 and 80 mg) were added to 30 mL deionized water and dispersed in an ultrasonic bath.

Afterwards, 6 mL of the Cu-trien solution were added and the suspensions were shaken for one hour by a rotary machine (B&B SA-12) at 60 rpm. The suspensions were then centrifuged. The concentration of Cu (II) complex in the supernatant was determined by ultraviolet-visible (UV-VIS) spectroscopy using a Varian Cary 50 Spectrophotometer from the peak absorbance between 580 and 587 nm. The difference between the concentration of the diluted Cu-trien solution and that of the supernatant was used to calculate the CEC.

3.3. Results and discussion

3.3.1. Morphology of clay mineral particles

Several TEM images were examined from both <0.2 and 0.2-2 μm fractions and in all cases the clay mineral particles were very similar in shape. In general, the particles could be divided into four categories based on their shapes: pseudo-hexagonal idiomorphic (A), subhedral (B), anhedral (C) and oval (D) (Fig. 3.2a and 3.2b). While most of the particles were anhedral or oval, subhedral and pseudo-hexagonal idiomorphic particles were occasionally observed. The majority of the particles were found as aggregates, although the samples were prepared from a very dilute solutions sonicated for more than 10 minutes (Fig. 3.2a).

The length and width of hundreds of particles were measured and the averages were compiled in Table 3-1 and the distributions shown in Fig. 3.3. Although many particles were irregular in shape, in the length-width measurements they were considered as oval meaning that the largest diameter of each particles was considered as the length and the largest diameter perpendicular to the length was measured as the width (Fig 3.3). Standard deviations for length, width and mean particle area were very close to the mean values for these parameters (Table 3-1). A similar relationship was reported for micas (Nadeau, 1987). The average length to width ratio (L/W) was similar for all samples, although the middlings had particles that were longer and wider (larger mean areas) than particles in the

primary froth and tailings in the 0.2–2 μm fractions. The average size of the particles was expected to increase following the order of primary froth, middlings, and tailings. Therefore, one might expect to have the longest and widest particles in the tailings. However, as can be seen from Table 3-1, the middlings stream had the longest and widest particles (Table 3-1). This may be explained by the presence of aggregates of clay mineral particles or sand grains covered by clay minerals. These large aggregates could settle quickly to the tailings stream. When the tailings samples were prepared for analysis, the aggregates would be destroyed and dispersed to their original small particle sizes.

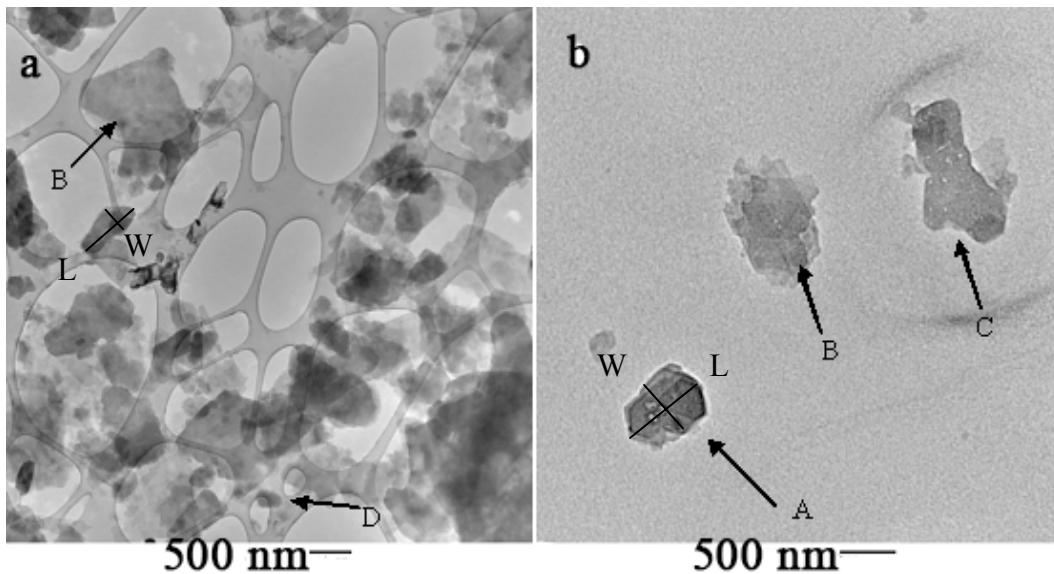


Fig. 3.2. TEM images of dispersed samples showing pseudo-hexagonal idiomorphic (A), subhedral (B), anhedral (C) and oval (D) particles. L – length and W – width.

In contrast, the $<0.2 \mu\text{m}$ size fractions showed the opposite trend, i.e., the middlings contained smaller particles in both length and width. Hydrophobicity of the clay mineral particles may be a key factor in this case. Small hydrophilic clay mineral particles covered by water molecules could be heavier than larger but hydrophobic clay mineral particles – attached to the air bubbles and found in large quantities in the primary froth – and, therefore, settled into the middlings. This hypothesis was in agreement with the enrichment of kaolinite, a relatively hydrophobic clay mineral, in the primary froth (Kaminsky et al., 2009). The

slightly hydrophobic kaolinite surfaces have been reported to interact with bitumen and non-polar solvents (Schoonheydt and Johnston, 2006). These kaolinite particles could attach to bitumen drops which themselves would attach to the air bubbles during aeration and, therefore, be found in large quantities in the froth stream.

Table 3-1. Length and width measurements for dispersed particles in primary froth and middlings samples. Mean area was calculated by multiplying the average length by the average width.

<u>Size Fraction</u>	<u>Stream</u>	<u># of Measured Particles</u>	<u>Average Length (nm)</u>	<u>Standard Deviation for Length (nm)</u>	<u>Average Width (nm)</u>	<u>Standard Deviation for Width (nm)</u>	<u>Average L/W Ratio</u>	<u>Mean Particle Area (1000 nm²)</u>	<u>Standard Deviation for Mean Particle Area (1000 nm²)</u>
0.2-2 µm	Primary froth	386	465	441	290	252	1.66	134.85	111.33
	Middlings	515	889	744	529	408	1.82	470.28	303.82
	Tailings	254	429	434	266	288	1.71	114.11	125.00
<0.2 µm	Primary froth	894	373	276	244	178	1.66	91.01	49.21
	Middlings	428	221	247	136	146	1.73	30.06	36.16
	Tailings	157	327	298	204	203	1.75	66.71	60.46

A final trend noted in the examination of the dispersed particles was the abundance of fine iron oxides. These areas were prevalent in both the middlings and the primary froth, but were more common in the primary froth samples. Ferrosityte and lepidocrocite were identified from selected area diffraction patterns of some of these areas. Other areas were identified as iron oxides by EDX but no diffraction patterns were obtained. Ferrosityte and most of the other iron (hydr)oxides were not detected in any of the XRD patterns (Kaminsky et al., 2009), as the extremely fine scale and relatively poor crystallinity of the particles likely caused their diffraction patterns to be lost in the background.

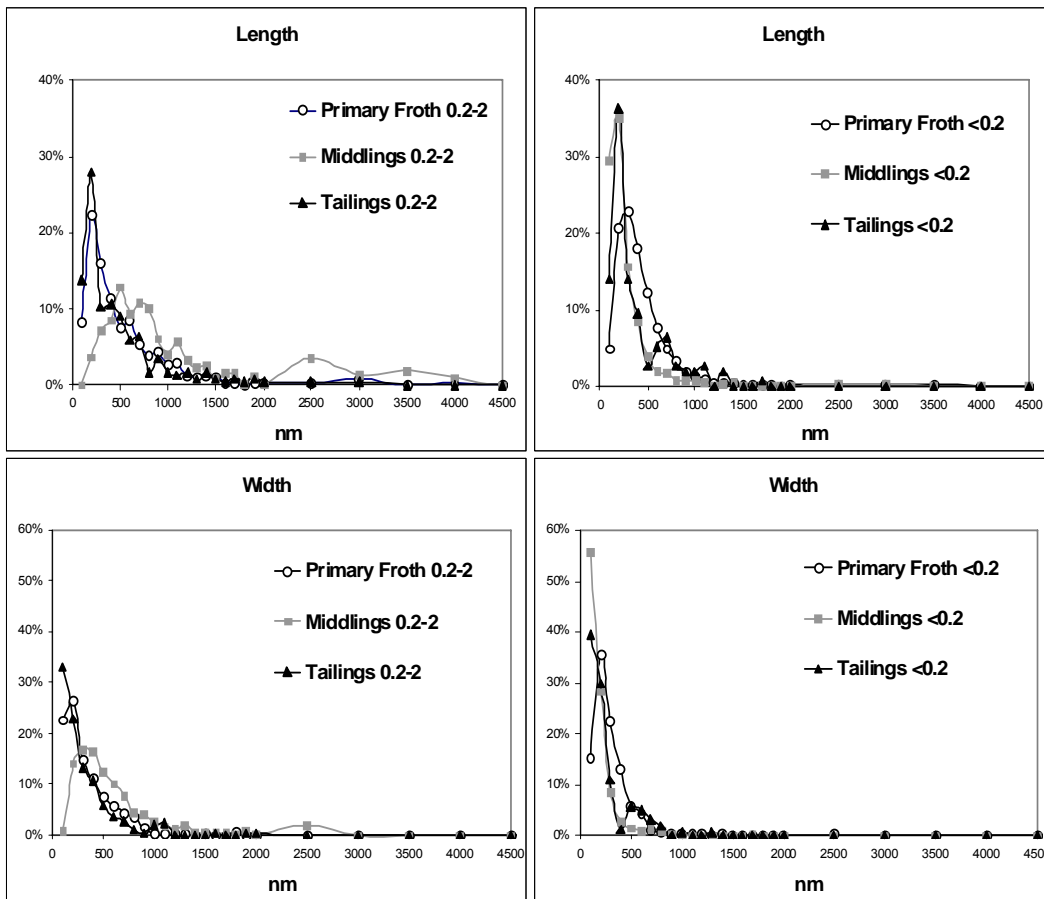


Fig. 3.3. Distributions of length and width of particles from extraction products measured from TEM images.

3.3.2. Particle thickness measurement by HRTEM

Ultrathin sections of clay mineral particles from the primary froth and middlings were studied by HRTEM. Particles with a wide range of thicknesses, from thin (Fig. 3.4a) to thick (Fig. 3.4b), were observed in both samples. The thickness of particles and the number of 2:1 aluminosilicate layers per particle were measured from several HRTEM images. The basal spacings of the samples were also calculated by using the data obtained from these measurements (Table 3-2). The number of layers per particle for both 0.2-2 μm and $<0.2 \mu\text{m}$ fractions of the primary froth and the middlings were compared one another in Table 3-2.

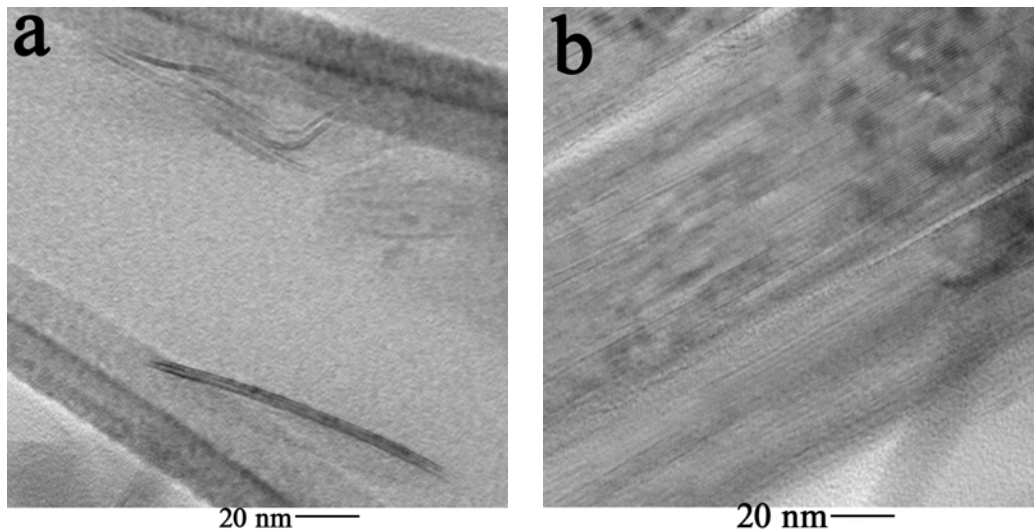


Fig. 3.4. HRTEM images of the 0.2-2 μm middlings sample showing a) thin and b) thick particles.

Table 3-2. Statistical parameters for particles observed by HRTEM. (*aspect ratio is calculated by using the area values from Table 3-1 and thicknesses only for illitic particles.)

<u>Stream</u>	<u>Size Fraction (μm)</u>	<u># of Particles</u>	<u>Average # of Layers per Particle</u>	<u>Standard Deviation for Layers per Particle</u>	<u>*Aspect Ratio (Area/Thickness) (nm)</u>
Middlings	<0.2	134	4.4	3.6	6.8×10^3
	0.2-2	239	6.6	6.0	6.6×10^4
Primary Froth	<0.2	191	3.4	2.4	2.7×10^4
	0.2-2	116	3.2	2.3	4.2×10^4

Differences were observed between the thickness distribution of the primary froth and the middlings particles. The middlings contain thicker particles (higher average number of layers per particle) than the primary froth, in both size fractions (Table 3-2). Although the primary froth 0.2-2 μm contained particles ranging in thickness from 1-2 nm to 10-15 nm (Fig. 3.5), thick particles (thicker than 10 nm) were not as abundant in this sample when compared to the middlings 0.2-2 μm (average number of layers per particle of 3.2 versus 6.6). It is significant to note the presence of about 7% of smectitic monolayers (smectitic fundamental particles based on Nadeau et al. (1984)) in both size fractions of the primary froth (Fig. 3.6). These monolayers were not detected by XRD since a single plane of atoms would not satisfy the Bragg condition. Also, the probability of inter-particle diffraction could be low due to the adsorbed Fe-oxides or organics.

Aspect ratios for both 0.2-2 μm and <0.2 μm fractions for the primary froth and the middlings were calculated (Table 3-2). The aspect ratio was calculated by dividing the mean area values for each fraction (Table 3-1) by the thickness of only illitic particles, since no HRTEM images were obtained from kaolinite fringes. Although this assumption, ignoring the thickness difference between kaolinitic and illitic particles, introduced an error to the calculation of aspect ratios, calculated values for aspect ratios showed two interesting features. Firstly, the aspect ratio for the <0.2 μm fraction of the middlings was in the same range as for Nadeau's data for illite-smectite. This was in agreement with the dominance of

illite-smectite in this sample (Kaminsky et al., 2009). Secondly, the aspect ratio was significantly higher for the 0.2-2 μm middlings in comparison with Nadeau's data for micaceous samples. This suggested that the presence of very thin particles with large surface areas in the middlings could be responsible for settling problems with suspended fines and clay minerals in the tailings basins (FTFC, 1995).

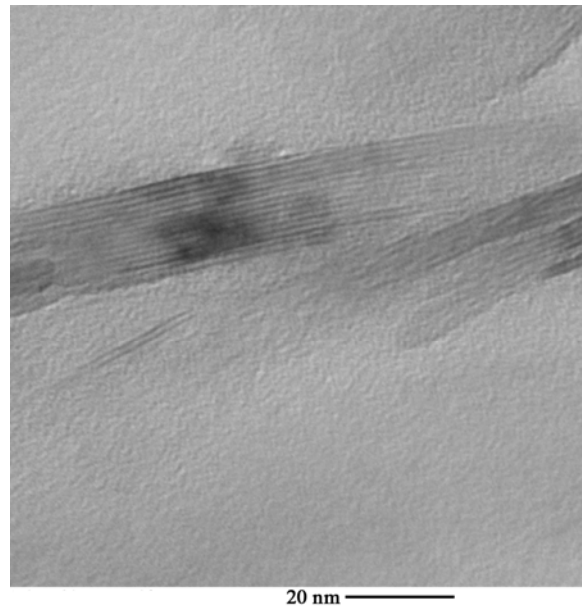


Fig. 3.5. HRTEM image of the 0.2-2 μm primary froth sample is showing thick (15 layers) and thin (2 layers) particles.

The 0.2-2 μm middlings samples not only contained thick particles in a larger quantity on average but also some very thick particles, e.g., particles containing 35 layers or more (Fig. 3.4b). The 0.2-2 μm middlings sample also had longer and wider particles when compared to the primary froth (Table 3-1). The 0.2-2 μm middlings samples had a polymodal distribution with peaks at about 2, 6, 9, 11 and 14 layers (Fig. 3.6). Fig. 3.4a and 4b are good examples of this polymodal size distribution. This thickness distribution is in agreement with the polymodal

distribution for length and width of particles for 0.2-2 μm middlings sample (Fig. 3.3). The polymodal size distribution is also reasonably consistent with the polymineral clay composition of this slurry (Kaminsky et al., 2009). Various clay minerals have different particle sizes. Generally, chlorite and illite have thicker particles than illite-smectite. By contrast, the 0.2-2 μm primary froth sample had a pronounced bimodal distribution with peaks at around 2 and 6 layers (Fig. 3.6).

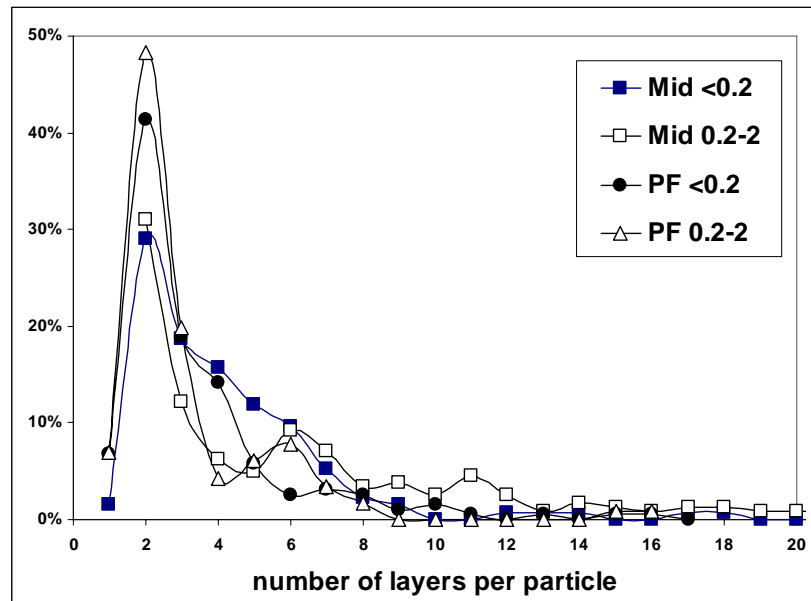


Fig. 3.6. Distribution of number of layers per particle measured from data obtained from HRTEM images.

The large number of very thin particles (peak of about 48% at 2 layers per particle) could explain the unexpected properties of this sample, such as its high CEC values, organic matter and iron content which will be discussed in subsequent sections. Since the basal spacing measurement error was significant for such thin particles, these bilayers were assumed to be illite fundamental particles based on Nadeau et al. (1984) although they could also be smectitic in nature. Fundamental illite particles were more likely, since R1 ordering was expected to be the dominant type of Reichweite ordering according to the

presence of the second-order superstructure reflection in these samples (Moore and Reynolds, 1997) and also based on the illite-smectite expandability calculations for these samples by Kaminsky et al. (2009, 20-30% smectite).

The $<0.2 \mu\text{m}$ primary froth sample contained many very thin particles, as thin as bi-layer particles as well (Fig. 3.7). There were some regions of nanometer sized particles in the $<0.2 \mu\text{m}$ primary froth sample, (Fig. 3.7). These areas were rich in iron compounds, based on EDX analysis. Kaminsky et al. (2006) have shown the presence of iron compounds by TEM electron diffraction analysis on similar areas of the same sample.

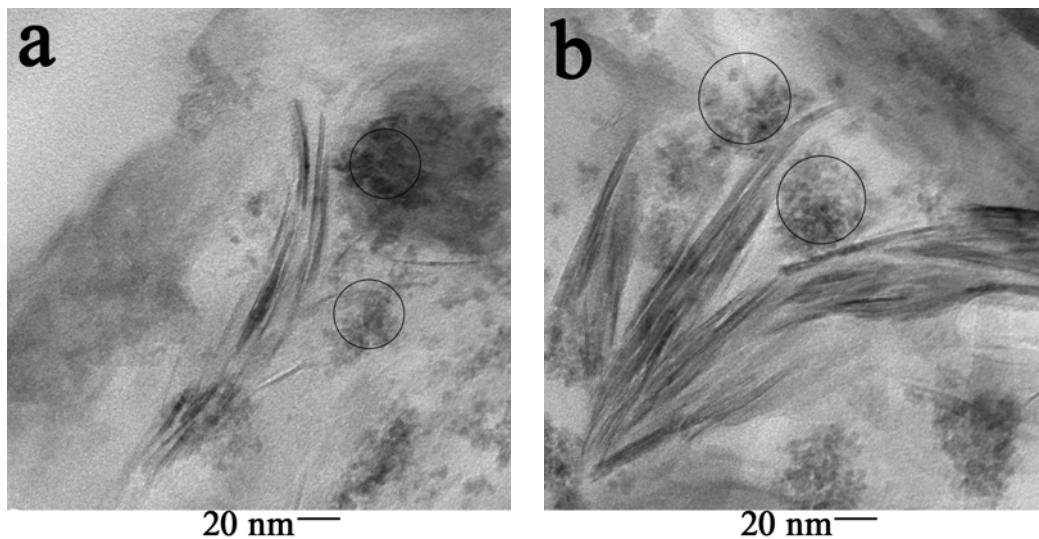


Fig. 3.7. HRTEM images of $<0.2 \mu\text{m}$ primary froth sample. Iron-rich regions are circled.

Based on the basal spacing measurements, no kaolinite lattice images were detected in these samples, likely due to the extreme sensitivity of kaolinite to the electron beam (Ma and Eggleton, 1999). Of the particles that were observed, most had the characteristic 1.0 nm basal spacing of illite. There were others, however, with measured spacings closer to 1.2 nm, possibly indicating the presence of

smectitic layers within a particle. Particles exhibiting inconsistent basal spacings (Fig. 3.8) were further indications of the latter possibility. Both phenomena may be due to an incorrect amount of defocus during imaging. However, the presence of well resolved layers, exhibiting 1.0 nm spacing close to the areas of inconsistency, suggested that it was a sample phenomenon rather than an experimental artefact. Lateral layer terminations were also observed in several other particles (Fig. 3.8). Lateral layer termination is a structural defect; the source of which is related to the origin of the particles and not with processing.

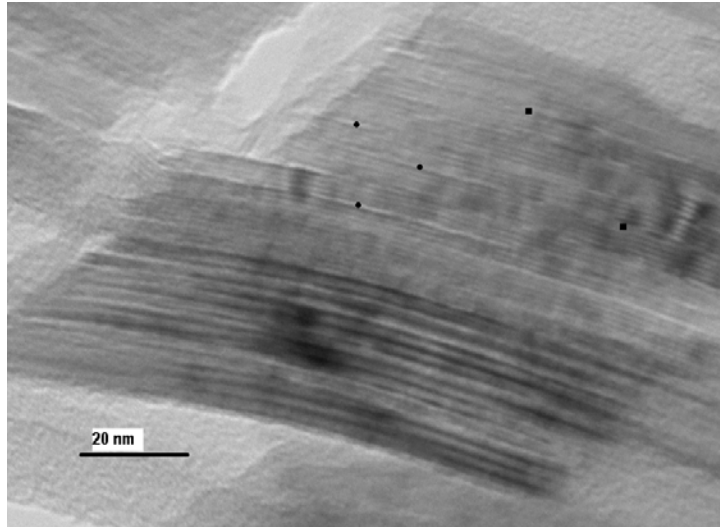


Fig. 3.8. HRTEM image of 0.2-2 μm middlings sample showing inconsistent basal spacings (circles) and lateral layer termination (squares).

Calculations of mixed-layer illite-smectite expandability from HRTEM images (Środoń et al., 1990) are more difficult when illite and illite-smectite are simultaneously present. The distribution of the number of layers per particle (Fig. 3.6) suggested the existence of at least two different phases corresponding to the peaks. A simplification was made by assuming that thinner particles (the first peak) were illite-smectite and thicker ones were illite particles, although it was not possible to exclude the presence of illite in thin particles (Dudek and Środoń, 2003).

In order to be more accurate, the illite-smectite expandability was calculated for all samples with the following considerations. Since the basal spacings of pure smectite and pure illite in epoxy resin were 1.35 and 1.00 nm, respectively (Środoń et al., 1990), the illite-smectite basal spacing was expected to be between these two limits. Therefore, any particle with a basal spacing of 1.4 nm or larger (chlorite particles) was not considered in the calculations. In addition, particles with 4 or less layers per particle were assumed to be illite-smectite, even if their basal spacings were in the range of 1 to 1.05 nm. This assumption is valid when the edges of the particles are considered to be smectitic in nature (Środoń et al., 1990), which is the case in all calculations presented in this paper. This assumption should not introduce significant error in the calculations, since only a few of such particles were found in HRTEM images. Particles with basal spacings in the range of 1.25-1.35 nm were assumed to be illite-smectite instead of pure smectite, since pure smectite was not identified by XRD. It is worth mentioning that less than 10% of the total number of particles was in this range, except for the 0.2-2 μm middlings sample which contained more particles in this range. In summary, all particles with basal spacings in the range of 1.05 to 1.35 nm, and also particles with 4 or less layers per particle with basal spacings less than 1.05 nm were used for illite-smectite expandability calculations. The expandability, %S Max, for the primary froth and middlings was calculated (Table 3-3). These results were about 10% higher than the illite-smectite expandability results calculated from XRD data, %S XRD, on the same samples (Kaminsky et al., 2009). This discrepancy is in agreement with previous work, as the maximum expandability calculated from TEM data, %S Max, is reported to be higher than the expandability calculated from XRD data, %S XRD, due to the assumption of the smectitic nature of the crystal edges (Nadeau and Bain, 1986, Środoń et al., 1990, Uhlík et al., 2000). A comparison was made between the %S Max and %S XRD (Fig. 3.9).

Table 3-3. Illite-smectite expandability calculated from HRTEM measurements (%S Max) and comparison with expandability measured by XRD (%S XRD). T – total measured thickness of particles; N – total number of interlayers in measured particles; No - number of measured particles.

Size (μm)	Stream	Without bilayers				With bilayers					
		T	No	N	%S Max	Bilayers	T	No	N	%S Max	%S XRD
< 0.2	Middlings	133.3	59	132	32.9	39	159.3	85	158	37.9	29
	Primary froth	397.5	131	366	44.5	79	483.5	218	452	45.8	26
0.2-2	Middlings	302.8	79	276	43.8	30	341.8	118	315	44.7	31
	Primary froth	281.0	86	256	46.0	56	327.0	132	302	47	37

The primary froth had higher illite-smectite expandability than the middlings in both size fractions (Table 3-3). This is in agreement with the lower average number of layers per particle for the primary froth (Table 3-2). An interesting point was that the <0.2 μm primary froth sample had higher expandability based on HRTEM calculations, but lower expandability based on XRD calculations (Kaminsky et al., 2009) when compared to the <0.2 μm middlings sample. This discrepancy may be explained by the presence of small amounts of illite-smectite phases with higher expandability. This explanation is consistent with the broadening of the illite-smectite XRD reflection from the <0.2 μm primary froth sample after EG saturation to a lower angle ($2\theta = 6.5 - 7.27^\circ$ (Co radiation; $d = 1.4 - 1.58 \text{ nm}$) (Kaminsky et al., 2009).

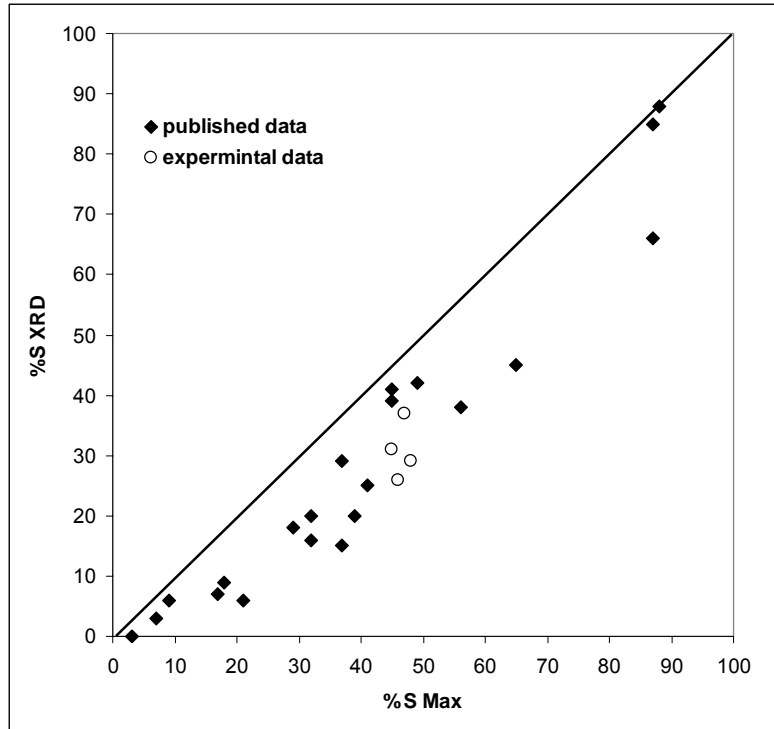


Fig. 3.9. Maximum percent smectite obtained from TEM plotted against expandability measured by XRD. Published data are from Środoń et al. (1992) and Uhlík et al. (2000).

3.3.3. Determination of iron content from amorphous and crystalline Fe Oxides

Fe content for some samples was determined by two methods, sodium dithionite and ammonium oxalate extraction (Fig. 3.10). Fe content was much higher in the 0.2-2 μm primary froth sample than in the other streams (Fig. 3.10). The results for both the ammonium oxalate and sodium dithionite extraction methods were very similar, indicating that the majority of soluble Fe was in the form of amorphous matter and/or nanocrystalline iron (hydr)oxides such as lepidocrocite. The difference between total Fe and soluble Fe (Fig. 3.10) showed the presence of 2-3% of insoluble Fe. This insoluble Fe must be the phyllosilicate structural Fe. From 1% to 2.8% of Fe was detected by EDX analysis from illitic clay minerals (Kaminsky et al, 2008). XRD results showed that the samples contained small

amounts of chlorite (Kaminsky et al., 2009). The chlorite appeared to be in Fe-chlorite form, another source of insoluble Fe, according to the lower intensities of odd basal reflections (001 and 003; Moore and Reynolds, 1997).

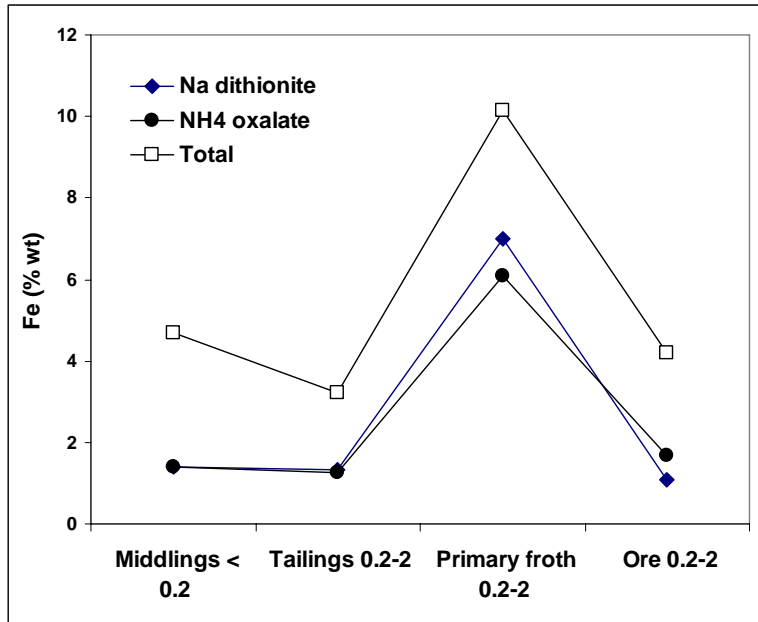


Fig. 3.10. Soluble Fe content (wt%) after sodium dithionite extraction and ammonium oxalate extraction is compared with the total amount of Fe determined by XRF (Kaminsky, 2008).

3.3.4. CEC Measurements

CEC values from both MB titration and Cu-trien adsorption methods were measured for the <0.2 and 0.2-2 μm fractions of the Dean Stark solids before and after the Jackson treatment (Table 3-4). As expected, the finer fractions had higher CEC due to smaller particle sizes.

Before the Jackson treatment, the CEC values of the primary froth samples determined by Cu-trien adsorption were higher than those by MB titration. However, after the Jackson treatment, the CEC value determined by Cu-trien

adsorption decreased to the same value obtained from MB titration. This may be due to the removal of Fe compounds from the samples by sodium dithionite in the Jackson procedure. Cu-trien was sensitive to the Fe content of the sample. Grygar et al. (2007) have mentioned the possibility of chemisorption of Cu^{2+} on hydrous ferric oxide admixtures.

In the $<0.2 \mu\text{m}$ fraction, clay mineral particles in the middlings had higher CEC than the clay mineral particles in the primary froth, according to both methods, which is in agreement with the calculated surface area from XRD results by Kaminsky et al. (2009). In the $0.2\text{-}2 \mu\text{m}$ fractions, on the other hand, CEC values from both methods were higher for the primary froth which contradicted the calculated SA values from XRD results. The $0.2\text{-}2 \mu\text{m}$ primary froth sample seemed to be an extraordinary case. Furthermore, the $0.2\text{-}2 \mu\text{m}$ primary froth sample contained the highest residual organic matter of all streams (Kaminsky, 2008). Therefore, more detailed discussion on this sample is presented below.

Table 3-4. CEC values before and after Jackson treatment.

<u>Fraction</u> (μm)	<u>Sample</u>	<u>Before Jackson Treatment</u>		<u>After Jackson Treatment</u> (Na)
		CEC MBI (meq/100g)	CEC Cu-trien (meq/100g)	CEC Cu-trien (meq/100g)
0.2-2	Primary Froth	22*	32	22
	Middlings	11*	10	
	Tailings	9*	11	10
<0.2	Primary Froth	31*	39	-
	Middlings	37*	41	35
	Tailings	38*	33	35

- not measured because of lack of sample

* published by Kaminsky et al. (2008a)

3.3.5. Special case of the 0.2-2 μm size fraction of the primary froth

The soluble Fe (Fe oxides) of the 0.2-2 μm primary froth sample was more than three times higher than that for the middlings (Fig. 3.10, ~6 wt% vs. less than 2 wt%). The presence of Fe compounds in this sample was also confirmed by TEM investigations. Fig. 3.7 shows a TEM image with areas of very small particles of crystalline Fe compounds. The 0.2-2 μm primary froth sample had the highest illite-smectite expandability (Table 3-3), Fe content (Fig. 3.10) and CEC among 0.2-2 μm fractions (Table 3-4). The extraordinarily high CEC was not in agreement with the mineralogy of this sample based on XRD analysis (showing more kaolinite than illite). The key point for this sample seemed to be the presence of smectitic layers observable only by HRTEM analysis.

As mentioned above, this sample had the highest %S Max, about 7% of smectite monolayers, and a large number of illite bilayer particles with smectitic external surfaces. These active smectitic surfaces could strongly bind to very fine Fe compounds which themselves could interact with organic matter (Kotlyar et al, 1985). The CEC for this sample decreased dramatically after the Jackson treatment (Table 3-4). Removing a major part of the Fe compounds with sodium dithionite in the Jackson treatment seemed to be responsible for this decrease in CEC values. An interesting point observable in Table 3-4 was that the CEC value of this sample determined by the Cu-trien method decreased after Jackson treatment to the same number obtained from MB titration before Jackson treatment. It has been reported that CEC determination by Cu-trien adsorption is sensitive to the Fe content of the sample, but this does not appear to be the case for MB titration. The MB was insensitive to the presence of iron oxides as the sample was titrated to below the isoelectric point of the iron oxides; hence they should not interact with methylene blue. The pH of the MB solution was below 3. The isoelectric points of the iron oxides are above 3 (Cornell and Schwertmann, 2003).

An important conclusion can be drawn from the 0.2-2 μm primary froth sample. To be able to explain the behaviour of the clay minerals in the extraction process, a detailed study on the mineralogical composition, particle size distribution, the properties of the clay minerals present, etc., is necessary. In this thesis, for example, only HRTEM analysis showing a large number of thin particles (bilayers and monolayers) with active smectite surfaces made it possible to explain the CEC.

3.4. Conclusions

This chapter has emphasized the importance of detailed characterization in explaining the properties of the clay minerals in the oil sands.

Based on transmission electron microscopic investigations on suspended solid samples, longer and wider clay mineral particles were found in the 0.2-2 μm fraction of the middlings, relative to the tailings. This may have been caused by aggregates of fine clay mineral particles or sand grains covered by clay minerals, which originated from the oil sands ores and survived the water extraction process, and settled to the tailings. Therefore, the effect of agglomeration/de-agglomeration of clay mineral particles must be taken into account in any method used for particle size measurements.

High-resolution transmission electron microscopy investigations showed the presence of about 7% smectitic monolayers in both fractions, <0.2 and 0.2-2 μm , of the primary froth while these monolayers were not detected by x-ray diffraction analyses.

X-ray diffraction based illite-smectite expandability calculations were not able to fully explain the observed properties of the clay minerals present in some streams, especially the 0.2-2 μm primary froth sample, because of the presence of illite bilayer and smectite monolayer fundamental particles. Only more accurate

expandability calculations based on high-resolution transmission electron microscopy analyses along with particle thickness distribution data made it possible to describe the behaviour of clay minerals in the extraction process streams. High-resolution transmission electron microscopy studies showed a pronounced bimodal thickness distribution of the clay mineral particles, containing a large number of very thin particles. The presence of thin particles was the cause of the extraordinarily high activity of the 0.2-2 μm primary froth sample. This effect was magnified by the presence of organic matter and iron compounds.

Investigations on iron in the clay fractions of the streams suggest that Fe may exist in several forms such as crystalline, nanocrystalline and/or amorphous iron (hydr)oxides, such as lepidocrocite and Fe in the clay mineral structure (e.g., chlorite). The cation exchange capacity data showed that the copper (II) triethylenetetramine adsorption method was sensitive to the presence of Fe oxides in the sample while the methylene blue titration method was not. Further studies on the role of iron in the bitumen extraction process could enrich knowledge in the field.

Acknowledgements

The authors are grateful to the Centre for Oil Sands Innovation (COSI) for providing research funding and to Suncor for providing oil sands ore sample.

3.5. References

- Alberta Energy (2011). Oil sands. Alberta Government, www.energy.gov.ab.ca/OurBusiness/oilsands.asp (accessed April 21, 2011).
- Bichard, J.A. (1987). Oil sands composition and behaviour research: The research papers of John A. Bichard 1957-65. *Alberta Oil Sands Technology and Research Authority (AOSTRA)*, Edmonton, Canada.
- Cornell, R.M., & Schvertmann, U. (2003). The Iron Oxides. 2nd edition. Wiley-VCH Verlag GmbH & Co. KGaA, Weinheim.
- Dudek, T., & Środoń, J. (2003). Thickness distribution of illite crystals in shales. II: Origin of the distribution and the mechanism of smectite illitization in shales. *Clays and Clay Minerals*, 51, 529-42.
- Eberl, D.D., Srodon, J., Lee, M., Nadeau, P. H., & Northrop, H. R. (1987). Sericites from the Silverton Caldera, Colorado: Correlation among structure, composition, origin, and particle thickness. *American Mineralogist*, 72, 914-34.
- Elsass, F., Beaumont, A., Pernes, M., Jaunet, A.-M., & Tessier, D. (1998). Changes in layer organization of Na- and Ca-exchanged smectite materials during solvent exchanges for embedment in resin. *The Canadian Mineralogist*, 36, 1475-83.
- FTFC (Fine Tailings Fundamentals Consortium) (1995). Vol.1, Clark hot water extraction fine tailings, In: *Advances in oil sands tailings research*, Alberta Department of Energy, Oil Sands and Research Division, Edmonton, Canada, 5-57.
- Grygar, T., Hradil, D., Bezdička, P., Doušová, B., Čapek, L., & Schneeweiss, O. (2007). Fe(III)-modified montmorillonite and bentonite: Synthesis, chemical and UV-VIS spectral characterization, arsenic sorption, and catalysis of oxidative dehydrogenation of propane. *Clay and Clay Minerals*, 55, 2, 165-76.
- Hang, P. T., & Brindley, G. W. (1970). Methylene blue adsorption by clay minerals. Determination of surface areas and cation exchange capacities. *Clays and Clay Minerals*, 18, 203-12.
- Kaminsky, H.A.W., 2008. Characterization of an Athabasca oil sands ore and process streams. Ph.D.Thesis, Department of Chemical and Materials Engineering, University of Alberta, Canada.
- Kaminsky, H.A.W., Etsell, T.H., Ivey, D.G., & Omotoso, O. (2006). Fundamental Particle size of clay minerals in Athabasca oil sands tailings. *Clay Science*, 12 (supplement 2), 217-22.

Kaminsky, H.A.W., Uhlik, P., Hooshiar, A., Shinbine, A., Etsell, T.H., Ivey, D.G., Liu, Q., & Omotoso, O. (2008). Comparison of morphological and chemical characteristics of clay minerals in the primary froth and middlings from oil sands processing by high resolution transmission electron microscopy. *Proceeding of the First International Oil Sands Tailings Conference*. Edmonton, Canada, 102-11.

Kaminsky, H.A.W., Etsell, T.H., Ivey, D.G., & Omotoso, O. (2009). Distribution of clay minerals in the process streams produced by the extraction of bitumen from Athabasca oil sands. *Canadian Journal of Chemical Engineering*, 87, 1, 85-93.

Kasongo, T., Zhou, Z., Xu, Z., & Masliyah, J. (2000). Effect of clays and calcium ions on bitumen extraction from Athabasca oil sands using flotation. *The Canadian Journal of Chemical Engineering*, 78, 674-80.

Kotlyar, L.S., Kodama, H., & Sparks, B.D. (1985). Isolation of inorganic matter-humic complexes from Athabasca oil sands. *Alberta Oil Sands Technology and Research Authority (AOSTRA)*, 2, 2, 103-11.

Ma, C., & Eggleton, R. A. (1999). Surface layer types of kaolinite; a high-resolution transmission electron microscope study. *Clays and Clay Minerals*, 47, 2, 181-191.

Meier, L.P., & Kahr, G. (1999). Determination of the cation exchange capacity (CEC) of clay minerals using the complexes of copper(II) ion with triethylenetetramine and tetraethylenepentamine. *Clays and Clay Minerals*, 47, 386-88.

Mikula, R.J., Omotoso, O., & Kasperski, K.L. (2008). The chemistry of oil sands tailings: production to treatment. *Proceedings of the First International Oil Sands Tailings Conference*. Edmonton, Canada, 23-32.

Moore, D. M., & Reynolds, Jr. R. C. (1997) 2nd Edition, *X-Ray Diffraction and the Identification and Analysis of Clay Minerals*, Oxford University Press, USA.

Moran, K., Yeung A., & Masliyah J. (2000). Factors affecting the aeration of small bitumen droplets. *Canadian Journal of Chemical Engineering*, 78, 8, 625-634.

Nadeau, P.H. (1987). Relationships between the mean area, volume and thickness for dispersed particles of kaolinites and micaceous clays and their application to surface area and ion exchange properties, *Clay Minerals*, 22, 351-56.

Nadeau, P.H., Wilson, M.J., McHardy, W.J., & Tait, J.M. (1984). Interstratified clay as fundamental particles. *Science*, 225, 923-35.

- Nadeau, P.H., & Bain, D.C. (1986). Composition of some smectites and diagenetic illitic clays and implications for their origin, *Clays & Clay Minerals*, 34, 455-64.
- Sanford, E.C. (1983). Processability of Athabasca oil sands: interrelationship between oil sand fine solids, process aids, mechanical energy and oil sand age after mining. *The Canadian Journal of Chemical Engineering*, 61, 554-67.
- Schoonheydt, R.A., & Johnston, C.T. (2006). Surface and interface chemistry of clay minerals. In: Bergaya, F., Theng, B.K.G., Lagaly, G., (Eds.), *Handbook of clay science, Development in clay science vol.1*, Elsevier Ltd., 87-114.
- Smith, B.F.L. (1984). The determination of silicon in ammonium oxalate extracts of soils. *Communications in Soil Science and Plant Analysis*, 15, 199-204.
- Środoń, J., Andreoli, C., Elsass, F., & Robert, M. (1990). Direct high-resolution transmission electron microscopic measurement of expandability of mixed-layer illite/smectite in bentonite rocks. *Clays and Clay Minerals*, 38, 373-9.
- Środoń, J., Elsass, F., McHardy, W.J., & Morgan, D.J. (1992). Chemistry of illite-smectite inferred from TEM measurements of fundamental particles. *Clay Minerals*, 27, 137-58.
- Šucha, V., Środoń, J., Zatkalíková, V., & Franců, J. (1991). Mixed layered illite/smectite: separation, identification, use. *Mineralia Slovaca*, 23, 267-74, (in Slovak, with English Abstract).
- Syncrude Research. (1979). "Determination of bitumen, water and solids content of oil sand, reject and slurry samples (Classical)". Method 2.7. Syncrude analytical methods for oil sand and bitumen processing. Syncrude Canada Limited.
- Tessier, D. (1984). Étude expérimentale de l'organisation des matériaux argileux. Ph.D. Thesis, Paris, France: University of Paris VII.
- Tu, Y., O'Carroll, J. B., Kotlyar, L. S., Sparks, B. D., Ng, S., Chung, K. H., & Cuddy, G. (2005). Recovery of bitumen from oil sands: Gelation of ultra-fine clay in the primary separation vessel. *Fuel*, 84, 653-60.
- Uhlík P., Šucha V., Elsass F., & Čaplovičová M. (2000). HRTEM of mixed-layer clays dispersed in PVP-10: a new technique to distinguish detrital and authigenic illitic material. *Clay Minerals*, 35, 781-9.

Wallace, D., Tipman, R., Komishke, B., Wallwork, V., & Perkins, E. (2004). Fines/water interactions and consequences of the presence of degraded illite on oil sands extractability. *The Canadian Journal of Chemical Engineering*, 82, 667-77.

Wang, N., & Mikula, R.J. (2002). Small scale simulation of pipeline or stirred tank conditioning of oil sands: Temperature and mechanical energy, *Journal of Canadian Petroleum Technology*, 41, 1, 8-10.

Chapter 4

Clay minerals in nonaqueous extraction of bitumen from Alberta oil sands. Part 1: nonaqueous extraction procedure¹

4.1. Introduction

The Alberta oil sands are large deposits of bituminous hydrocarbons located in North-eastern Alberta, Canada. With 170 billion barrels of oil that can be recovered by current technology, the Alberta oil sands are the second largest known oil reserve in the world after Saudi Arabia. In 2008, 1.3 million barrels of crude oil per day was produced from the oil sands (206,000 m³/day), and it is anticipated that daily production will grow to three million barrels by 2018 (Alberta Energy, 2010).

There are currently two types of commercial bitumen extraction operations from the oil sands: surface mining and in-situ. The in-situ technologies involve the use of thermal energy to heat the bitumen in-place and allow it to flow to the well bore to be pumped to the surface, e.g., the steam assisted gravity drainage (SAGD) process. Bitumen recovery by the in-situ technologies is typically less than 60%. Surface mining operations, on the other hand, use shovels and trucks to dig out the oil sands, which are then mixed with hot water and caustic and sent through a hydrotransport pipeline to the extraction plant where the bitumen is recovered (Alberta Energy, 2010; Camp, 1976). Typical bitumen recovery is as high as 90%. Currently, about 55% of the oil production from the Alberta oil sands is through surface mining operations (Alberta Energy, 2010).

¹ The contents of this chapter have been submitted for publication in the journal *Fuel Processing Technology*. Hooshiar, A., Uhlik, P., Etsell, T. H., Ivey, D. G., & Liu, Q. (2011). Clay minerals in nonaqueous extraction of bitumen from Alberta oil sands. Part 1. nonaqueous extraction procedure. *Fuel Processing Technology* (submitted).

However, commercial surface mining and hot water bitumen extraction operations have several shortcomings, most significant of which are high fresh water and energy consumption. In this process, approximately 17 to 21 barrels of water are required to produce one barrel of oil. Although the majority of the process water is recycled, some of the water is trapped in the unsettled tailings (mature fine tailings, MFT). As a result, the Alberta oil sands industry requires a net intake of approximately 2 to 4.5 barrels of fresh water from the Athabasca River to produce one barrel of oil. Also, large tailings ponds are required to contain the unsettling and unconsolidated tailings, which have accumulated to about 650 million m³ by 2006 (FTFC, 1995; Sustainable Development Business Case Report, 2006).

The Alberta government currently allocates 359 million m³ of Athabasca River water per year to oil sands mining and production (PTAC, 2007). This is equivalent to about 3% of the average annual flow of the Athabasca River. However, in winter seasons, due to the low water level, the government typically limits water withdrawal from the river to less than 1.3% of the average annual flow, effectively limiting water withdrawal to less than half of the allocation during the winter months (Alberta Energy, 2010). Taken together, the allocated amount of water would limit oil production from Alberta oil sands to approximately 1.15 to 2.3 million barrels per day based on the current water consumption rate. Daily production was 1.13 million barrels in 2006 and increased to 1.3 million barrels in 2008. Obviously, a significant increase in oil production from the Alberta oil sands will not be possible unless more fresh water is allocated to oil sands production. Given the current climate and perception surrounding the oil sands operations, an increase in water allocation to the oil sands industry is unlikely. Therefore, unless new technologies are developed that use much less fresh water, expansion of oil production from the Alberta oil sands to three million barrels per day will not be feasible.

Because of the potential for high recovery of bitumen, the elimination of sludge tailings ponds and a significant decrease in water consumption, nonaqueous

solvent extraction processes have been investigated since the mid 1960s. Investigators have focused on several extraction parameters such as solvent type, agitation rate, oil sands to solvent ratio, contact time and oil sands ore grade. Most of the studies and processes are not completely nonaqueous, since they use at least small amounts of water as a binding agent for the clays. Although the results have been encouraging, nonaqueous solvent extraction has not yet been used commercially to extract bitumen from Alberta oil sands. The reason seems to be related to poor solvent recovery from the oil sands extraction tailings, which is probably the most critical technical problem for any nonaqueous bitumen extraction process (Benson, 1969; Cormack et al., 1977; Funk, 1979; Funk et al., 1984; Meadus et al., 1982).

In the oil sands industry, it is generally recognized that the coarse sands do not cause any problem in either water or nonaqueous solvent extraction processes. On the other hand, clay minerals, especially clay minerals with an organic coating, are most detrimental. They contribute to the formation of unsettled MFT in water-based bitumen extraction processes (Omotoso & Mikula, 2004). While little is known about clay mineral behaviour and its influence on nonaqueous solvent extraction processes, it is suspected that the clay minerals are responsible for the poor recovery of nonaqueous solvents from the extraction tailings. Consequently, an understanding of the clay mineral types and their reactivities in a nonaqueous extraction process is necessary. In this work, a simulated nonaqueous extraction process was developed with the primary purpose of generating clay mineral samples. The clay minerals were studied by mineralogical and microstructural analyses as well as reactivity analyses, such as cation exchange capacity and specific surface area, in relation to the nonaqueous oil sands extraction process. In this paper, results for the nonaqueous extraction process itself are reported. Clay mineral properties and behaviour during nonaqueous extraction will be reported in a separate paper.

4.2. Materials and experimental procedures

4.2.1. Samples

Two oil sands ores, a high grade, low fines, good processing ore and a medium grade, high fines, poor processing ore, from a Syncrude lease were selected for the experiments. Here, “good” or “poor” processing is with reference to the Clark hot water extraction process (Camp, 1976). Table 4-1 shows the composition of the samples.

Table 4-1. Composition of oil sands ore samples.

Sample	Characteristics	Bitumen (wt%)	Solids (wt%) >45 μm	Solids (wt%) 2-45 μm	Solids (wt%) <2 μm	Water (wt%)
A	high grade, low fines, good processing	13.5	78.7	4.5	0.8	2.5
B	medium grade, high fines, poor processing	10.5	62.5	15.2	8.1	3.7

4.2.2. Solvent extraction tests

A mixture of aromatic (toluene) and paraffinic (heptane) solvents was used to extract bitumen from the oil sands ore samples. Toluene to heptane mass ratios were varied at 70/30, 30/70, 10/90 and 0/100. For each test, 150 grams of the oil sands ore sample were placed in a 250 mL glass bottle, to which 100 grams of the solvent were added (i.e., oil sands/solvent = 60/40). The bottle was then sealed and agitated through an end-to-end tumbling action for 10 min at 60 rpm in a rotary mixer. The mixture was then transferred to a 250 mL graduated cylinder, which was set in the upright position to allow the mixture to settle for 30 min. Two distinct layers (phases) were formed in the settling mixture. The dark liquid phase in the upper portion of the cylinder was slowly siphoned from above the demarcation line and this formed the “supernatant” product. The remaining slurry

was mixed with half of the original amount of the same solvent, agitated for a further 10 min using the rotary mixer and poured onto a 45- μm aperture stainless steel sieve. The material that went through the sieve was collected as the “secondary product”. The material remaining on the sieve was collected as the “tailings”.

Tailings produced from two solvent ratios, i.e., toluene to heptane ratios of 30/70 and 0/100, were chosen for extra washing only for bitumen recovery calculations. For this purpose, a sieve vibrator was used to shake the 45- μm sieve and another aliquot of the solvent (half of the original amount, i.e., tailings/solvent = 75/25) was used to wash the “tailings” twice. The remaining material on the sieve was collected as “tailings after the 2nd wash”. This additional tailings wash significantly increased the bitumen recovery. To emphasize, the extra wash of the tailings was performed only to improve bitumen recovery. All other data presented in this paper were obtained from samples without the extra tailings wash.

When pure heptane was used in the extraction (i.e., toluene/heptane = 0/100), a third transition layer, comprised mostly of fine solids, was formed between the supernatant and tailings. The third layer was almost the same colour as the supernatant. The heptane to bitumen ratio in the pure heptane extraction test exceeded the critical value to trigger asphaltene precipitation (Speight, 2004). Therefore, one would expect that this layer consisted mainly of asphaltene and fine solids.

Settling tests were conducted on supernatants generated from the 30/70 and 0/100 (toluene/heptane) extraction tests, to determine the water and solids contents at different settling times. Small samples of the settling supernatant, approximately 10 mL in volume, were collected for water and solids content analyses at the following time intervals: 1, 2, 3, 4, 5, 10, 15, 20 and 30 min.

4.2.3. Analytical methods

Bitumen, solids and water contents for all three fractions, i.e., the supernatant, secondary product and tailings, were determined by the Dean Stark (DS) extraction method (Bulmer & Starr, 1979). For all extraction products, supernatants and secondary products, the water content was also determined by the Karl Fischer (KF) titration method using a Mettler Toledo DL39 system. The mean value of at least three measurements is reported in this paper. Measurement accuracy was repeatedly verified by testing a standard sample with 0.1% water content. The standard deviation of the water content for KF titration was about $\pm 0.05\%$ compared to $\pm 1\%$ for Dean Stark analysis (Bulmer & Starr, 1979). The water content in the secondary product was 4 to 40 times higher and in the supernatant 10 to 900 times higher by Dean Stark analysis than by KF titration (Fig. 4.1). In addition, for some samples, the water content obtained by Dean Stark analysis was even higher than the water content in the original oil sands ore samples. For example, the water content in the secondary product of the high fines ore, B, at a toluene to heptane ratio of 10/90 was 4.8% - larger than the 3.8% value in the raw ore (Fig. 4.1 and Table 4-1). Therefore, the KF titration method was used for the samples with a low water content ($<1\%$). It cannot be used for samples with higher water contents, e.g., tailings, due to experimental limitations of this method.

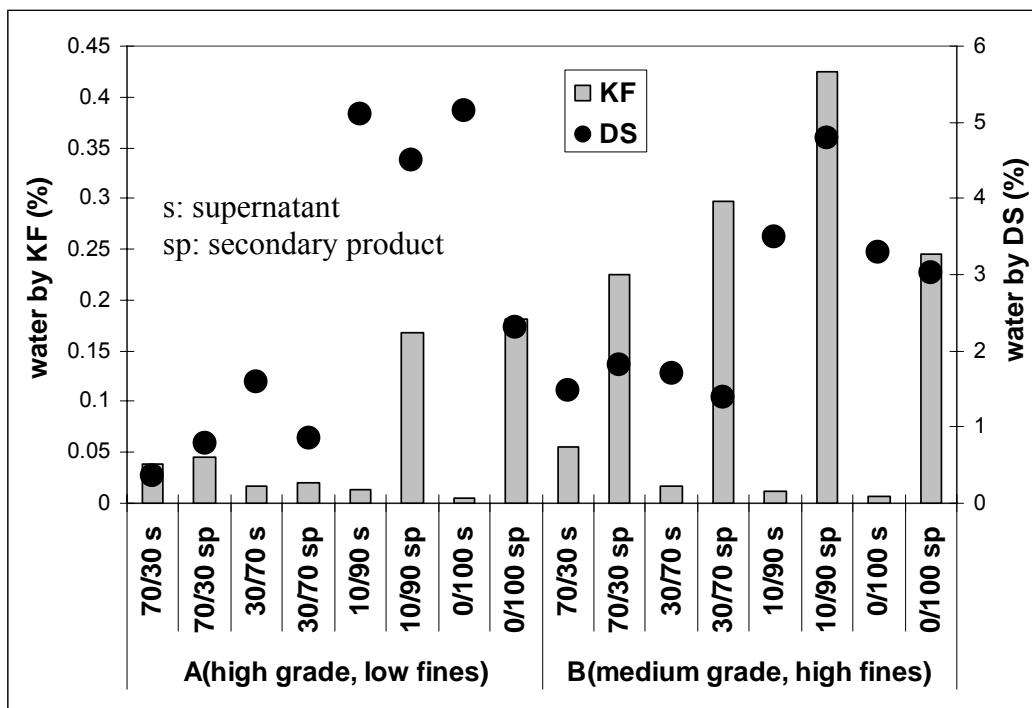


Fig. 4.1. A comparison between water content measured by the Karl Fischer titration method (KF) and Dean Stark analysis (DS) in the extraction products.

The solids content of some samples was also determined by thermogravimetric analysis (TGA) performed in Setaram Instrumentation LABSYS evo. In this analysis, the supernatant was poured in to the TG crucible and then placed on a balance, with an accuracy of 0.01 mg, for four hours to ensure the entire volatile part of the supernatant evaporated. The four-hour evaporation time was determined through trial and error. Initially, a sample was placed on the balance for only 30 min before transferring to the TG crucible. Chaotic weight recording by the TGA balance, an indication of rapid solvent evaporation, was observed in this case. The same test was repeated for 1, 2 and 3 hours evaporation time for several samples. Although no chaotic behaviour in the TGA was observed for samples left for 3 hours to evaporate, 4 hours was chosen to eliminate any possible error due to solvent evaporation. Samples were then heated in the TG analyzer to 1000 °C at 20 °C/min and then cooled down at the same rate. The weight of the sample as a function of time was recorded.

Mass balance tables were prepared using the KF results for the water content of the extraction products and DS results for the water content of the tailings. Solids and bitumen contents of all samples are based on DS analysis. Also, mass balance calculations were done with and without considering the solvent (solvent-free basis). In the former case, the total feed was calculated as the sum of the ore and solvent. It was assumed that any mass loss was due to solvent loss, mainly through solvent evaporation. In the latter case, the solvent-free basis, the solvent was not taken into account in mass balance calculations. The results presented in the current paper were obtained from the latter approach unless indicated otherwise.

Three important types of diagrams, i.e., assay, distribution and bitumen recovery, were extracted from the mass balance calculations. The assay of each component (e.g., solids) was the mass of that component in the fraction (e.g., the supernatant) over the total mass of the fraction. The distribution was calculated as the mass of the component in the fraction over the sum of that component in all fractions. Bitumen recovery was the sum of the bitumen in the main products (the supernatant and secondary product) over the sum of the bitumen in all fractions (the supernatant, secondary product and tailings).

4.3. Results and discussion

4.3.1. Bitumen recovery

The distribution of bitumen in all products is depicted in Fig. 4.2. The bitumen content in the supernatant decreased for both samples, as the toluene to heptane ratio was decreased. In the secondary product, on the other hand, the opposite trend was observed (Fig. 4.2). The total bitumen recovery (in the supernatant and secondary product) for the low fines, high grade ore sample (A) was unaffected

by the toluene to heptane ratio (Fig. 4.3); thus the loss of bitumen to the tailings was more or less the same for the toluene to heptane ratios tested (Fig. 4.2). As such, one can conclude that the lower recovery of bitumen in the supernatant (primary recovery) was compensated by an increase in the bitumen recovery in the secondary product (secondary recovery) resulting in a constant total bitumen recovery. For the high fines, medium grade ore sample (B), on the other hand, the total bitumen recovery decreased as the toluene to heptane ratio was decreased, meaning that the loss of bitumen to the tailings increased at lower toluene to heptane ratios (Figs. 4.2 and 4.3).

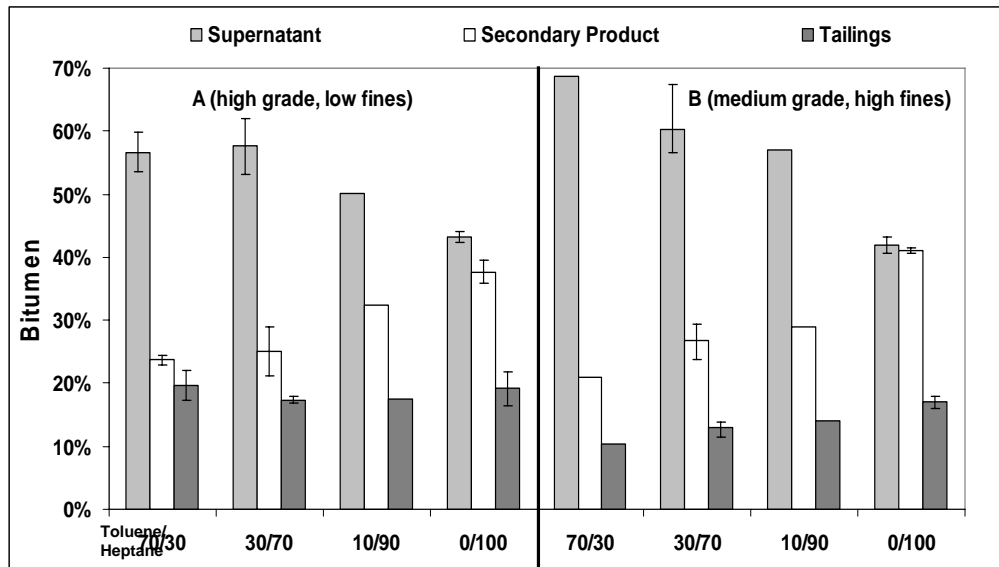


Fig. 4.2. Bitumen distribution in all three products. Error bars show differences in the values of two or three extraction tests.

At first glance, it might seem unexpected that bitumen recovery is higher for the medium grade, high fines ore (Fig. 4.3). However, when analyzing data presented in Fig. 4.3, it has to be taken into account that the mass ratio of solvent to ore (not solvent to bitumen, S:B, also plotted in Fig. 4.3) was kept constant during the extraction procedure. Therefore, more solvent was used relative to the amount of

bitumen for the high fines ore sample, since this sample had a lower bitumen content.

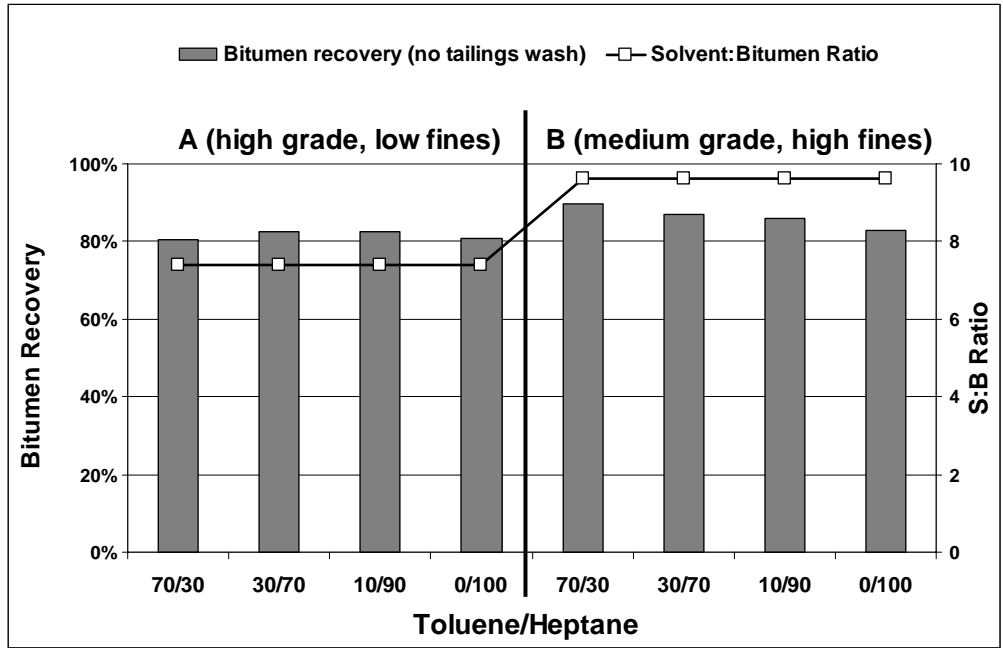


Fig. 4.3. Bitumen recovery and corresponding solvent to bitumen (S:B) ratio.

Toluene to heptane ratio did not notably influence bitumen recovery (Fig. 4.3), especially for the low fines ore sample. This seemed to contradict the conventional wisdom about the solubility of bitumen in paraffinic solvents. Paraffinic solvents, such as heptane, are not able to dissolve the resin and asphaltene components of bitumen entirely. Therefore, one would expect to see a decrease in bitumen recovery with decreasing toluene to heptane ratio, especially for pure heptane. It should be noted that total bitumen recovery was about 80% for the low fines ore sample (A) and slightly higher for the high fines ore sample (B) by using the one-step tailings wash. It was not clear if the lost bitumen was due to the non-aggressive (gentle mixing) extraction procedures or due to the precipitated resins and asphaltenes. It is possible that some of the bitumen – likely trapped in clays aggregates - was not exposed to enough solvent during extraction,

contributing to the low bitumen recovery shown in Fig. 4.3. However, in the high fines ore sample (B) extraction tests, the bitumen distribution in the tailings increased from 10 to 16% with decreasing toluene content in the solvent (Fig. 4.2), suggesting that the residual bitumen in the tailings was likely in the form of asphaltene-clay aggregates with sizes greater than 45 μm so that they were retained on the 45 μm sieve.

The purported advantage common to solvent extraction processes is the high bitumen recovery for all grades of oil sands (Benson, 1969; Savage, 1971). In order to obtain high bitumen recovery, an extra two-step tailings wash was applied, together with sieve shaking, to dissolve the residual bitumen and/or liberate the trapped bitumen. The total bitumen recovery after the additional two-step tailings wash (Fig. 4.4) was increased to 98.2% for the low fines ore sample (A) and 98.4% for the high fines ore sample (B) at a toluene to heptane ratio of 30/70, and to 96.1% for the low fines ore sample (A) and 96.2% for the high fines ore sample (B) at a toluene to heptane ratio of 0/100. Precipitation of resins and asphaltenes, insoluble components of bitumen in pure heptane, was responsible for the decrease in bitumen recovery using pure heptane (e.g., see (Sparks et al., 1992).

Total bitumen recovery is very high (>96%) for both samples, “good” and “poor” processing (Fig. 4.4). This could be an advantage for the proposed nonaqueous extraction process over the hot water extraction process. When comparing bitumen recovery values for the two ores, i.e., high grade, low fines, “good” processing (A) and medium grade, high fines, “poor processing” (B), it has to be taken into account that more solvent was used relative to the amount of bitumen for sample B since the mass ratio of solvent to ore (not solvent to bitumen; S:B) was kept constant during the extraction procedure.

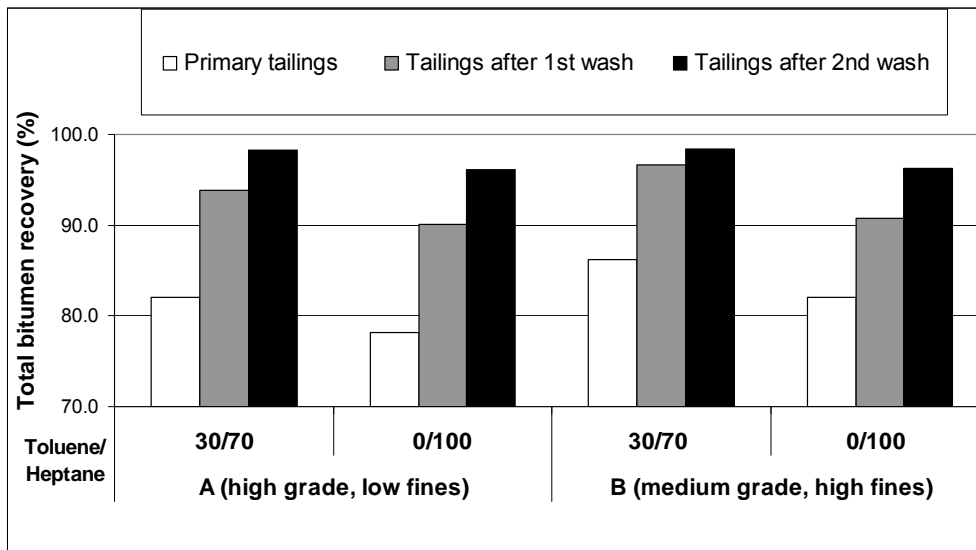


Fig. 4.4. Total bitumen recovery based on the mass of the remaining bitumen in the tailings after a 2nd wash.

However, the primary objective of the current solvent extraction study was not to develop an “optimized” solvent extraction procedure. The purpose was to treat the oil sands with organic solvents of different aromaticity (i.e., mixtures of different proportions of typical aromatic and aliphatic solvents), and collect clay samples to study their mineralogy and deportation during the solvent extraction process. Therefore, the 2nd wash was not used in all tests to maximize bitumen recovery.

4.3.2. Product quality

The supernatant was almost pure bitumen (over 99.5 wt% bitumen) in most cases. The amount of bitumen was lower (from 94.28 wt% to 98.85 wt%) in some cases, especially when pure heptane was used (Table 4-2, Fig. 4.5). As mentioned before, data were based on solvent-free based mass balances. It should be noted that the solvent was the main component of both the supernatant and secondary products (82-88 wt%). The amount of bitumen in the supernatant varied from about 16 to 18 wt% for the low fines ore (A) and from about 12 to 15 wt% for the high fines ore (B) if the solvent was included in the mass balance calculations. In

both cases, with and without solvent, the supernatant and secondary products from the low fines ore sample had higher bitumen contents than the extraction products from the high fines ore sample, except when pure heptane was used in the extraction (Table 4-2 and Fig. 4.5).

There was a very small amount of solids in the supernatant (less than 0.1 wt% for the low fines ore sample and less than 0.2 wt% for the high fines ore sample) when toluene was included in the extraction process. The exception was the toluene to heptane ratio of 30/70. The higher solids content when only heptane was used for extraction was likely due to the precipitation of paraffin insoluble components of bitumen, i.e., resins and asphaltenes. As mentioned above, a transitive layer was formed between the supernatant and tailings when pure heptane was used as the solvent. This layer is probably composed of aggregates of clay particles and asphaltene precipitates.

Table 4-2. Supernatant assays based on solvent-free mass balance calculations*.

<u>Ore</u>	<u>Toluene/Heptane</u>	-	<u>Bitumen</u> <u>(wt%)</u>	<u>Solids</u> <u>(wt%)</u>	<u>Water</u> <u>(wt%)</u>
A	70/30	min-max	99.68-99.75	0.03-0.11	0.21-0.22
		average	99.72	0.07	0.21
	30/70	min-max	96.62-99.88	0.02-3.33	0.09-0.10
		average	98.24	1.67	0.09
	10/90		99.84	0.08	0.08
	0/100	min-max	96.12-97.34	2.63-3.78	0.03-0.04
average		96.75	3.21	0.04	
B	70/30		99.5	0.13	0.37
	30/70	min-max	94.76-99.75	0.13-5.14	0.07-0.11
		average	96.78	3.13	0.09
	10/90		99.72	0.19	0.09
	0/100	min-max	98.85-94.28	5.65-1.10	0.07-0.05
		average	96.57	3.37	0.06

* The average values given are from two extractions, except for sample B treated in toluene/heptane = 30/70 which is from three extractions. Only one extraction test was performed on samples without an average value.

The heptane to bitumen ratios for both samples and all solvent ratios were calculated and are presented in Table 4-3. Comparison of Table 4-2 and Fig. 4.5 indicates that the water content in the supernatant decreases with increasing heptane to bitumen ratio. In paraffinic froth treatment, it is well known that heptane removes the emulsion water from the hydrocarbon phase. Tipman et al. (Tipman et al., 2001) also showed that aromatic impurities such as toluene in heptane increase the required heptane to bitumen ratio for removing emulsion water from the hydrocarbon phase. Therefore, the observed relationship between water content and heptane to bitumen ratio is in an excellent agreement with the findings from the paraffinic froth treatment, even though addition of water was eliminated in the nonaqueous extraction used here. In fact, except for the toluene to heptane ratio of 70/30, the water content for each of the supernatants was very low (less than 0.1 wt%, Table 4-2 and Fig. 4.5). At the heptane to bitumen ratios used the water-in-oil emulsion was broken (Tipman et al., 2001), so that the very low water content detected in the supernatant was most likely due to water that was attached to the very fine solids. Although water content in the secondary product is almost one order of magnitude higher than in the supernatant for the high fines ore, it is in the same range for the low fines ore (Fig. 4.6). This could be another indication of the above hypothesis about the relationship between water and fine solids. This relationship is explained in more detail in the settling time section (Section 4.3.3).

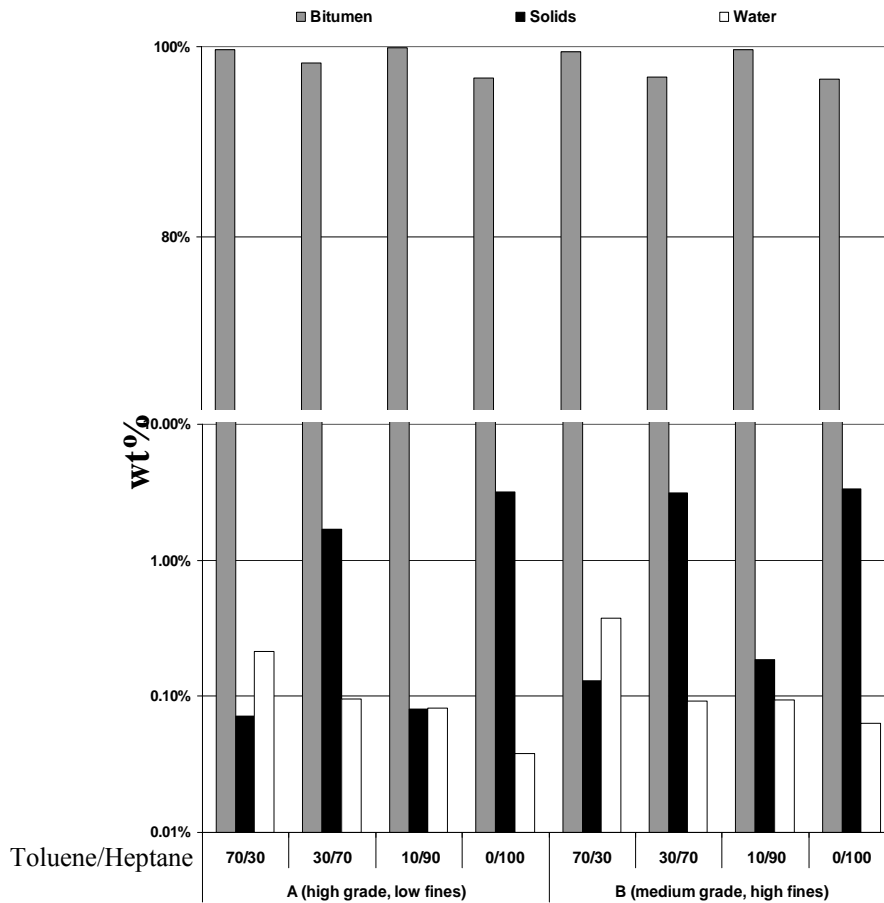


Fig. 4.5. Supernatant assays from mass balance calculations – average values are from Table 4-2, using water content values from the KF titration method. Standard deviation is $\pm 1\%$ for bitumen and solids (measured by Dean Stark) and $\pm 0.05\%$ for water (measured by Karl Fischer titration)

Solids content, on the other hand, does not show such a relationship with the heptane to bitumen ratio. Comparing Table 4-3 and Fig. 4.5 shows a very low solids content (~ 0.1 wt%) for the lowest heptane to bitumen ratio and very high solids content (> 3 wt%) for the highest heptane to bitumen ratio. Therefore, it appears that the solids content in the supernatant increases when the heptane to bitumen ratio increases, with the exception of the toluene to heptane ratio of 30/70 which seems to be an anomaly. The high solids content, for samples with heptane to bitumen ratios equal to about five and higher, was possibly due to the precipitation of asphaltene. In fact, Tipman et al. (Tipman et al., 2001) observed massive asphaltene precipitation at room temperature when the heptane to

bitumen ratio was five, although their work was performed on a bitumen froth that was produced from water-based extraction.

Table 4-3. Calculated values for heptane to bitumen ratio at different toluene/heptane ratios for the two oil sands samples.

	<u>Toluene/Heptane</u>			
	70/30	30/70	10/90	0/100
Ore	<u>Heptane/Bitumen</u>			
A	1.48	3.46	4.44	4.94
B	1.90	4.44	5.71	6.35

The oil sands industry desires bitumen products from the oil sands that contain less than 0.5 wt% water and solids, because this product can be sent directly to the upgraders. The proposed extraction procedure in this research was, therefore, successful with respect to bitumen product quality.

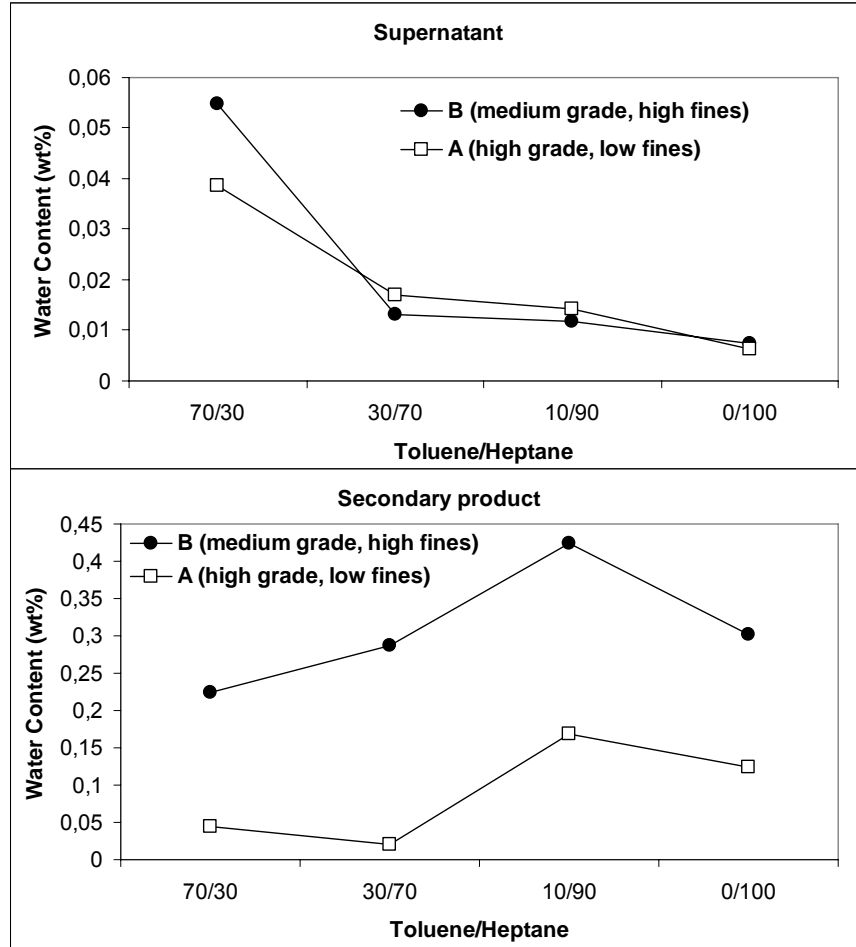


Fig. 4.6. Water content in extraction products by Karl Fischer titration. Standard deviation is $\pm 0.05\%$.

4.3.3. Settling time

Settling tests on the supernatants from the extraction tests at toluene to heptane ratios of 30/70 and 0/100 were conducted to see if the settling time could be shortened while still maintaining bitumen product quality. In these tests, water and solids contents were measured by KF titration and TGA, respectively.

For the toluene to heptane ratio of 30/70, initially, the solids content in the high fines sample (B) was significantly higher than that in the low fines sample (Fig. 4.7). The higher fines content in the poor processing ore (B) seemed to be

responsible for the high solids content of the supernatant. Water and solids contents decreased dramatically after 2-3 min for both samples, especially the high fines ore sample (B). The amounts of solids and water in the supernatant were negligible after 10 min settling, indicating that the optimum settling time in the extraction could be shortened to less than 10 min without affecting product quality (Fig. 4.7).

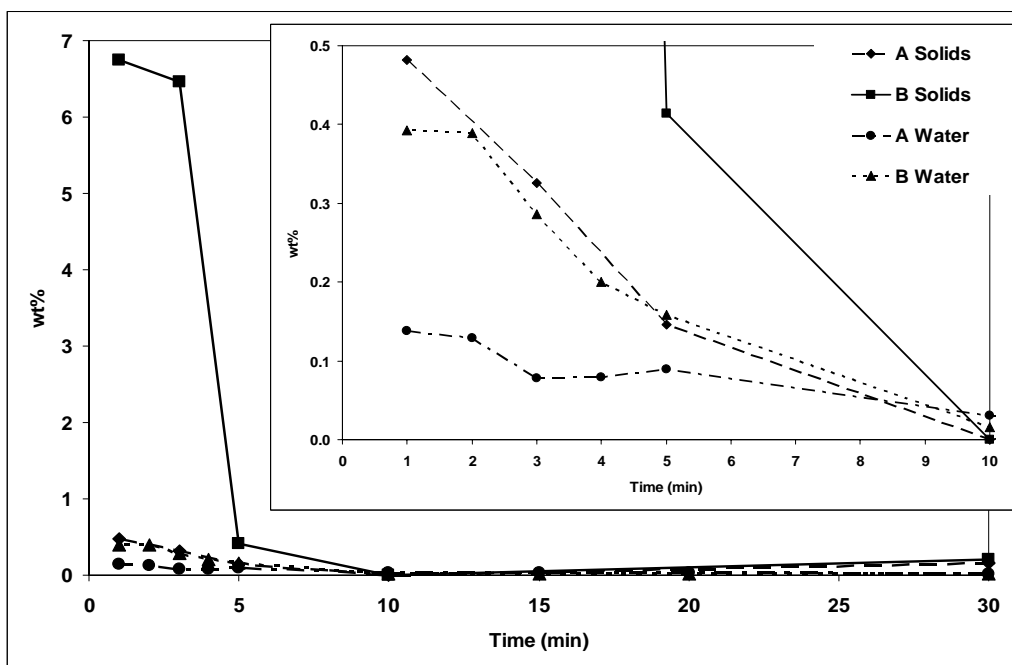


Fig. 4.7. Water and solids contents of the supernatant with a toluene to heptane ratio of 30/70 at different settling times analyzed by the KF titration and TGA, respectively. Standard deviation is $\pm 0.05\%$ for water contents.

For the toluene to heptane ratio of 0/100, no trend was observed for any of the samples at the beginning of the settling ($t < 10$ min). As mentioned in Section 3.2., precipitation of asphaltene increased when only heptane was used in the extraction. The asphaltene precipitates seem to be responsible for the initial chaotic-look of the plots in Fig. 4.8 for initial settling times ($t < 10$ min). There may be an “incubation” period for the fine asphaltene particles to assemble themselves into relatively larger aggregates as settling begins.

It seems that settling started with a delay for pure heptane, when compared with the toluene to heptane ratio of 30/70. In any event, the solids and water content dropped after 10 min in all instances (Fig. 4.8). The desirable product quality was reached after 30 min, based on the solids and water content when pure heptane was used as the solvent.

An interesting feature was observed in Figs. 4.7 and 4.8 when comparing the solids and water contents in the supernatant. Although the amount of water was small, the decrease in the water content seemed to follow the trend for decrease in the solids content. This could indicate that the small amount of water detected in the supernatant was attached to the solid particles rather than in a separate phase.

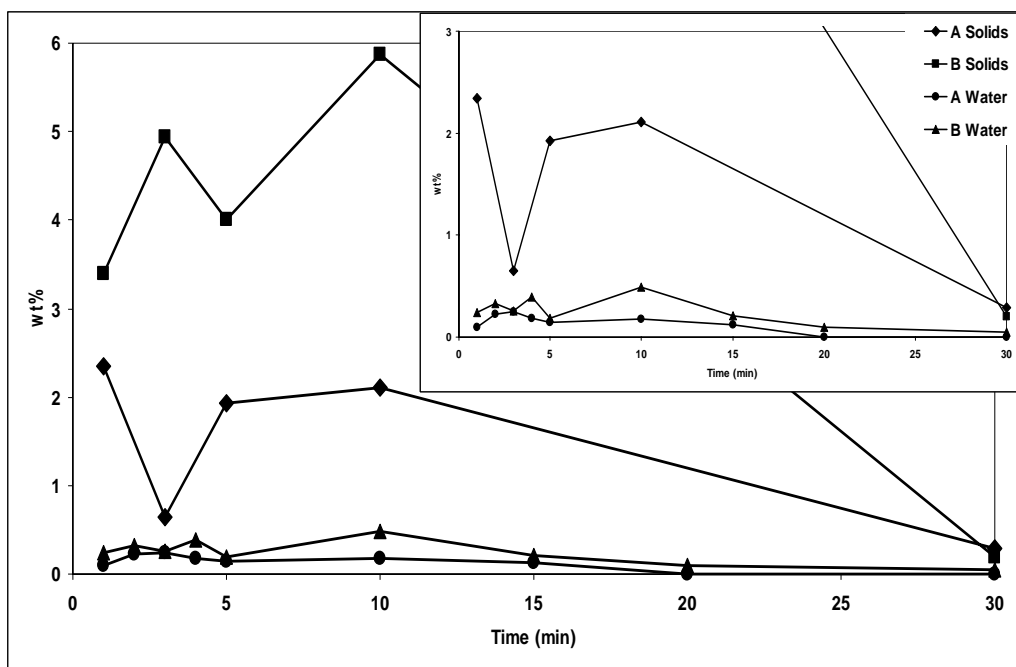


Fig. 4.8. Water and solids contents of the supernatant with a toluene to heptane ratio of 0/100 at different settling times analyzed by the KF titration and TGA, respectively. Standard deviation is $\pm 0.05\%$ for water contents.

4.4. Conclusions

Two different oil sands samples were treated by simulated, nonaqueous solvent extraction in laboratory conditions without the use of any water. Total bitumen recovery was higher than 98% for both the high grade, low fines ore (A) and the medium grade, high fines ore (B). The results indicated that, unlike the water extraction process, the solvent extraction procedure was not sensitive to the fines and clays contents of the oil sands ores or to the ore grade, at least for medium and high-grade ores.

The solvents used in the extraction process were toluene and heptane at four different ratios, 0/100, 10/90, 30/70, 70/30. The toluene to heptane ratio did not affect bitumen recovery from the high grade, low fines, good processing ore (A), but it affected the medium grade, high fines, poor processing ore (B). Bitumen recovery for the poor processing ore (B) decreased as the amount of toluene decreased. In addition, as the amount of toluene was decreased, bitumen content decreased in the supernatant and increased in the secondary product.

A desirable product, bitumen with less than 0.5 wt% solids and water, was produced during extraction at room temperature. Carrying out the extraction process at room temperature would lower the extraction cost significantly. Heptane to bitumen ratios used in this study were high enough for the paraffinic solvent, heptane, in the presence of the aromatic component, toluene, to remove emulsion water from the hydrocarbon phase, but mostly were below the critical ratio for the precipitation of asphaltene. Based on the solids and water contents in the supernatant during gravity settling tests, the optimum settling time to achieve desirable product quality was about 10 and 30 min when toluene to heptane ratios were 30/70 and 0/100, respectively.

Acknowledgements

The authors are grateful to the Centre for Oil Sands Innovation (COSI) for providing research funding and to Syncrude Canada Ltd and Imperial Oil Resources Ltd for providing samples.

4.5. References

- Alberta Energy (2010). Oil sands. Alberta Government, www.energy.gov.ab.ca/OurBusiness/oilsands.asp.
- Benson, A. M. (1969). Filtration of solvent/water extracted tar sand. US Patent No. 3 459 653.
- Bulmer, J.T., & Starr, J. (1979). Syncrude analytical methods for oil sand and bitumen processing. Alberta Oil Sands Technology and Research Authority (AOSTRA), Edmonton, Canada.
- Camp, F. W. (1976). The tar sands of Alberta, 3rd ed., Cameron Engineers Inc., Colorado, USA.
- Cormack, D. E., Kenchington, J. M., Phillips, C. R., & Leblanc, P. J. (1977). Parameter and mechanisms in the solvent extractions of mined Athabasca oil sand. *The Canadian Journal of Chemical Engineering*, 55, 572-80.
- FTFC (Fine Tailings Fundamentals Consortium) (1995). Vol.1, Clark hot water extraction fine tailings, In: *Advances in oil sands tailings research*, Alberta Department of Energy, Oil Sands and Research Division, Edmonton, Canada, 5-57.
- Funk, E. D. (1979). Behaviour of tar sand bitumen with paraffinic solvents and its application to separations for Athabasca tar sands. *The Canadian Journal of Chemical Engineering*, 57, 333-41.
- Funk, E. D., Pirkle, J. C., & May, W. G. (1984). Processing approach for the solvent extraction of Athabasca tar sands. *Energy Progress*, 14, 12-16.
- Meadus, F. W., Bassaw, B. P., & Sparks, B. D. (1982). Solvent extraction of Athabasca oil-sand in a rotating mill part 2. Solids—liquid separation and bitumen quality. *Fuel Processing Technology*, 6(3), 289-300.
- Omotoso, O. E., & Mikula, R. J. (2004). High surface areas caused by smectitic interstratification of kaolinite and illite in Athabasca oil sands. *Applied Clay Science*, 25(1-2), 37-47.
- Savage, W. E. (1971). Process for extracting tar from tar sand. US Patent No. 3 553 099.

Sparks, B. D, Meadus, F. W, Kumar, A., Woods, J. R. (1992). The effect of asphaltene content on solvent selection for bitumen extraction by the SESA process. *Fuel*, 71(12), 1349-53.

Speight, J. G. (2004). Petroleum asphaltenes Part 1 Asphaltenes, resins and the structure of petroleum. *Oil and Gas Science and Technology - Rev. IFP*, 59, 467-77.

Sustainable Development Business Case Report (2006). “Clean Conventional Fuel - Oil and Gas”, version 1, November.

Tipman, R., Long, Y-Ch., Shelfantook, W. E. (2001). Solvent process for bitumen separation from oil sands froth. US Patent No. 6 214 213 B1.

Water Use in Alberta Oil Sands. (2007). PTAC – May 29, Water Innovation in the Oil Patch Forum.

Chapter 5

Clay minerals in nonaqueous extraction of bitumen from Alberta oil sands. Part 2: characterization of clay minerals¹

5.1. Introduction

The Alberta oil sands deposit is the second largest source of oil after Saudi Arabia and the largest oil sands deposit on the planet with approximately 1.7 trillion (1.7×10^{12}) barrels of bitumen in-place. Of the 1.7 trillion barrels of bitumen, 170 billion (0.17 trillion) barrels are proven reserves (Alberta Oil Sands Technology and Research Authority, 1990; Alberta Energy, 2010). This deposit consists of bitumen (4-18 wt%), sands (55-80 wt%), fine solids (particles smaller than 44 μm (5-34 wt%)) and water (2-15 wt%) (Bichard, 1987). In 2008, the average production of crude oil from the Alberta oil sands was 1.31 million barrels/day according to the Alberta Energy and Utilities Board (AEUB). The production is anticipated to reach three million barrels per day by 2018 (Alberta Energy 2010).

The important role of clay minerals in the bitumen extraction process has been reported by many researchers. Clay minerals cause problems in all crucial stages of bitumen extraction, and affect bitumen recovery and waste management. Certain clay minerals, such as montmorillonite and kaolinite, have been reported to have a negative influence on bitumen extraction from the oil sands (Liu et al., 2004). Mutual interactions between organic materials, especially bitumen, and clay minerals significantly affect both extraction recovery and product quality. Such interactions were reported to result in clay-organic complexes making the

¹ The contents of this chapter have been submitted for publication in the journal *Fuel Processing Technology*. Hooshiar, A., Uhlik, P., Etsell, T. H., Ivey, D. G., & Liu, Q. (2011). Clay minerals in nonaqueous extraction of bitumen from Alberta oil sands. part 2. characterization of clay minerals. *Fuel Processing Technology* (submitted).

bitumen extraction process complicated (Clementz, 1976; Czarnecka & Gillott, 1980; Ignasiak et al., 1983). In addition, the flocculation/dispersion behaviour of the clay minerals has been found to directly control the settling behaviour of the tailings. Clay minerals can also have major influences on the bitumen extraction process by affecting water chemistry (Omotoso et al., 2002). The mineralogy of clay minerals in the Alberta oil sands has been studied and a summary of these studies can be found in papers by Kaminsky et al. (2009) and Omotoso and Mikula (2004). Based on such studies, the mineralogy of clay minerals in the Alberta oil sands deposit varies across the deposit. Kaolinite, illite, smectite and chlorite are found to be the major clay minerals in the Alberta oil sands deposits with the first two being the most abundant. However, the mixed layer clay minerals, illite-smectite and kaolinite-smectite, cannot be neglected even when present in low quantities. These mixed layer clay minerals have been shown to be responsible for the extraordinarily high surface areas and cation exchange capacities of the tailings solids (Omotoso and Mikula, 2004; Kaminsky et al., 2008).

Although the behaviour of clay minerals in water-based bitumen extraction has been studied by many researchers, there is limited information on the behaviour of clay minerals in nonaqueous bitumen extraction. This information is of great importance since clay minerals may behave completely differently in the presence or absence of water. Several studies have been reported on the solvent-based bitumen extraction from the oil sands, but none included the role clay minerals played (Funk et al., 1984; Tis et al., 1984; Leung & Phillips, 1985; Tipman et al., 2001). Although the study by Meadus et al. (1982) has included the role of fine solids in the solvent extraction-spherical agglomeration (SESA), this process cannot be considered as nonaqueous extraction since a large amount of water was used at the agglomeration stage. To the authors' knowledge, there has not been any study on the clay minerals in a completely nonaqueous bitumen extraction process. This shortage of information on the clay mineralogy, distribution and behaviour of clay minerals during nonaqueous bitumen extraction from the

Alberta oil sands was the motivation for the current study. The details about nonaqueous bitumen extraction from the Alberta oil sands have been described in the previous chapter. The current chapter is focused on the clay minerals in such an extraction process.

5.2. Materials and experimental procedures

5.2.1. Oil sands ore samples

Two oil sands ores, designated as A and B, from a Syncrude lease, were selected for the experiments. Ore A is a high grade (13.5% bitumen), low fines (5.3%), good processing ore and ore B is a mid grade (10.5% bitumen), high fines (23.3%), poor processing ore. The clay ($< 2 \mu\text{m}$) contents of ores A and B are 0.8 and 8.1 wt%, respectively. “Good processing” and “poor processing” are terms indicating the level of bitumen recovery and quality for water-based bitumen extraction. Visual inspection showed some differences between the samples in terms of the presence of clay lumps. While ore B contained visible clay lumps ranging in size from a few mm up to 100 mm, ore A appeared to be homogenous without visible clay lumps. Detailed specifications of the two ore samples can be found in Hooshlar et al. (2011). The raw ore samples were manually homogenized and kept frozen in portions of 3-4 kg in sealed plastic bags.

5.2.2. Solvent extraction

In a typical extraction test, the oil sands ore sample and the solvent were mixed at a ratio of 60 wt% oil sands (150 g) and 40 wt% solvent (100 g). The solvent that was used in the extraction was a mixture of aromatic (toluene) and paraffinic (heptane) solvents at two weight ratios, i.e., toluene to heptane weight ratios (T/H) of 30/70 and 0/100. These two ratios were selected among the four ratios previously used for the nonaqueous extraction (Hooshlar et al., 2009). The 30/70

toluene to heptane ratio was selected because it was the optimum ratio for the bitumen extraction. The 0/100 toluene to heptane ratio was chosen in order to compare the system in the presence and absence of an aromatic solvent (toluene). The extraction resulted in three products, i.e., the supernatant, secondary product and tailings (the nonaqueous extraction procedure is described in more detail in Chapter four). Solids that were contained in the top 100 mL (of the 250 mL graduated cylinder) of the supernatant after settling for either 1 min or 7.5 min were used in the mineralogical characterization studies.

5.2.3. Clay particle separation

After homogenizing, approximately 50 g of each of the oil sands ores were centrifuged with toluene to remove the bitumen. The centrifugation was repeated several times, each time with fresh toluene, until a clear liquid over the solids was obtained. After extraction bitumen was removed from the solids obtained from the supernatants (extraction products) using the same procedure. Subsequently, after the solids were dispersed in water, clay (0.2-2 μm) and ultrafine clay (<0.2 μm) size fractions were separated by gravity sedimentation and centrifuging. Stokes' law was used to calculate the sedimentation time and centrifugation conditions in order to obtain the desired particle size.

5.2.4. X-ray diffraction (XRD) analyses

The Millipore[®] filter transfer method, a glass slide method, was used to prepare oriented XRD samples from a fully dispersed water suspension of clay (0.2-2 μm) and ultrafine clay (<0.2 μm) fractions. In order to promote the basal plane preferred orientation and prevent the flocculation of clay particles in the suspension, the suspension was treated in an ultrasonic bath for 10 min. In order to identify possible expandable clay minerals such as smectite or illite-smectite pre-treatments, such as saturating the samples with ethylene glycol (EG) or at

54% relative humidity (54% RH), were applied (Moore and Reynolds, 1997). XRD profiles were obtained from a Rigaku RU-200B diffractometer with a cobalt rotating anode operating at 40 kV. The samples were run from $2\theta=3^\circ$ to $2\theta=58^\circ$ at a step of 0.02° . The areas under the peaks on the XRD profiles were measured using JADE 7 software after identifying XRD peaks manually. Profiles of the pure clay minerals, illite and kaolinite, were simulated using NEWMOD[®]. The reference intensity ratio (RIR) method was used for quantifying the clay minerals in the samples (Moore & Reynolds, 1997). The first two peaks of kaolinite and the first and third peaks of illite, I(001) and I(003), were used to quantify the amount of illite and kaolinite in each sample. The second peak of illite, I(002), was used as the standard. I(003) and one of the quartz peaks, Q(101; $d=0.343$ nm), overlapped at 2θ of about 31° in XRD profiles. Instead of deconvoluting this peak to two peaks using JADE 7, the area under each peak was calculated manually. Based on the intensities for quartz peaks, the area under the peak for Q(101) was 4.3 times larger than the area under the peak for Q(100; $d=0.426$ nm). Therefore, the area under the peak for I(003) was calculated by subtracting the calculated area for Q(101) from the area under the peak at 2θ of about 31° .

5.2.5. Transmission electron microscopy (TEM) investigations

Two types of samples, dispersed samples and ultrathin sections, were used in TEM analysis. Clay size particles were diluted with deionized water to an approximate concentration of 1 mg solids/40 mL water in the preparation of the dispersed samples. In order to fully disperse the clay mineral particles, the resulting slurry was treated in an ultrasonic bath for at least 5 min. One drop of the solution was then placed on a lacey, carbon-coated, copper grid. A JEOL 2010 transmission electron microscope (TEM), operated at 200 kV, was used in the TEM investigations of dispersed samples. The length and width of several hundred clay mineral particles in the images were then measured and compiled.

Ultrathin sections were prepared using fragments of the dried solids after clay size separation. The solids were first coated with agar and then immersed in water. Afterwards, they were embedded in resin using the method of Tessier (1984) and Elsass et al. (1998). The water was replaced in the agar-coated solids by sequentially immersing them in methanol, propylene oxide and finally Spurr resin to ensure all pores and free spaces had been impregnated. The Spurr resin was then polymerized for 72 hr. After polymerization, ultrathin sections (<70 nm thick) were cut using a Reichert Ultracut E microtome with a diamond knife. The microtome slices were captured on a lacey, carbon-coated, copper grid.

Bright field high-resolution TEM (HRTEM) images were taken with both JEOL 2010 and JEOL 2022 FS microscopes operated at 200 kV. In order to minimize beam damage to the sample, the electron beam was defocused so that the image was barely visible on the screen. Sample height was adjusted to the point of minimum contrast and the objective lens was slightly under focused for lattice fringe imaging. In order to find the proper orientation for imaging, the maximum contrast for lattice fringes of the aluminosilicate layers normal to the stacking direction of the layers in each case was used. In HRTEM lattice fringe images from clay minerals, the distance between the two sequential similar lines (dark-dark or bright-bright) corresponds to the basal spacing of the clay mineral. The thickness and basal spacing of many particles were measured from HRTEM images. Illite RM30, with a known basal spacing of 1.0 nm, was used as a standard for calibration purposes in such measurements. Detailed information about illite RM30 is available in the study by Eberl et al. (1987). In order to calculate the maximum expandability of illite–smectite (%S Max) according to the following equation by Środoń et al. (1990), particle thickness and the number of interlayers per particle were used:

$$\%S \text{ Max} = \frac{(T + N_0 D_s) - (D_l (N + N_0))}{(N + N_0)(D_s - D_l)} \times 100\% \quad (5-1)$$

In the above equation, T is the “total” measured thickness, N_0 is the number of crystals measured for a given sample, and N is the “total” number of measured interlayers. D_S and D_I are the basal spacings for smectite (1.35 nm) and illite (1.0 nm), respectively. Here, the percentage of smectitic interlayers per illite–smectite crystal is calculated as the maximum expandability, %S Max, since the edge layers are smectitic in nature (Środoń et al., 1990).

5.2.6. Scanning electron microscopy (SEM) investigations

A small amount of each of the solid samples, ores and tailings, was placed on carbon tape supported by aluminum holders (12 mm in diameter). A drop, approximately 0.05 mL, of each supernatant was placed on similar holders covered with carbon tape. Afterwards, the liquid was allowed to evaporate. Since samples contained organic materials, they were studied in a low-pressure SEM (Hitachi S-3000N), operated at 15 kV, at a working pressure of 50-70 Pa. Frozen oil sands ores were also studied using a JEOL 6301F SEM equipped with an Emitek K1250 cryogenic system. Both secondary electron (SE) and backscattered electron (BSE) detectors were used for imaging. Unknown particles were chemically analyzed using energy dispersive x-rays (EDX). Unfortunately, EDX could not be used to differentiate the clay minerals from each other, since the clay mineral particles were very small and agglomerated.

5.3. Results and discussion

5.3.1. Characterization of clay minerals in the oil sands ores

5.3.1.1. Low-pressure SEM investigations

Environmental SEM images of the raw oil sands ores showed the existence of very fine particles – considered to be mostly clay particles due to the small size –

not only in the water layer but also attached to the sand grains and, more importantly, inside the bitumen phase (Fig. 5.1). This contradicts the old model for the oil sands components, which considered that the clays were only in a water film (Camp, 1976). Therefore, it is not only during bitumen extraction that clay particles come in contact with the bitumen phase, but some clay particles are initially bound to the bitumen in the raw oil sands ore. Our observation is in agreement with a previous paper by Sparks et al. (2003). They have described the strong organic matter-clay particle interaction and reported that this interaction existed in the original oil sands.

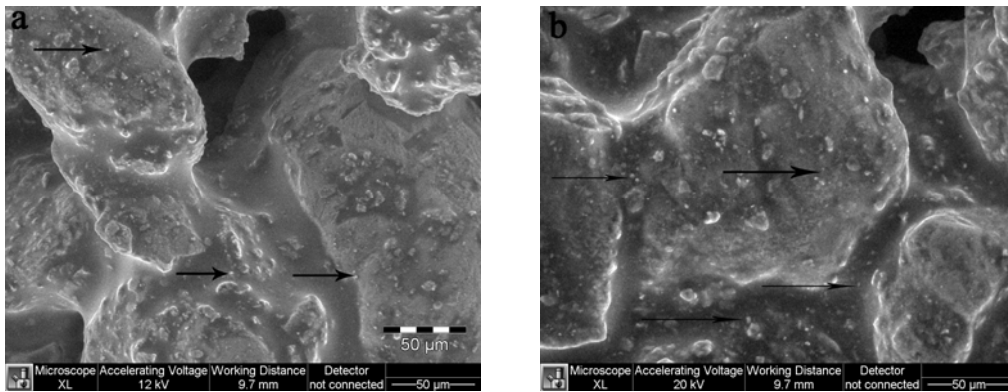


Fig. 5.1. Environmental SEM images of the raw oil sands ore showing the very fine (clay) particles attached to the large sand grains. Bitumen is most probably present in dark channels among sand grains. Arrows show some small clay particles as an example.

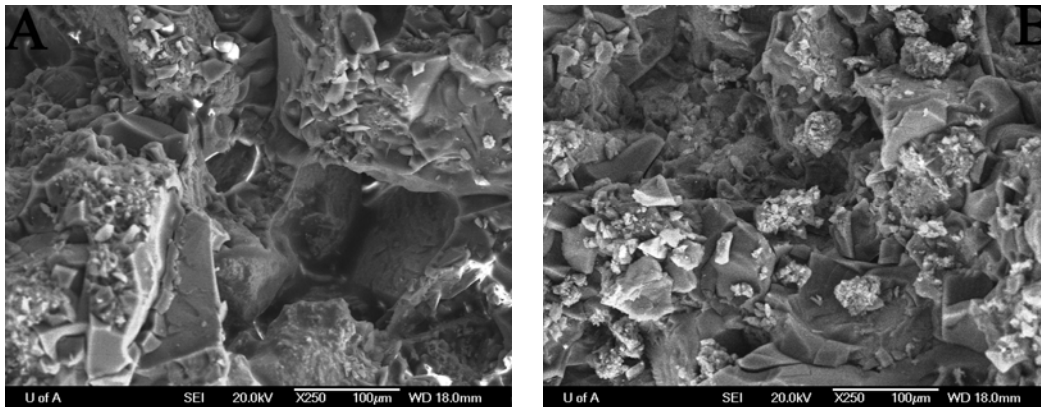


Fig. 5.2. Cryo-SEM secondary electron images of raw oil sands ores, A and B, showing agglomerates of clay particles in ore B.

SEM observations showed some differences between the raw oil sands ores, A and B. While a significant number of clay aggregates (less than $\sim 200 \mu\text{m}$ in size) were found in SEM images from ore B, these aggregates were not observed in ore A (Fig. 5.2). Similar aggregates have been observed by Sparks et al. (2003) after a cold water agitation test. The bitumen trapped in these aggregates may be one of the reasons for the lower bitumen recovery from ore B than from ore A in the water extraction process (Hooshiar et al., 2009).

5.3.1.2. TEM analyses

Several TEM images from the clay ($0.2\text{--}2 \mu\text{m}$) fraction of the oil sands ores were analyzed. A wide range of particle sizes, from a few nanometres to hundreds of nanometres, was observed in both samples A and B. In general, most particles were pseudo-hexagonal or irregular in shape. Some lath-like particles were also observed in the TEM images (Fig. 5.3). Although the samples were prepared from a very dilute solution sonicated longer than 10 min, the majority of the particles were found in the form of aggregates (Fig. 5.3a).

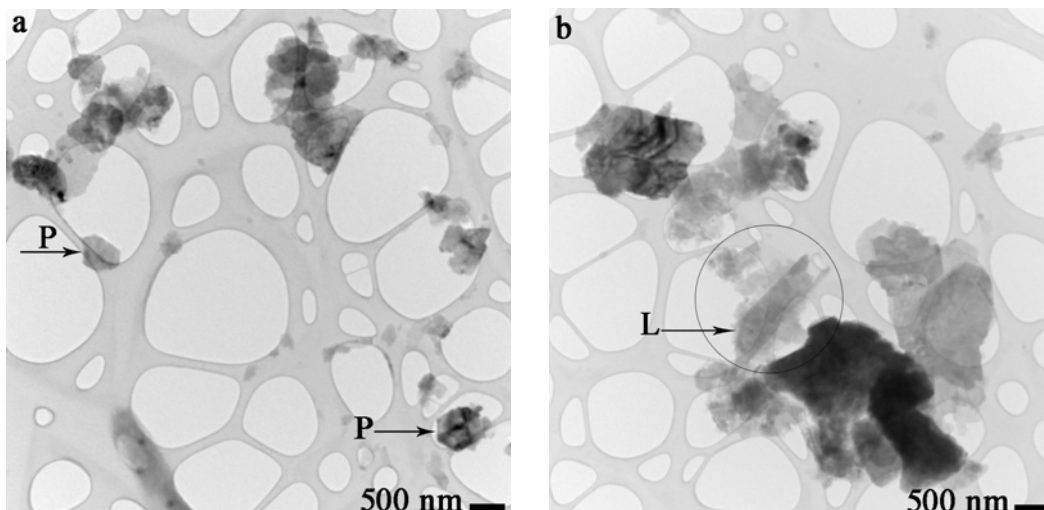


Fig. 5.3. TEM images of dispersed samples from the $0.2\text{--}2 \mu\text{m}$ fraction of oil sands ore A showing pseudo-hexagonal (P) and lath-like (L) particles.

TEM images were used for measuring the length and width of several hundred particles. These measurements as well as their average values, length to width ratios, mean particle areas and their standard deviations are shown in Table 5-1. The mean particle area was calculated by multiplying the average length by the average width. Standard deviation values for length, width and mean particle area were very close to the mean values for these parameters (Table 5-1). A similar relationship was reported for micas (Nadeau, 1987). The mean particle area for sample B (high fines content) is significantly smaller than for sample A (low fines content). Slightly higher length to width ratios for sample B may be due to the higher abundance of the lath-like particles (characteristic of illitic particles). These observations are in agreement with the higher illite content (including illite-smectite) of this sample based on XRD analysis which will be discussed later.

Table 5-1. Length and width measurements for dispersed particles in oil sands ores A and B. Mean area was calculated by multiplying the average length by average width.

	<u>Size fraction</u>	
	0.2-2 μm	
Sample	A	B
Number of measured particles	261	103
Average length (nm)	348	238
Standard deviation for length (nm)	225	295
Average width (nm)	212	135
Standard deviation for width (nm)	155	161
Average (L/W)	1.64	1.76
Mean particle area (1000 nm ²)	53.7	38.2
Standard deviation for mean particle area (1000 nm ²)	34.79	47.36

5.3.2. Comparison between clay minerals in the oil sands ore and extraction product

5.3.2.1. XRD analyses

The clay (0.2-2 μm) and ultrafine clay (<0.2 μm) fractions extracted from both oil sands ores, A and B, as well as from the main products of the nonaqueous

extraction (supernatant for toluene to heptane ratios of 30/70 and 0/100 at two settling times of 1 and 7.5 min), were analyzed by XRD. The ultrafine clay fraction of the supernatant from sample A was not analyzed by XRD due to the very small amount of sample obtained from nonaqueous extraction. It should be noted that only 1 wt% of the solids in ore A are in the $< 2 \mu\text{m}$ clay fraction. Therefore, the low yield of solids in the ultrafine clay fraction was to be expected. XRD profiles of the 0.2-2 μm fraction from both oil sands ores as well as their nonaqueous extraction products (supernatants at a toluene to heptane ratio of 30/70 after 7.5 min of settling) are illustrated in Fig. 5.4. All samples consisted of predominantly illite and kaolinite, with very small amounts of quartz and chlorite, and traces of illite-smectite (Fig. 5.4). The presence of quartz in the clay size fraction is a common phenomenon. The occurrence of illite-smectite with expandable smectitic interlayers was identified by the difference between the EG saturated and 54% RH patterns in the 2θ range of 8-10°. There were no differences in peak positions of kaolinite before and after EG saturation as shown in Fig. 5.4. However, changes in the kaolinite peak intensities and slight peak broadening were observed after EG saturation of clay-rich sample B (Uhlik et al., in preparation). Therefore, traces of kaolinite-smectite are present at least in sample B.

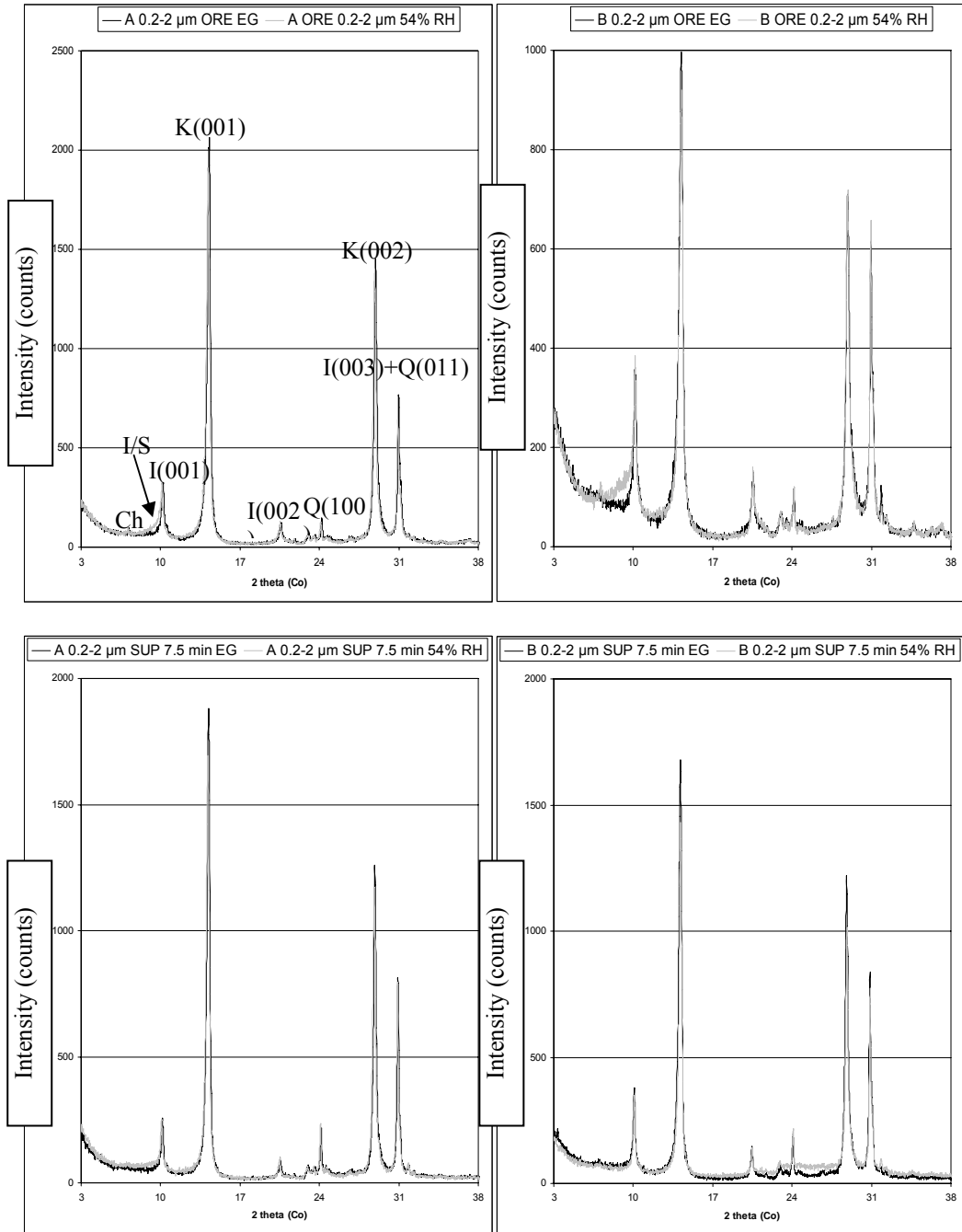


Fig. 5.4. XRD profiles of oriented samples of the 0.2-2 μm fraction of the oil sands ores as well as their nonaqueous extraction products (supernatants at a toluene to heptane ratio of 30/70 and a settling time of 7.5 min). Ch-chlorite, I/S – mixed-layered illite-smectite, I-illite, K-kaolinite, Q-quartz, EG-sample saturated with ethylene glycol, RH-relative humidity, SUP-supernatant.

Although both ores were kaolinitic (kaolinite to illite ratio was higher than one), the kaolinite to illite ratio (K/I) was significantly higher for sample A than sample

B (2.6 vs. 1.4). Comparison of the kaolinite to illite ratios in the ore and supernatant revealed that kaolinite was enriched in the supernatant (settled more slowly from the supernatant to the tailings) in both ore samples, A and B. Although the actual values for K/I were higher for the supernatants obtained from sample A, the enrichment of kaolinite was more pronounced in supernatants obtained from sample B (Fig. 5.5). The relative enrichment of kaolinite was calculated from the following formula:

$$\text{Relative enrichment of kaolinite in product} = \frac{K/I_{\text{product}} - K/I_{\text{ore}}}{K/I_{\text{ore}}} \times 100 \% \quad (5-2)$$

The relative enrichment of kaolinite is depicted in Fig. 5.5 for all samples. The important feature in Fig. 5.5 is the enrichment of kaolinite in all cases. The enrichment of kaolinite in the supernatant, a phase composed predominantly of bitumen and the organic solvent, is probably due to the higher affinity of kaolinite particles for the bitumen and the solvents. Illite particles, on the contrary, are more likely to form aggregates, thereby settling to the tailings quickly, although they can have similar shapes as kaolinite particles (Beutelspacher & Van Der Marel, 1968). The neutral siloxane surfaces found on kaolinite are hydrophobic meaning kaolinite has a higher affinity to hydrocarbons such as bitumen and organic solvents than illite. The slightly hydrophobic kaolinite surfaces have been reported to interact with non-polar solvents (Schoonheydt & Johnston, 2006).

For both sets of samples, A and B, the K/I and also kaolinite enrichment in the supernatant increased with increased settling time from 1 min to 7.5 min when the toluene to heptane ratio was 30/70, while the trend was different when the solvent was pure heptane (T/H = 0/100) (Fig. 5.5). Kaolinite enrichment in the supernatant was discussed above. One would expect this enrichment to be observed to a higher degree as the settling time was increased, which was the case

for a toluene to heptane ratio of 30/70. The opposite trend for pure heptane can be explained only by considering the settling behaviour of these samples. In the previous chapter it was shown that the settling of solids started with a delay for these samples. The settling of solids by assembly into larger aggregates was characterized by an “incubation” period due to the precipitation of asphaltene which was possibly attached to clay mineral particles. The settling of solids in pure heptane started in a chaotic way and only after some delay became similar to the settling of solids with a toluene to heptane ratio of 30/70. Therefore, in the beginning, only large aggregates of mostly asphaltene and illite particles settled quickly thereby increasing the K/I ratio relative to that in the ore. The K/I ratio had the highest value at this stage (e.g., at a settling time of 1 min). After this stage, settling continued in the same manner as the other sets of samples, i.e., those extracted with a toluene to heptane ratio of 30/70, when both kaolinite and illite particles (possibly covered by some asphaltene precipitates) settled, with a higher rate of settling for illite particles. Therefore, the K/I ratio at this point (e.g., settling time of 7.5 min) was still higher than that for the ore but lower than the K/I ratio at the beginning of the settling (Fig. 5.5).

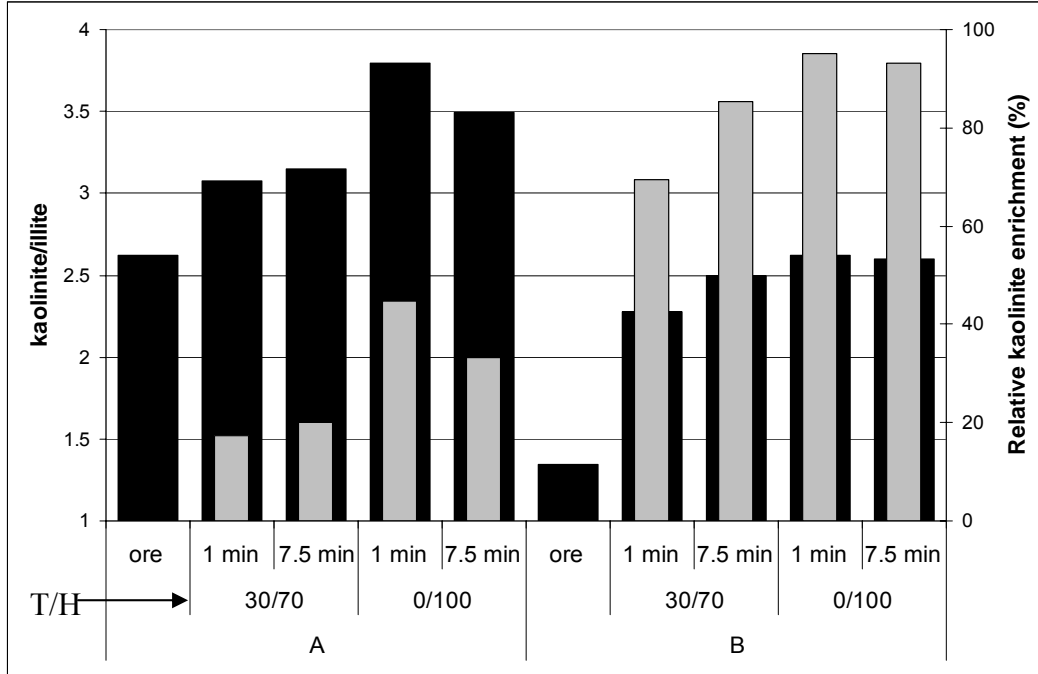


Fig. 5.5. K/I ratio (black bars) and relative enrichment of kaolinite to the supernatant (gray bars) for the entire clay fraction ($< 2 \mu\text{m}$) from the ore and supernatant after 1 and 7.5 min of settling, based on quantitative XRD analysis. T/H - toluene to heptane ratio.

Kaminsky et al. (2008) observed the enrichment of kaolinite in the bitumen froth during water-based batch extraction. Quantitative XRD analysis on clay fractions of streams after water-based batch extraction of samples A and B revealed the same behaviour. The primary froth had a higher K/I value than those of the ore and the middlings in both samples, showing the enrichment of kaolinite in the primary froth (Fig. 5.6). Similar to nonaqueous extraction, the relative enrichment of kaolinite in the extraction product (the primary froth) was higher for sample B than sample A (98% vs. 36%) during water-based batch extraction.

Sample B had a lower K/I value than any of the extraction products, which cannot be true in reality (Fig. 5.6). This discrepancy is due to the inhomogeneity of the oriented XRD samples and possible errors in the quantitative analysis. It should be noted that, among all the streams after the batch extraction, the middlings contain the majority of the clay mineral particles. The very small difference

between the K/I for ore B (1.70) and the middlings (1.82), therefore, shows the insignificance of the mentioned error.

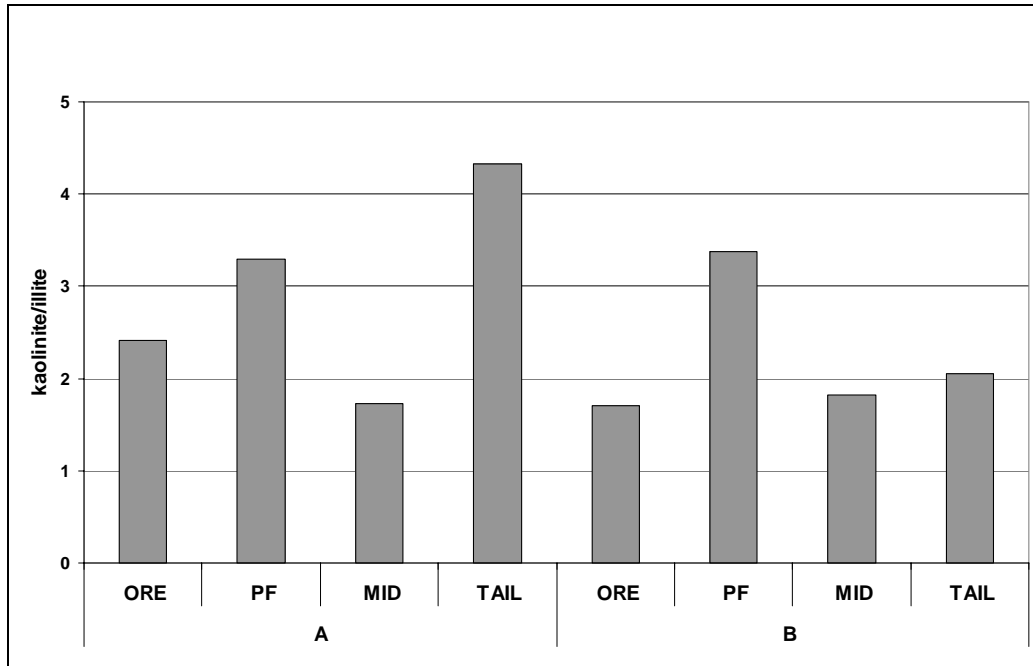


Fig. 5.6. K/I ratio for the entire clay fraction (<2 μm) from the ore and products after water-based batch extraction of samples A and B, based on quantitative XRD analysis. PF - primary froth, MID - middlings, TAIL -tailings.

An experiment was designed to evaluate kaolinite enrichment using the established nonaqueous extraction procedures on an artificial oil sands ore sample. The artificial oil sands ore was prepared by mixing 85 wt% real tailings (completely free of clay and organic matter and with particle sizes larger than 45 μm), 10 wt% pure bitumen obtained from Syncrude and the balance a one-to-one mixture of illite-smectite from Dolná Ves, Slovakia (Šucha et al., 1992; identical to Special Clay ISCz-1, with particle sizes smaller than 2 μm) and poorly crystalline highly defective kaolinite source clay minerals (KGa-2) in their natural fraction (mixture of <2 μm and >2 μm particles). KGa-2 was obtained from the Clay Minerals Society Source Clays Repository.

The reason for selecting significantly larger kaolinite particles (compared to illite-smectite particles) was to eliminate any effect of the clay mineral particle size in the segregation of the clay minerals during the extraction process. In fact, larger kaolinite particles are expected to settle more quickly to the tailings rather than remain in the supernatant if only the discrete particle size plays a role. The artificial ore went through exactly the same nonaqueous extraction process as the real oil sands ores, with a weight ratio of toluene to heptane of 30/70. In spite of the larger particle size of kaolinite (than the illite-smectite), XRD analysis of the supernatant after 1 min of settling revealed significant enrichment of kaolinite in the supernatant (kaolinite/illite-smectite ratio of 4:1 in the supernatant versus 1:1 in the artificial ore feed). Therefore, enrichment of kaolinite in the main product of nonaqueous bitumen extraction does not depend on the discrete particle sizes of the clay minerals.

5.3.2.2. HRTEM investigations

Ultrathin sections of the 0.2-2 μm fractions of the clay mineral particles from the oil sands ore and supernatant (main product of nonaqueous bitumen extraction at a toluene to heptane ratio of 30/70 as the solvent) for sample B were studied by HRTEM. Sample B was chosen for the HRTEM investigations due to its higher clay content (almost 8 wt%) than sample A (less than 1 wt% clays).

Although the method used for HRTEM analysis was successful in obtaining lattice fringe images from well crystallized kaolinite source clay mineral, KGa-1B (Fig. 5.7) (detailed information about KGa-1B is available at Pruet & Webb (Pruett & Webb, 1993)), lattice fringe images of kaolinite were not observed in samples from the oil sands. The presence of other clay minerals such as illite and illite-smectite in addition to kaolinite in oil sands samples and the lower crystallinity of kaolinite in oil sands are possible causes for not observing kaolinite lattice fringes. Therefore, only 2:1 layer clay minerals (illite and illite-smectite) were investigated by HRTEM.

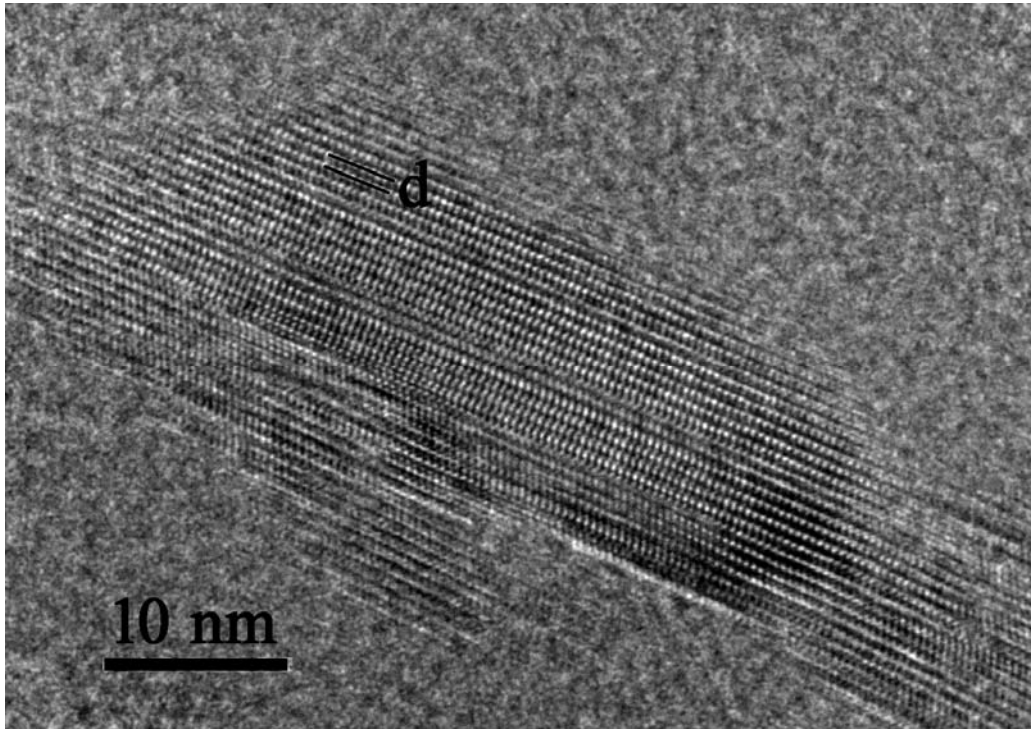


Fig. 5.7. HRTEM lattice fringe image from KGa-1B. Measured d (basal spacing) = 0.7 nm.

Both samples, the ore and supernatant, contained particles varying in thickness from a monolayer (~ 1 nm) to thick multilayers (Fig. 5.8). More bilayers were found in the supernatant than in the ore. Some extremely thick particles (particles with more than 50 layers) (e.g., Figs. 5.8b and 5.8f) were found in both the ore and supernatant.

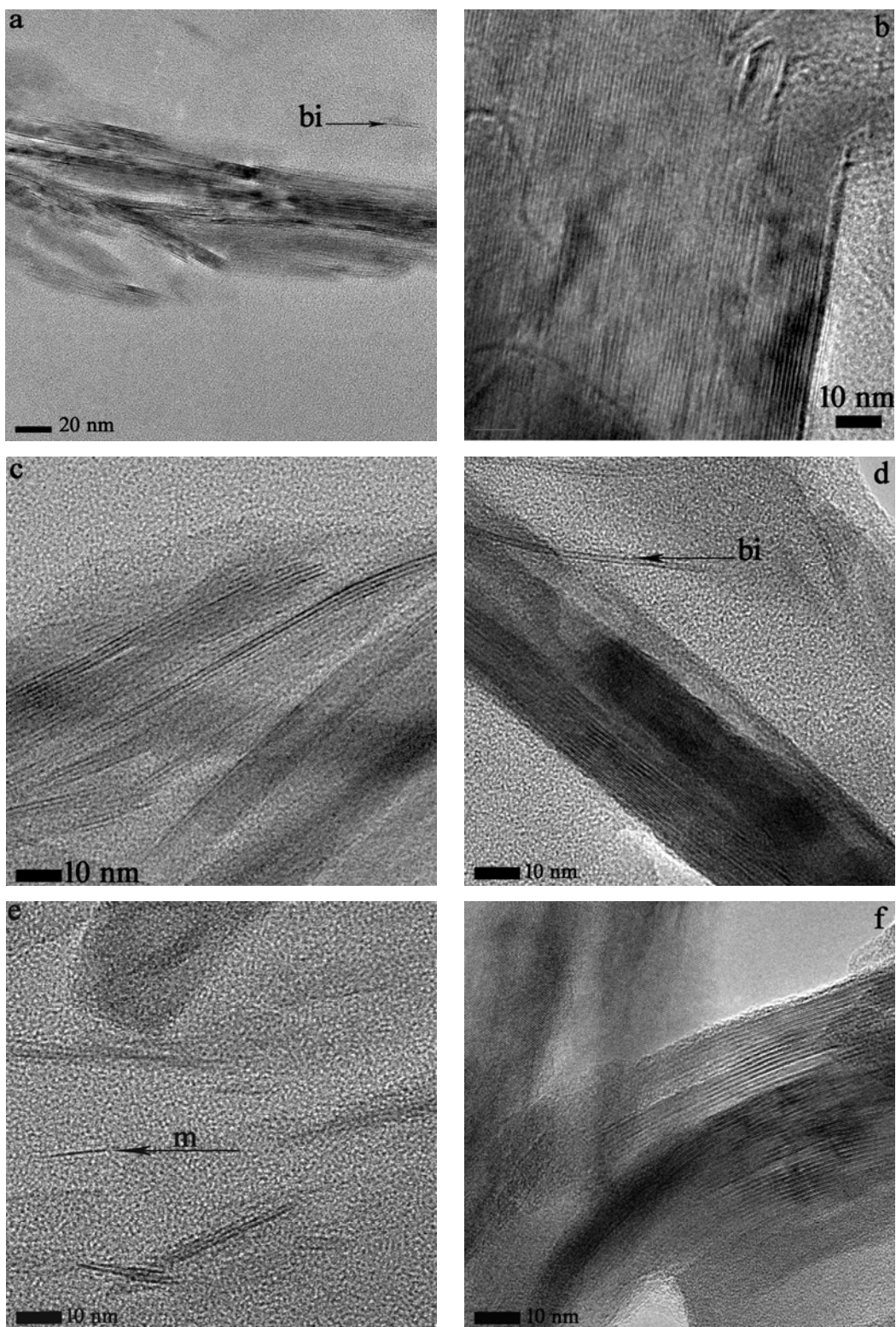


Fig. 5.8. HRTEM lattice fringe images from the clay fractions of sample B: a), b) the oil sands ore and c), d), e), f) the extraction product (supernatant) showing particles varying in thickness. bi: bilayer, m: monolayer.

Both the ore and supernatant from sample B contained particles with a polymodal thickness distribution, with modes at a thickness of 3-4 layers (Fig. 5.9). This figure also shows that the supernatant contained significantly higher percentages of ultrathin – with 4 or less layers per particle – 2:1 layer (illite and illite-smectite) clay mineral particles than the ore. Similar selective segregation of the ultrathin portion of the 2:1 layer clay mineral particles was observed in water-based bitumen extraction to the primary froth (Hooshiar et al., 2010). A strong relationship between the amount of these ultrathin illite (and illite-smectite) particles in the oil sands and bitumen recovery in a water-based extraction was reported by Mercier et al. (2008). They showed that the bitumen recovery dramatically decreased when the content of these particles exceeded 1 wt%.

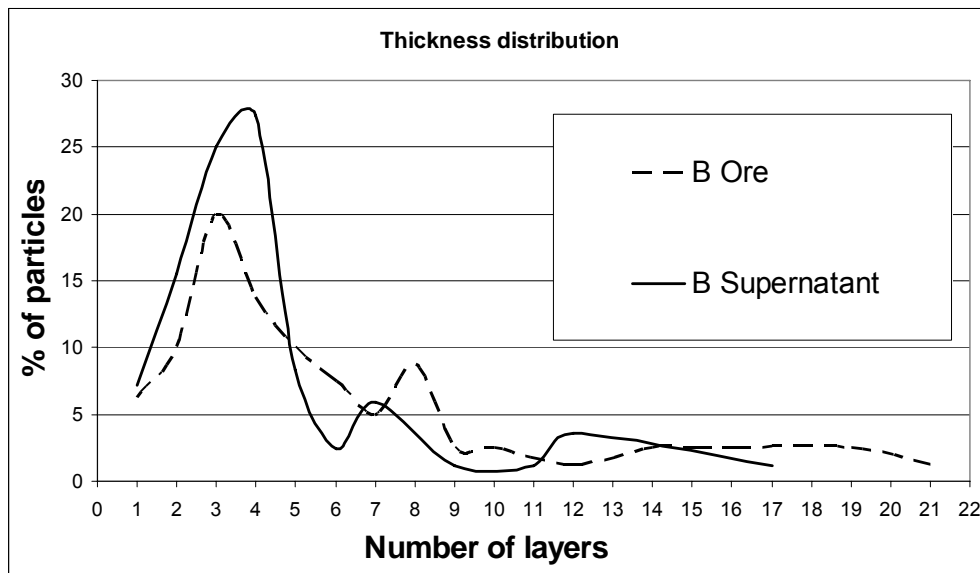


Fig. 5.9. Distribution of number of layers per particle measured from data obtained from HRTEM images. Samples are clay fractions ($< 2\mu\text{m}$) separated from ore B (dashed line) and supernatant produced from sample B at a toluene to heptane ratio of 30/70 after 7.5 min of settling.

Similar to water-based extraction, the presence of ultrathin clay mineral particles is expected to play a negative role during nonaqueous bitumen extraction. One of the reasons for the lower bitumen recovery for sample B than sample A (Hooshiar

et al., 2009) may be the presence of ultrathin clay minerals particles, although this is only a hypothesis since sample A was not studied by HRTEM. However, the difference in bitumen recovery between samples A and B diminished after additional solvent washing (Hooshiar et al., 2011). Therefore, it may be concluded that this segregation was more pronounced in the water-based bitumen extraction compared to what was observed in the nonaqueous extraction.

In order to investigate the effect of the smectitic layers on the extraction process, the maximum expandability was calculated and the results are shown in Table 5-2 for both the oil sands ore and supernatant, based on the method by Środoń et al. (1990). The following considerations were taken into account in expandability calculations. The basal spacing of an illite-smectite particle is expected to be between 1.05 nm and 1.35 nm, the basal spacing values of pure illite and pure smectite in epoxy resin, respectively (Środoń et al., 1990). Particles with basal spacings of 1.4 nm or larger (chlorite particles) were completely excluded from expandability calculations regardless of their thicknesses. Particles with 4 or less layers per particle were considered to be illite–smectite, even if their basal spacings were between 1.00 and 1.05 nm. This assumption is valid if the outer surfaces of these particles are assumed to be smectitic surfaces (Środoń et al., 1990). The assumption does not introduce significant error into expandability calculations, because only a few such particles were observed in HRTEM images. Particles with basal spacings between 1.25 nm and 1.35 nm were assumed to be illite–smectite rather than pure smectite, because pure smectite was not identified by XRD. In short, all particle with a basal spacing between 1.05 nm and 1.35 nm, and particles with 4 or less layers per particle with basal spacings less than 1.05 nm, were used in illite–smectite expandability calculations.

In addition, the supernatant had higher percentages of bilayers (14.8% vs. 9.9%) and larger average basal spacing than the ore (1.13 nm vs. 1.09 nm) (Table 5-2). Bilayer particles are highly smectitic (at least 50%) due to the high ratio of the outer surfaces (surfaces were smectitic in nature) to the interlayer surfaces when

compared with multilayer particles. Larger average basal spacings and higher numbers of bilayer particles showed the higher degree of smectitic characteristic for the 2:1 layer clay minerals in the supernatant than in the ore.

Furthermore, the supernatant contained slightly higher percentages of monolayers (completely smectitic in nature) than the ore (Table 5-2), which is in agreement with the more smectitic characteristic of the supernatant although the difference may not be statistically significant. The presence of these smectitic monolayers even in such small quantities (7.1% of the 2:1 layer clay minerals equal approximately 0.2 wt% of the entire ore for sample B) could still affect the extraction process due to their very high surface area. (Mercier et al. (2008) showed that even very small amounts of ultrathin 2:1 layer clay minerals affect bitumen recovery.) HRTEM is one of the few methods, if not the only one, capable of detecting such monolayers. These smectitic monolayers cannot be detected by XRD since they do not satisfy Bragg's condition for constructive interference (Cullity, 1978).

Table 5-2. Statistical parameters for particles observed by HRTEM - %Smax and d-spacing are calculated maximum illite-smectite expandability and basal spacing, respectively.

<u>Sample</u>	<u>B Ore</u>	<u>B Supernatant</u>
Size fraction (µm)	0.2-2	0.2-2
Number of measured particles	81	87
Average number of layers per particle	6.2	4.6
Average d-spacing (nm)	1.09	1.13
% of monolayers	6.3	7.1
% of bilayers	9.9	14.8
Number of particles used for expandability calculations	42	64
%Smax	37	36

5.3.2.3. Low-pressure SEM investigations

Low-pressure SEM images were obtained from supernatants produced from samples A and B after two different settling times, 1 and 7.5 min. Particles

ranging in sizes from less than 10 μm to as large as 100 μm were observed in the supernatants produced from both A and B samples, with finer particles dominating. It is also interesting to note that larger particles appeared to be more abundant in the supernatant produced from sample A than from sample B. Rapid settling of very fine particles (mostly clay minerals) in the supernatant was observed. At the beginning (1 min of settling), a relatively uniform distribution of very fine particles (less than a few μm) was observed in the supernatants produced from both samples A and B (Figs. 5.10 and 5.11). Although more particles were observed for the supernatant produced from sample B at the beginning (after 1 min of settling) rather than sample A (note that scale bars are almost one order of magnitude different in Figs. 5.10 and 5.11), the difference was more pronounced after 7.5 min of settling (Figs. 5.12 vs. Fig. 5.13). This is in good agreement with the shorter settling time for sample A (settling time of less than 10 min) than sample B (settling time of about 30 min) based on the sum of solids and water content in the supernatant reported in the previous chapter.

Particle size in the supernatant decreased with increasing settling time in both cases (compare Fig. 5.10 with 5.12, and Fig. 5.11 with 5.13). Several isolated clusters of particles were observed in the supernatant produced from sample A (Fig. 5.12), while no clusters were observed in the supernatant produced from sample B.

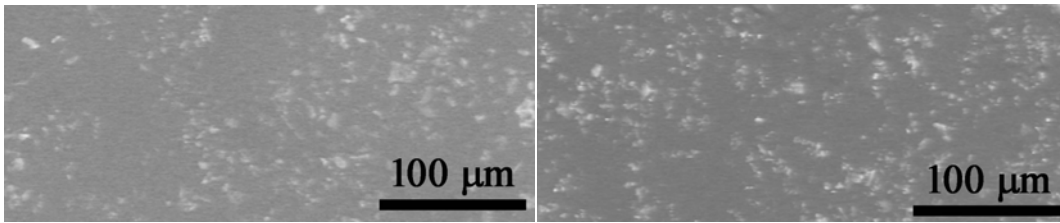


Fig. 5.10. BSE SEM image of the A supernatant after 1 min of settling.

Fig. 5.11. BSE SEM image of the B supernatant after 1 min of settling.

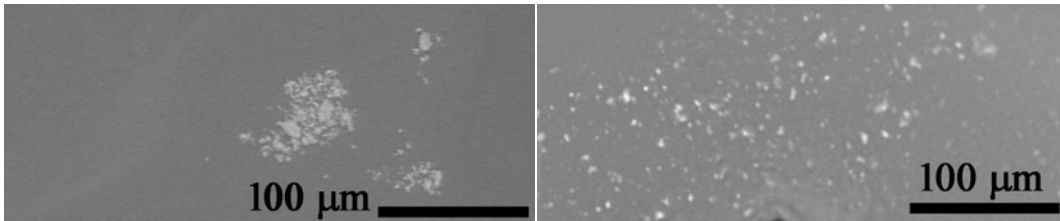


Fig. 5.12. BSE SEM image the of A supernatant after 7.5 min of settling.

Fig. 5.13. BSE SEM image of the B supernatant after 7.5 min of settling.

5.3.3. Characterization of the tailings

The tailings from the nonaqueous extraction process were composed of mainly solids (>94 wt% of the total), with a small amount of water (2.8-3.6 wt%) and bitumen (1.4-2.5 wt%). The solvent was excluded from the composition since solvent evaporation was not controlled during the extraction process. In addition, the entire mass lost (up to 14%) was attributed to the solvent loss (Hooshiar et al., 2009). It should be noted that the tailings discussed here were the primary tailings, which had not gone through extra washing, and the corresponding supernatant recovered 80% of the bitumen (see previous chapter).

Tailings solids consisted of predominantly quartz and some feldspar particles. Clay minerals were the next most abundant components of the tailings (Fig. 5.14). The tailings from the two oil sands ores, A and B, were different with respect to clay mineral contents. The clay minerals were found in significantly larger quantity in the tailings produced from sample B than from sample A. The

compositions of the clay fraction in the tailings were very similar to the compositions of the same fraction from the oil sands ore.

In addition, and more importantly, the arrangement of clay minerals was different in the two tailings (tailings produced from samples A and B). Clay minerals were mostly found in the form of relatively large aggregates (several hundreds μm in size) in the tailings produced from sample B, while in the tailings produced from sample A they existed as small, discrete particles on the surface of quartz or feldspar grains (Fig. 5.15). In the tailings produced from sample B, it appeared that the clay mineral aggregates were intact after nonaqueous bitumen extraction. Although this may affect bitumen recovery, it could potentially benefit bitumen product quality and tailings management since these aggregates naturally settle faster compared to dispersed clay minerals. Dispersed clay minerals were the cause of major problems, e.g., very long settling time, in unconsolidated tailings in hot water bitumen extraction. They also affect upgrading, since they are tightly bound to the bitumen (FTFC, 1995).

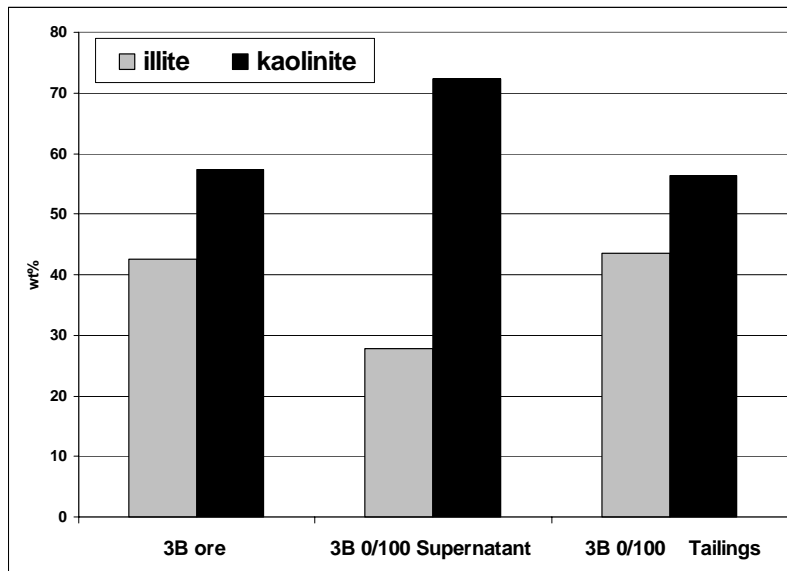


Fig. 5.14. Comparison of clay fraction ($<2 \mu\text{m}$) composition of the ore and products after nonaqueous extraction (supernatant and tailings), showing the kaolinite enrichment in the supernatant. 0/100 = toluene to heptane ratio.

The origin of the difference in the arrangement of the clay minerals in the tailings may be due to the higher clay content for the raw B ore (8 wt%) than the A ore (1 wt%), and the difference in the clay minerals composition (the K/I ratio for A ore was almost twice as high as for B ore). In addition, only very mild agitation was used in the nonaqueous extraction tests. A more turbulent process condition may result in tailings with a different morphology in terms of clay minerals.

The morphology and abundance of clay aggregates in the tailings produced from B ore were almost identical to those of the original B ore. The aggregates appeared to settle almost immediately (in less than 1 min) with the large sand grains. However, the possibility of initial dispersion and later re-aggregation of the aggregates during the extraction process could not be ruled out. If re-aggregation did happen, it must have occurred sometime between 1 and 7.5 min of settling, since no aggregates were found in the investigated supernatants, obtained after 1 min and 7.5 min of settling (Figs. 5.10-5.13). The close association of clay aggregates with quartz grains supports the first hypothesis.

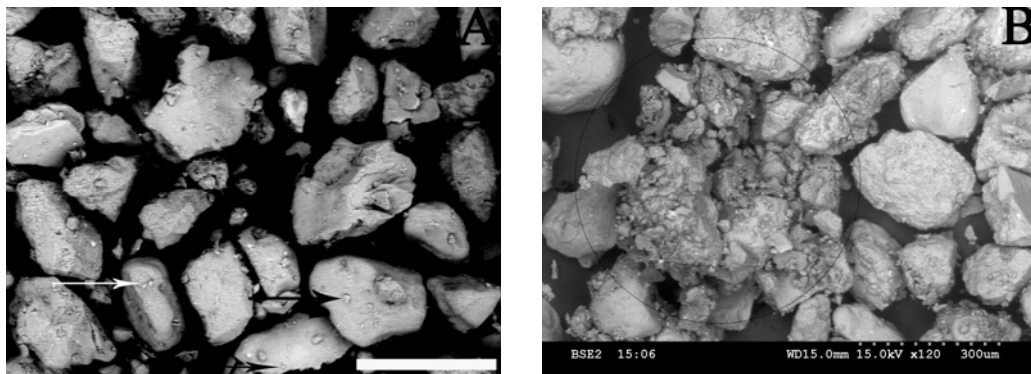


Fig. 5.15. BSE low pressure SEM images of tailings from nonaqueous extraction with a toluene to heptane weight ratio of 30/70. Sample A (left), sample B (right), scale bars are 100 μm . Large grains: quartz/feldspar, small particles: clays. Arrows show some small clay particles. The circle shows an area of clay agglomerates.

Since current tailings thickening and waste management processes all use water, the tailings mentioned above were agitated with water to observe their settling behaviour in an aqueous environment. This test was done only for the sake of

scientific curiosity. Cleaning the tailings produced in the solvent extraction process with water in the oil sands industry is not the best option since it has at least two disadvantages, dispersion of the clay aggregates and contamination of the water.

After agitating with water, major differences were observed between the tailings produced from samples A and B as expected. Agitating with water dispersed the clay aggregates. The tailings produced from sample B were found to settle much more slowly than those from sample A due to the significantly higher content of the clay minerals (Fig. 5.16). Unlike the tailings from sample B, the majority of the solids in the tailings of sample A were consolidated after 5 min of sedimentation. The water layer above the mudline was completely transparent after 6 hr of settling while it did not reach the same level of transparency even after 102 hr for the tailings from sample B. The settling behaviour of the tailings from sample B was quite different. An opaque suspension of dispersed clay mineral particles was observed after the first hour of sedimentation. A dense slurry started to form when a large volume of dispersed clay mineral particles started to flocculate at the end of the third hour. Afterwards, a diffuse interphase with a considerable amount of clay mineral particles started to form between the water phase and the dense slurry. This dense slurry is considered to be partly consolidated tailings, in contrast to the consolidated tailings at the bottom of the graduated cylinders. Both tailings, partly consolidated and consolidated, were the origin of the sharp rise in the solids volume as shown in Fig. 5.16. The dense slurry became more and more consolidated as the water phase on top became clearer with increasing settling time.

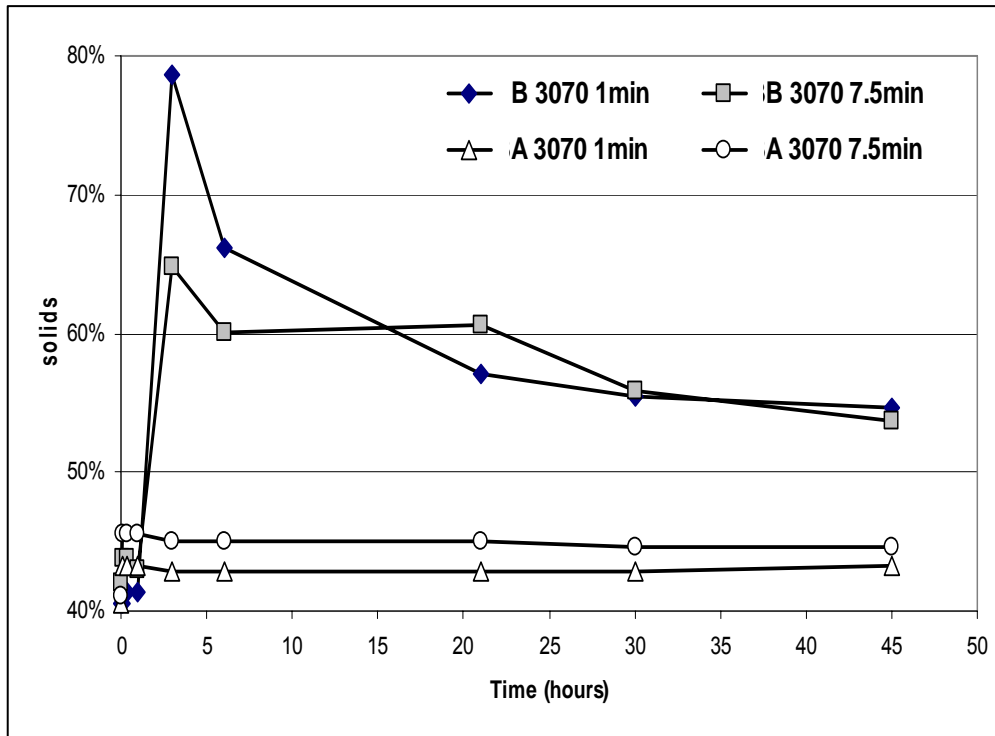


Fig. 5.16. Sum of the consolidated and partly consolidated tailings solids volume vs. gravity settling time. (Solids% = (Volume of consolidated tailings + Volume of partly consolidated tailings)/Total volume).

5.4. Conclusions

Two Alberta oil sands ores, a high grade, low fines, good processing ore (A) and a mid grade, high fines, poor processing ore (B), were studied during nonaqueous bitumen extraction. A mixture of toluene and heptane at two weight ratios, 30/70 and 0/100, were used as the extraction solvents. A significant number of aggregates (less than $\sim 200 \mu\text{m}$ in size) composed of clay mineral particles and bitumen were found in SEM images from ore B, but not in ore A. Very similar aggregates were found in the tailings produced from sample B. These aggregates appeared to be unaffected by the nonaqueous extraction process, since they were very similar in morphology and quantity in both the ore feed and the tailings from sample B.

Kaolinite and illite were the dominant clay minerals found in both samples with a small amount of illite-smectite and chlorite based on XRD investigations. Quantitative XRD analysis revealed enrichment of kaolinite in the supernatant when compared to the ore, with the enrichment being pronounced for sample B. Kaolinite enrichment in the supernatant was likely due to the higher affinity of the kaolinite particles for bitumen than illite. No significant difference was found between the two oil sands ores in terms of clay mineral particle size and morphology from TEM observations. HRTEM studies showed a higher amount of ultrathin illite-smectite particles (2:1 layer clay minerals) in the supernatant than in the ore. HRTEM, performed only on sample B, revealed the presence of smectite monolayers – not detectable by XRD – in both the ore and supernatant.

When agitated with water, the tailings from the nonaqueous extraction behaved differently. The settling rate of the tailings produced from sample A was much higher than that from sample B. The very low settling rate of the tailings from sample B was due to the dispersion of clay mineral particles, which were intact during nonaqueous extraction, by agitating with water. Producing tailings with a very small amount of dispersed clay mineral particles may be an advantage of nonaqueous extraction.

Acknowledgements

The authors are grateful to the Centre for Oil Sands Innovation (COSI) for providing research funding and to Syncrude and Imperial Oil for providing oil sands ore samples. The authors also wish to thank Arek Derkowski, Daniel Solomon and Shiraz Merali for their assistance with the characterization work.

5.5. References

- Alberta Energy (2010). Oil sands. Alberta Government, www.energy.gov.ab.ca/OurBusiness/oilsands.asp.
- Author not stated. (1990). A 15 Year Portfolio of Achievement. *Alberta Oil Sands Technology and Research Authority (AOSTRA)*, Edmonton, Canada.
- Beutelspacher, H., & Van Der Marel, H.W. (1968). Atlas of Electron Microscopy of Clay Minerals and their Admixtures. *Elsevier*, Amsterdam-London-New York.
- Bichard, J.A. (1987). Oil sands composition and behaviour research: The research papers of John A. Bichard 1957-65. *Alberta Oil Sands Technology and Research Authority (AOSTRA)*, Edmonton, Canada.
- Camp, F. W. (1976). The Tar Sands of Alberta. 3rd ed., *Cameron Engineers, Inc.*, Colorado, USA.
- Clementz, D. M. (1976). Interaction of petroleum heavy ends with montmorillonite. *Clays and Clay Minerals*, 24, 6, 312-19.
- Cullity, B.D. (1978). Elements of X-Ray Diffraction, 2nd Edition, *Addison-Wesley Publishing Company, Inc.* Notre Dame, Indiana, USA.
- Czarnecka, E., & Gillott, J. E. (1980). Formation and characterization of clay complexes with bitumen from Athabasca oil sand. *Clays and Clay Minerals*, 28, 3, 197-203.
- Eberl, D. D., Srodon, J., Lee, M., Nadeau, P. H., & Northrop, H. R. (1987). Sericite from the silverton caldera, Colorado; correlation among structure, composition, origin, and particle thickness. *American Mineralogist*, 72, 9-10, 914-34.
- Elsass, F., Beaumont, A., Pernes, M., Jaunet, A. M., & Tessier, D. (1998). Changes in layer organization of Na- and Ca-exchanged smectite materials during solvent exchanges for embedment in resin. *Canadian Mineralogist*, 36, 6, 1475-83.
- FTFC (Fine Tailings Fundamentals Consortium) (1995). Vol.1, Clark hot water extraction fine tailings, In: Advances in oil sands tailings research, *Alberta Department of Energy, Oil Sands and Research Division*, Edmonton, Canada, 5-57.
- Funk, E.W., May, W.G., & Pirkle, J.C. (1984). Processing approach for the solvent extraction of Athabasca tar sands. *American Institute of Chemical Engineers (AIChE) Energy Progress Quarterly*, 4, 12, 12-16.

Hooshiar, A., Uhlik, P., Adeyinka, B. O. B., Etsell, T. H., Ivey, D. G., & Liu Q. (2009). Nonaqueous bitumen extraction of Alberta oil sands. 8th World Congress of Chemical Engineering, Montreal, Canada.

Hooshiar, A., Uhlik, P., Kaminsky, H. W., Shinbine, A., Omotoso, O., Liu, Q., et al. (2010). High resolution transmission electron microscopy study of clay mineral particles from streams of simulated water-based bitumen extraction of Athabasca oil sands. *Applied Clay Science*, 48, 3, 466-74.

Hooshiar, A., Uhlik, P., Etsell, T. H., Ivey, D. G., & Liu, Q. (2011). Clay minerals in nonaqueous extraction of bitumen from Alberta oil sands. Part 1. Nonaqueous extraction procedure. *Fuel Processing Technology* (submitted).

Ignasiak, T. M., Kotlyar, L., Longstaffe, F. J., Strausz, O. P., & Montgomery, D. S. (1983). Separation and characterization of clay from Athabasca asphaltene. *Fuel*, 62, 3, 353-62.

Kaminsky, H.A.W., Uhlik, P., Hooshiar, A., Shinbine, A. Etsell, T.H., Ivey, D.G., et al. (2008). Comparison of morphological and chemical characteristics of clay minerals in the primary froth and middlings from oil sands processing by high resolution transmission electron microscopy. Proceedings of the First International Oil Sands Tailings Conference, Edmonton, Canada, 102-11.

Kaminsky, H. A. W., Etsell, T. H., Ivey, D. G., & Omotoso, O. (2009). Distribution of clay minerals in the process streams produced by the extraction of bitumen from Athabasca oil sands. *The Canadian Journal of Chemical Engineering*, 87, 1, 85-93.

Leung, H., & Phillips, C. R. (1985). Solvent extraction of mined Athabasca oil sands. *Industrial & Engineering Chemistry Fundamentals*, 24, 3, 373-79.

Liu, J., Xu, Z., & Masliyah, J. (2004). Role of fine clays in bitumen extraction from oil sands. *AIChE Journal*, 50, 8, 1917-27.

Meadus, F. W., Bassaw, B. P., & Sparks, B. D. (1982). Solvent extraction of Athabasca oil-sand in a rotating mill part 2. Solids—liquid separation and bitumen quality. *Fuel Processing Technology*, 6, 3, 289-300.

Mercier, P. H. J., Page, Y. L., Tu, Y., & Kotlyar, L. (2008). Powder x-ray diffraction determination of phyllosilicate mass and area versus particle thickness distributions for clays from the Athabasca oil sands. *Petroleum Science & Technology*, 26, 3, 307-21.

Moore, D. M., & Reynolds Jr., R. C. (1997). X-ray Diffraction and the Identification and Analysis of Clay Minerals, 2nd Edition, *Oxford University Press*, USA.

- Nadeau, P. H. (1987). Relationships between the mean area, volume and thickness for dispersed particles of kaolinites and micaceous clays and their application to surface area and ion exchange properties. *Clay Minerals*, 22, 3, 351-56.
- Omotoso, O. E., & Mikula, R. J. (2004). High surface areas caused by smectitic interstratification of kaolinite and illite in Athabasca oil sands. *Applied Clay Science*, 25, 1-2, 37-47.
- Omotoso, O. E., Munoz, V. A., & Mikula, R. J. (2002). Mechanisms of crude oil–mineral interactions. *Spill Science & Technology Bulletin*, 8, 1, 45-54.
- Pruett, R. J., & Webb, H. L. (1993). Sampling and analysis of KGa-1B well-crystallized kaolin source clay. *Clays and Clay Minerals*, 41, 4, 514-19.
- Schoonheydt, R.A., & Johnston, C.T. (2006). Surface and interface chemistry of clay minerals, In: Handbook of Clay Science (Bergaya, F., Theng, B.K.G., & Lagaly, G. (editors)), *Elsevier Science*, Amsterdam, 87-114.
- Sparks, B. D., Kotlyar, L. S., O'Carroll, J. B., & Chung, K. H. (2003). Athabasca oil sands: Effect of organic coated solids on bitumen recovery and quality. *Journal of Petroleum Science and Engineering*, 39, 3-4, 417-30.
- Środoń, J., Andreoli, C., Elsass, F., & Robert, M. (1990). Direct high-resolution transmission electron microscopic measurement of expandability of mixed-layer illite/smectite in bentonite rock. *Clays and Clay Minerals*, 38, 4, 373-79.
- Šucha, V., Kraus, I., Mosser, Ch., Hroncová, Z., Soboleva, K.A., & Širáňová, V. (1992). Mixed-layer illite/smectite from Dolná Ves hydrothermal deposit, Kremnica Mountains, The West Carpathians. *Geologica Carpathica Clays*, 43, 1, 13-19.
- Tessier, D. (1984). Étude expérimentale de l'organisation des matériaux argileux. Ph.D. Thesis, *University of Paris VII*, Paris, France.
- Tipman, R., Long, Y-Ch., & Shelfantook, W. E. (2001). Solvent process for bitumen separation from oil sands froth. US Patent No. 6 214 213 B1.
- Tis, D. J., Culbertson, R. W., & Kelley, M. N. (1984). Recent developments with the Dravo solvent extraction process for tar sand. *Energy Progress*, 4, 1, 56-8.

Chapter 6

Summary

The results of the present studies can be summarized in three main categories:

1. Study of the nature of clay minerals in both good and poor processing raw oil sands ores, and the clay lenses.
2. Study of the behaviour and characteristics of clay minerals during nonaqueous extraction.
3. Comparison study of the behaviour of clay minerals during water extraction.

6.1. Study of the nature of clay minerals in both good and poor processing raw oil sands ores and the clay lenses

Three oil sands ores were selected for testing. These included a high grade, low fines, good processing ore (A) and a medium grade, high fines, poor processing ore (B), from a Syncrude lease, and a low grade, high fines, good processing ore (HK). Here “good” or “poor” processing is with reference to the Clark Hot Water Extraction process. Samples A and B were used in both nonaqueous and aqueous processes, while sample HK was used solely in water-based bitumen extraction.

Several characterization techniques such as x-ray diffraction (XRD), scanning electron microscopy (SEM), transmission electron microscopy (TEM), elemental analysis, cation exchange capacity (CEC) measurements and thermogravimetric analysis (TGA) were used. The standard Dean Stark extraction procedure was used to remove organic matter from the oil sands samples and to determine the solids, bitumen and water content. The modified Jackson procedure was used to further remove organic matter, carbonates and Fe compounds in many cases. Fines content (<45 μm) of the samples was determined by wet sieving. In order to

study the clay minerals, the clay fractions ($<2\ \mu\text{m}$) of samples were separated by sedimentation according to Stoke's law. In some cases, the ultrafine clay fraction ($<0.2\ \mu\text{m}$) was separated from the clay fraction by centrifugation.

Particle size analyses of the raw oil sands ores showed that more than 60 wt% of sample A and 50 wt% of sample B particles were in the range of 125 to 250 μm . The largest difference between the two ores was in terms of the fines (6 wt% vs. 23 wt%) and clay (1 wt% vs. 8 wt%) contents.

XRD analyses on the clay fractions of the ore samples showed that the dominant clay minerals were kaolinite and illite. There were only trace amounts of chlorite and mixed-layer clay minerals (illite-smectite and kaolinite-smectite) in the raw oil sand ores, although the high fines ore (B) contained slightly more mixed-layer clay minerals relative to the low fines ore (A). More importantly, no discrete smectite was found in the raw oil sands ores. A small amount of lepidocrocite ($\text{FeO}(\text{OH})$) was found in the HK ore sample, as well as in the clay lenses. In general, the mineral composition of the clay lenses was very close to the raw oil sand ores.

Extensive TEM analysis was performed on the clay fractions of the raw oil sands ores (A and B) in order to investigate the clay particle size and shape. Based on TEM data, the average length to width ratio (L/W) was in the range of 1.7 to 2. The distribution of L/W was also very similar in all cases, indicating a similar particle shape distribution in the clay and ultrafine clay fractions for both ores.

6.2. Study of the behaviour and characteristics of clay minerals during nonaqueous extraction

A mixture of aromatic (toluene) and paraffinic (n-heptane) solvents was used to extract bitumen from the oil sands ore samples. Toluene to heptane ratios were varied as T/H = 70/30, 30/70, 10/90 and 0/100. Bitumen recovery, product

(supernatant) quality, settling time and settling behaviour of the tailings were investigated to evaluate the extraction process.

6.2.1. Bitumen recovery

The bitumen content in the supernatant decreased for both samples, as the toluene to heptane ratio was decreased. In the secondary product, on the other hand, an opposite trend was observed. The total bitumen recovery (supernatant and secondary product combined) for the low fines, high grade ore sample (A) was unaffected by the toluene to heptane ratio, and the loss of bitumen to the tailings was more or less the same across the toluene to heptane ratios tested. As such, one can conclude that the lower recovery of bitumen in the supernatant (primary recovery) was compensated by an increase in the bitumen recovery in the secondary product (secondary recovery). However, for the high fines, low grade ore sample (B), the total bitumen recovery decreased as the toluene to heptane ratio was decreased and the loss of bitumen to the tailings increased at lower toluene to heptane ratios.

Toluene to heptane ratio did not notably influence the total bitumen recovery, especially for the low fines ore sample. This seems to contradict conventional wisdom about the solubility of bitumen in paraffinic solvents. Paraffinic solvents, such as heptane, are not able to entirely dissolve the resin and asphaltene components of bitumen. Therefore, one would expect to see a decrease in bitumen recovery with decreasing toluene to heptane ratio, especially for the case of pure heptane. It should be noted that total bitumen recovery was only about 80% for the low fines ore sample and even less for the high fines ore sample when using a one-step tailings wash. It was not clear if the lost bitumen was due to the non-aggressive extraction procedures or due to precipitated asphaltenes and resins. It is possible that some of the bitumen – likely trapped in clay aggregates - was not exposed to enough solvent during extraction, contributing to the low bitumen recovery. However, in the high fines ore sample extraction tests, the bitumen distribution in the tailings increased from 10 to 16% with decreasing toluene

content in the solvent, suggesting that the residual bitumen in the tailings was likely in the form of asphaltene-clay aggregates with sizes greater than 45 μm so that they were retained on the 45 μm sieve.

In order to obtain high bitumen recovery, an extra two-step tailings wash was applied, together with sieve shaking, to dissolve the residual bitumen and/or liberate the trapped bitumen. The final bitumen recovery after the additional two-step tailings wash was increased to 98.2% for the low fines ore sample and 98.4% for the high fines ore sample at T/H = 30/70, and to 96.1% for the low fines ore sample and 96.2% for the high fines ore sample in pure heptane. Precipitation of resins and asphaltenes, which are insoluble components of bitumen in pure heptane, was responsible for the decrease of bitumen recovery in pure heptane.

6.2.2. Product quality

The supernatant was almost pure bitumen (over 99.5 wt% bitumen) except for sample B with T/H = 30/70 (94.8 wt% bitumen) and for both samples where pure heptane was used (97.3 wt% bitumen for sample A and 98.9 wt% bitumen for sample B). There was a very small amount of solids in the supernatant (less than 0.1 wt% for sample A and less than 0.2 wt% for sample B) when toluene was included in the extraction process. The exception was sample B with T/H = 30/70, which seemed to be an anomaly. The extraction was repeated three times in order to make sure that the anomaly was not due to experimental error. The higher solids content when only heptane was used for extraction was likely due to the precipitation of paraffinic insoluble components of bitumen, i.e., resins and asphaltenes. The heptane to bitumen ratio (H/B) seems to have a key role in the precipitation of asphaltenes, since the solids content in the supernatants with H/B of about 5 and higher was significantly higher than for samples with H/B ratios lower than 4. Samples with H/B ratios below 4.44 contained a very small amount of water and solids. This showed that even the lowest heptane to bitumen ratio (H/B = 1.48) used in the current study was high enough for the paraffinic solvent (heptane), in the presence of the aromatic component (toluene) to remove

emulsion water from the hydrocarbon phase. The removal of water was likely due to the breaking of the water-in-oil emulsion for the heptane to bitumen ratios used.

6.2.3. Settling time

Settling tests on the supernatants from the extraction tests, for T/H = 30/70 and 0/100, were conducted to see if the settling time could be shortened while still maintaining the product quality. Initially, the solids content in the high fines sample (B) was significantly higher than that in the low fines sample (A). The higher fines content in the sample B raw ore appeared to be responsible for the initially high solids content of the supernatant. Water and solids contents decreased dramatically after 2-3 min for both samples, especially the high fines sample (B). When the toluene to heptane ratio was 30/70, the amounts of solids and water in the supernatant were negligible after 10 min settling, indicating that the optimum settling time in the extraction could be shortened to less than 10 min without affecting product quality. For pure heptane, a longer settling time was required in order to achieve the best supernatant quality. In this case, optimum settling time was between 25 and 30 min.

An interesting feature was observed when comparing the solids and water contents in the supernatant. Although the amount of water was small, a decrease in water content seemed to follow a decrease in solids content. This could indicate that the small amount of water detected in the supernatant was likely attached to the solid particles rather than as a separate phase.

6.2.4. Settling behaviour of the tailings

Cryo-SEM and environmental SEM analyses were performed on both raw oil sands ores and tailings. A significant difference was observed between the two

ores. The high fines ore (B) contained clay aggregates in large quantities, while these aggregates were not observed in the low fines ore (A). Instead, the clays in the low fines ore (A) were found as isolated particles mostly attached to the large sand grains. SEM investigations revealed the same features as the corresponding raw ore for each of the tailings. Based on the similar morphology and the abundance of clay aggregates in both the B ore and tailings, it appears that the aggregates were essentially unaffected by nonaqueous solvent extraction. The non-aggressive agitation and/or the absence of water could be the reasons for this phenomenon. After nonaqueous extraction, the tailings were mixed and agitated with water to study their behaviour in the presence of water. The tailings from the A and B ores showed very different settling behaviour after treating with water. While the tailings solids from sample A completely settled in less than 32 hours, the tailings solids from sample B did not settle even after 102 hours. This dramatic difference in the settling behaviour of the tailings was due to the dispersion of the clay minerals in the presence of water, which broke the clay aggregates.

Clay fractions ($<2\ \mu\text{m}$) after 1 and 7.5 min settling were separated from the supernatant and analyzed by XRD and TEM. The mineral components of the clay minerals from the supernatant were very similar to the raw oil sands ores, indicating that kaolinite and illite were the major clay minerals. Segregation of kaolinite to the supernatant relative to the ore was observed in all cases, although the high fines ore (B) was more illitic compared to the low fines ore (A). The enrichment of kaolinite in the supernatant was more pronounced for sample B, possibly due to the higher initial absolute amount of kaolinite (more kaolinite even though the illite/kaolinite ratio was higher). This phenomenon could be due to the difference in the surface charge density of kaolinite and illite. In a nonaqueous environment when only a small amount of water exists, highly charged illite particles flocculate rapidly and form large agglomerates which quickly settle into the tailings while no or very low charge kaolinite particles stay suspended in the supernatant.

More detailed studies were performed on the clay minerals separated from the high fines ore (B) and the supernatant after 7.5 min settling with T/H = 30/70 by high resolution transmission electron microscopy (HRTEM). Only 2:1 layer clay minerals (illite and illite-smectite) were investigated since there is no HRTEM method currently available to study kaolinite in the presence of other clay minerals (kaolinite tends to breakdown in the electron beam). HRTEM investigations revealed the presence of significant amounts of monolayers (6.3% in the ore and 7.1% in the supernatant) not detectable by XRD. In addition, 9.9% bilayer clay minerals in the ore and 14.8% in the supernatant were identified by HRTEM observations. These monolayers (100% smectitic) and bilayers (at least 50% smectitic) were very expandable due to the presence of loose cations on their surfaces; therefore, they settled very slowly compared with thicker particles. In summary, the solids in the supernatant had a more smectitic nature when compared with the ore.

6.3. Comparison study of the behaviour of clay minerals during water extraction

In water-based extraction, bitumen recovery from the high grade, low fines, good processing ore (A) was higher than from the medium grade, high fines, poor processing ore (B) (97% vs. 90%), unlike nonaqueous extraction. The major difference between the two ores with respect to bitumen recovery was observed during secondary recovery, where the bitumen to solids ratio in the secondary froth was 2.33 for A and 0.70 for B.

Quantitative XRD analyses revealed enrichment of kaolinite in the froth fraction for both samples A and B. This phenomenon was more pronounced for sample B, which was significantly more kaolinitic in the raw oil sands ore (contained more kaolinite although had a higher illite/kaolinite ratio) when compared with sample A. Enrichment of kaolinite in the froth product was consistent with previous results on the HK sample (Kaminsky, 2008).

Based on TEM investigations on suspended solid samples, longer and wider clay mineral particles were found in the 0.2–2 μm fraction of the middlings, relative to the tailings. This may have been caused by aggregates of fine clay mineral particles or sand grains covered by clay minerals, which originated from the oil sands ores, survived the water extraction process, and settled to the tailings. Therefore, the effect of agglomeration/dispersion of clay mineral particles must be taken into account in any method used for particle size measurements.

HRTEM investigations showed the presence of about 7% smectitic monolayers in both size fractions, < 0.2 and 0.2–2 μm , of the primary froth (similar to the supernatant in nonaqueous extraction where 7.1% monolayers were observed). These monolayers were not detected by XRD analysis. Because of these monolayers, XRD based illite–smectite expandability calculations were not able to fully explain the observed properties of the clay minerals present in some streams, especially the 0.2–2 μm primary froth sample. Only more accurate expandability calculations based on HRTEM analyses along with particle thickness distribution data made it possible to describe the behaviour of clay minerals in the extraction process streams. HRTEM studies showed a pronounced bimodal thickness distribution of the clay mineral particles, containing a large number of very thin particles. The presence of thin particles was the cause of the extraordinarily high activity of the 0.2–2 μm primary froth sample (high CEC and specific surface area values). This effect was magnified by the presence of organic matter and Fe compounds.

Investigations on Fe in the clay fractions of the streams suggest that Fe compounds may exist in several forms including crystalline, nanocrystalline and/or amorphous iron (hydr)oxides, such as lepidocrocite, and Fe in the clay mineral structure (e.g., chlorite). The CEC data showed that the Cu-trien adsorption method was sensitive to the presence of Fe oxides in the sample, while

the methylene blue titration method was not. Further studies on the role of Fe in the bitumen extraction process could enrich knowledge in the field.

Chapter 7

Conclusions and future work

7.1. Conclusions

Illite and kaolinite were the dominant clay minerals in both the raw oil sands ores and the clay lenses. Only small amounts of chlorite and mixed-layers clay minerals (illite-smectite and kaolinite-smectite) were detected with the exception of the HK ore which contained high quantities of mixed-layer clay minerals.

Cation exchange capacity (CEC) and surface area (SA) measurements should be used carefully since measurements are sensitive to the experience of the operator for methylene blue titration and the presence of ultrafine iron compounds for the copper triethylenetetramine titration method. Detailed mineral composition analysis of samples is required in order to evaluate the CEC and SA measurements, since these properties are very sensitive to the mineral composition of the samples.

Amorphous and/or ultrafine iron compounds were detected in the oil sands samples. These compounds are believed to dramatically influence the bitumen extraction process. Further studies in this area are essential.

A nonaqueous bitumen extraction process using a mixture of aromatic (toluene) and paraffinic (n-heptane) was established. The proposed extraction process resulted in very high bitumen recovery (96-98%) and an extraction product with high purity (>99.5% bitumen). The bitumen recovery was the same for so called “good” and “poor” processing ores, indicating a possible advantage of the nonaqueous extraction process over the current hot water extraction process. Another advantage of the nonaqueous extraction process was the settling

behaviour of the tailings. Unlike water extraction, nonaqueous extraction did not disperse the clays, thereby dramatically shortening the settling time of the tailings. Both solvent to bitumen and heptane to bitumen ratios need to be optimized in the extraction process, since they play important roles in dissolving bitumen and precipitating asphaltenes.

Unlike bitumen recovery, extraction time and product quality were sensitive to the fines and/or clay content of the oil sands ore. Shorter extraction times and better product quality were obtained for the low fines ore. Similar trends for the changes of solids and water contents in the main extraction product (supernatant) with settling time were observed. This could indicate that the small amount of water detected in the supernatant was likely attached to the solid particles rather than as a separate phase.

Segregation of kaolinite relative to illite to the extraction product (supernatant in nonaqueous extraction and primary froth in water extraction) was observed in all cases.

HRTEM investigations on 2:1 layer clay minerals (illite and illite-smectite) revealed the presence of significant amounts of smectitic monolayers in the extraction product (not detectable by XRD). These monolayers (100% smectitic) and also bilayers (at least 50% smectitic) were very expandable due to the presence of loose cations on their surfaces and, therefore, settled very slowly compared with thicker particles. In summary, the solids in the supernatant had a more smectitic nature when compared with the ore. In addition, the expandability calculations based on HRTEM data explained the extraordinarily high activity of the primary froth generated from sample HK, while XRD calculations failed to do so.

7.2. Future work

Suggestions for the future work are categorized as follow:

- Establishment of a systematic sampling method.
- Detailed characterization of the clay minerals and Fe nanominerals in the representative oil sands end members (estuarine sand, estuarine clay, marine sand, and marine clay) and artificial oil sands samples.
- Study of the influence of clay minerals on solvent extraction in a completely water-free environment.
- Study of the influence of different smectites on water-based and nonaqueous bitumen extraction.
- Influence of clay minerals on solvent recovery.

7.2.1. Establishment of a systematic sampling method

As mentioned in the Introduction chapter, several parameters such as bitumen grade, fines content, clays content, processability of the ore, etc. are used for categorizing oil sands ores in oil sands research and industry. These parameters, although useful from some perspectives, cannot be used as a standard criterion for systematic studies. For instance, it was shown in the current study that the terms “good processing” and “poor processing” as defined in water-based bitumen extraction are meaningless in a nonaqueous bitumen extraction process. In addition, there is little knowledge about the processability of different petrologic types in the oil sands deposit during nonaqueous bitumen extraction. Any difference in the processability of the petrologic types would significantly affect the calculation of economic reserves from the perspective of nonaqueous bitumen extraction from the oil sands. Therefore, the establishment of a systematic sampling method is necessary in mineralogical studies on oil sands. A geological approach defining four petrologic end members (estuarine sand, estuarine

claystone, marine sand, and marine claystone) is suggested by the author. The properties of different oil sands ore zones are believed to be an averaged combination of the properties of the end members. Therefore, understanding the four end members will go a long way towards understanding the entire deposit. Detailed analysis of the end member compositions, quantifying solid and water content in the supernatant during nonaqueous extraction, and testing post-extraction solvent recovery are necessary in order to interpret the “solvent-based processability” of the end member rocks. Using this type of classification will make it possible to recommend the types of oil sands ores suitable for solvent-based extraction, as well as the types of ores that should be avoided or specially treated.

7.2.2. Detailed characterization of the clay minerals and Fe nanominerals in the representative oil sands end members (estuarine sand, estuarine clay, marine sand, and marine clay) and artificial oil sands samples

Detailed mineralogical studies focusing on the clay and Fe nanominerals of each end member are proposed. The same methodology used in the current study can be used in order to meticulously analyze the clay minerals in the four end members. In addition to the methodology used in this research for XRD analysis, full profile fitting methods such as Rietveld refinement are necessary in order to quantitatively analyze the amount of mixed-layering within illite and kaolinite. Preparing extra pure, fully homogenized, well oriented XRD samples is an important prerequisite for such investigations. A modified glass slide method using the largest possible glass slide that can be used for Rigaku refractometers has been already developed by the author of this thesis. Using more powder on the glass slide will result in a higher signal to background ratio (higher intensity) in the XRD profiles which is crucial for doing such accurate analysis.

The negative influence of the Fe nanominerals on water-based bitumen extraction (properties of the primary froth) was investigated in the present study, but the

behaviour of Fe nanominerals in nonaqueous extraction is still unknown. Specific surface properties of ultrafine Fe minerals may cause them to concentrate in the supernatant, for the same reason that they concentrate in the froth after water-based extraction. Nevertheless, their high density should cause them to settle down along with the coarse minerals. Studying Fe nanomineral distribution in fractions after solvent extraction tests and artificial samples with the addition of various Fe nanominerals may lead to a better understanding of the role they play in nonaqueous bitumen extraction.

In order to verify the complicated mineralogical studies of natural oil sands ores (four end members), these studies are recommended to be applied to artificial samples as well. Artificial samples can be made by mixing Athabasca bitumen, minerals and water in the same ratio obtained from the studies on the natural system. Using bitumen and minerals with previously known properties (or determining their properties prior to making artificial samples) can be extremely helpful in understanding the interactions among bitumen, minerals, water and solvent (if added) during the extraction process. Another advantage of such simulated systems (artificial samples) is the possibility of varying each important parameter independently. For instance, the effect of clay minerals or Fe nonominerals can be studied in separate systems. However, it must be pointed out that the results of such simplified simulated studies have to be used only in conjunction with the results from studies on natural systems, as they could be very misleading.

It was also shown in the present study that the aggregates of clay mineral particles, organic matter, and possibly water were present only in the high fines ore and not the low fines ore during nonaqueous bitumen extraction. The reason for this phenomenon is speculated to be related to differences in the adsorption of organic matter on the surfaces of clay minerals in the two mentioned ores. Another possibility is that the number of such aggregates if formed during the extraction of the low fines ore was so small so they were not observed in any

SEM images. Detailed studies on the adsorption of organic matter on the clay surfaces in a nonaqueous extraction process are necessary. Such studies, if successful, could also be applied to the four end members in order to answer the question about the difference between the surface properties of estuarine and marine claystones. Unlike the light laminated estuarine claystones, the black colour of marine clays is problematic in commercial oil sands mining and bitumen extraction as they cannot be identified on-site during processing by fly-by large-scale infrared spectroscopy. For that reason the marine ore is recognized as rather “poor-processing”, although it may contain in total only a little less bitumen than the estuarine ore. While the estuarine ore is mixed with water and hydro-transported to the processing plant, the marine ore has to be transported on a train and undergoes pre-processing. The reason for the visual (colour) difference between marine and estuarine deposits is also speculated to be related to the adsorption of organic matter on the surfaces of clay minerals. A fundamental study is required to identify the relationship between the surface properties of the marine clay minerals and the toluene insoluble organic matter adsorbed on their surfaces. Only such studies may explain the difference between the interaction of organic matter with the surfaces of estuarine and marine claystones. Preliminary elemental analysis investigations by the author of this study suggest that the origin of the adsorbed organic matter is likely kerogen. Further experiments, such as detailed elemental analysis and Fourier transform infrared spectroscopy (FTIR), are suggested to verify this hypothesis.

7.2.3. Study of the influence of clay minerals on solvent extraction in a completely water-free environment

The enrichment of kaolinite in the extraction product (froth in water-based and supernatant in nonaqueous bitumen extraction) was found in the current study as well as other studies (e.g. Kaminsky, 2008). This phenomenon could not be linked to particle size as kaolinite is typically coarser than illite (illite-smectite).

Therefore, clay mineral segregation must have been related to the specific hydrophobic vs. hydrophilic surface properties of the clay minerals (Saada et al., 1995; Liu et al., 2004). Clay minerals, especially smectite, naturally contain adsorbed water; thus their surfaces are hydrophilic. Natural ore always contains water as well. Based on the clay segregation found in the supernatant, it seems that due to hydrophilic surfaces covered by a water film, clays tend to flocculate in an organic solvent. This is, however, a working hypothesis. Further studies are required to verify this hypothesis. If this hypothesis is true, there will be a number of important questions to be answered. For instance, how much water is needed for flocculation to occur and what is the maximum water/clay ratio which can remove water from the supernatant by clay flocculation? Studying the clay minerals during a completely water free solvent extraction (by removing water from the oil sands ore by microwaving, for example, and using extra pure solvent in controlled humidity) might lead to an understanding of the mechanism of this phenomenon.

7.2.4. Study of the influence of different smectites on water-based and nonaqueous bitumen extraction

It was shown in the current research that the presence of smectite, both discrete (monolayer particles) and smectitic layers, in the structure of illite-smectite strongly influences the bitumen extraction process. The most common smectite in the oil sands deposits is montmorillonite. Its electrical charge originates almost exclusively from $\text{Mg}^{2+} \rightarrow \text{Al}^{3+}$ substitution in the octahedral sheet. Although montmorillonite has been studied extensively as the most abundant smectite in the oil sands, it is not the only smectite present. Besides montmorillonite, beidellite, saponite and nontronite are smectitic structures (see review by Emmerich et al., 2009), which occur typically in various rocks as pure minerals or as smectitic interstratifications in mixed-layer clay minerals and form the outer surfaces of the non-expandable clay minerals. Smectitic surfaces in the illite-smectite mixed-layer phase may show montmorillonitic as well as beidellitic (electrical charge

provided exclusively by substitution of Al^{3+} for Si^{4+} in the tetrahedral sheet) properties. Glauconite, abundant in the Clearwater Formation, contains nontronitic interstratifications. Moreover, besides the structural features, smectites differ by the total charge density. The cation exchange capacity (CEC) originating from the charge density ranges from 70 to 130 meq/100 g for pure smectite (see e.g., Środoń and McCarty, 2008).

Different smectites behave in extremely different ways when adsorbing polar and non-polar, ionic and non-ionic, and hydrophilic and hydrophobic molecules. Evidence for such properties comes from studies on the sorption of hydrophobic pesticides and other soil pollutants on clays, e.g., Laird et al. (1992) and Hundal et al. (2001). As an example, the order of atrazine adsorption starts from beidellite and hectorite, followed by saponite and mixed-charge montmorillonite-beidellite, and then ends with the high charge Otay montmorillonite, which provides almost no adsorption (Laird et al., 1992). The difference between the highest and lowest measured adsorption on smectite is several orders of magnitude. Rana et al. (2009) observed dramatic changes in dioxine adsorption on smectites when applying various interlayer cations. Generally, the lower the hydration potential of interlayer cations, the higher the adsorption of hydrophobic compounds. There is a lack of characterization of different smectites and their influences on bitumen extraction (especially nonaqueous extraction). Smectites with different particle sizes and exchangeable cations are suggested to be used and studied in the artificial systems mentioned earlier.

7.2.5. The role of clay minerals on solvent recovery

Solvent recovery has to be considered as an important parameter in any possible commercial solvent extraction process. Solvent recovery is not only important from an economical standpoint but also from an environmental perspective, as the maximum concentration of solvents, such as toluene, that can be tolerated in the extraction tailings is 500 ppm. The interactions between organic matter and clay

mineral surfaces are believed to have a key impact on solvent recovery. A study of solvent recovery was beyond the scope of the current research, but is required for nonaqueous bitumen extraction to be commercialized. The capability of the tailings in retaining the organic solvent (e.g., toluene and heptane) is expected to be controlled by the same parameters controlling the adsorption of organic matter on the clay mineral surfaces (see the Introduction chapter).

7.3. References

Emmerich, K., Wolters, F., Kahr, G., & Lagaly, G. (2009). Clay profiling: the classification of montmorillonites. *Clays and Clay Minerals*, *57*, 104–14.

Hundal, L., S., Thompson, M., L., Laird, D., A., & Carmo, A., M. (2001). Sorption of phenanthrene by reference smectites. *Environmental Science & Technology*, *35*, 3456-61.

Kaminsky, H., A., W. (2008). Characterization of an Athabasca oil sands ore and process streams. Ph.D.Thesis, Department of Chemical and Materials Engineering, University of Alberta, Canada.

Laird, D., A., Barriuso, E., Dowdy, R., H., & Koskinen, W., C. (1992). Adsorption of atrazine on smectites. *Soil Science Society of America Journal*, *56*, 62-67.

Liu, J., Xu, Z., & Masliyah, J. (2004). Role of fine clays in bitumen extraction from oil sands. *American Institute of Chemical Engineers (AIChE) Journal*, *50*, 8, 1917-27.

Rana, K., Boyd, S., A., Teppen, B., J., Li, H., Liu, C., & Johnston, C., T. (2009). Probing the microscopic hydrophobicity of smectite surfaces. A vibrational spectroscopic study of dibenzo-p-dioxin sorption to smectite. *Physical Chemistry Chemical Physics*, *11*, 2976–85.

Saada, A., Siffert, B., & Papirer, E. (1995). Comparison of the hydrophilicity/hydrophobicity of illites and kaolinites. *Journal of Colloid and Interface Science*, *174*, 185-190.

Środoń, J. & McCarty, D., K. (2008). Surface area and layer charge of smectite from CEC and EGME/H₂O-retention measurements. *Clays and Clay Minerals*, *56*, 155-74.